LSDS-2082
Version 1.0

Department of the Interior
U.S. Geological Survey

Landsat 9 Data Users Handbook

Version 1.0

February 2022

Landsat 9
Data Users Handbook

February 2022

Document Owner:

KRISTI SAYLER Digitally signed by KRISTI SAYLER
Date: 2022.02.18 09:19:10 -06'00'

Kristi Sayler Date
LSRD Project Manager
U.S. Geological Survey

Approved By:

TIMOTHY GLYNN Digitally signed by TIMOTHY GLYNN
Date: 2022.02.24 11:25:45 -06'00'

Timothy Glynn Date
LSDS CCB Chair
U.S. Geological Survey

EROS
Sioux Falls, South Dakota

Executive Summary

The Landsat 9 (L9) Data Users Handbook is prepared by the U.S. Geological Survey (USGS) Landsat Project Science Office at the Earth Resources Observation and Science (EROS) Center in Sioux Falls, S.D., and the National Aeronautics and Space Administration (NASA) Landsat Project Science Office at NASA's Goddard Space Flight Center (GSFC) in Greenbelt, Maryland.

The purpose of this handbook is to provide a basic understanding and associated reference material for the L9 Observatory and its science data products. In doing so, this document does not include a detailed description of every technical detail for the L9 mission, but instead focuses on the information that the users need to gain an understanding of the science data products.

This document is controlled by the USGS Land Satellites Data System (LSDS) Configuration Control Board (CCB). Please submit changes to this document, as well as supportive material justifying the proposed changes, via a Change Request (CR) to the Process and Change Management Tool.

Document History

Document Number	Document Version	Publication Date	Change Number
LSDS-2082	Version 1.0	February 2022	CR 20910

Contents

List of Figures

List of Tables

Section 1 Introduction

1.1 Background

The Landsat 9 (L9) mission is a joint mission formulated, implemented, and operated by the National Aeronautics and Space Administration (NASA) and the Department of the Interior (DOI) U.S. Geological Survey (USGS). L9 is a remote-sensing satellite mission providing coverage of the Earth's land surfaces. This mission ushers in 50 years of global data collection and distribution provided by the Landsat series of satellites. Landsat images provide information that meets the broad and diverse needs of business, science, education, government, and national security.

The goal of L9 is to continue the collection, archival, and distribution of multispectral imagery affording global, synoptic, and repetitive coverage of the Earth's land surfaces at a scale where natural and human-induced changes can be detected, differentiated, characterized, and monitored over time. Landsat represents the only source of global, calibrated, moderate spatial resolution measurements of the Earth's surface that are preserved in a national archive and freely available to the public.

The L9 goal is consistent with the Landsat programmatic goals stated in the United States Code, Title 15 Chapter 82 "Land Remote Sensing Policy" (derived from the Land Remote Sensing Policy Act of 1992). This policy requires that the Landsat Project provide data into the future that are sufficiently consistent with previous Landsat data to allow the detection and quantitative characterization of changes in or on the land surface of the globe. L9 was conceived as a follow-on mission to the highly successful Landsat series of missions that have provided satellite coverage of the Earth's continental surfaces since 1972. The data from these missions constitute the longest continuous record of Earth's surface as seen from space.

L9 is intended to ensure that Landsat data be provided to the USGS National Satellite Land Remote Sensing Data Archive (NSLRSDA) for at least five years. The intent with the implementation of L9 is to leverage, to the extent practical, the designs and systems used for Landsat 8 (L8).

1.2 Mission Objectives

The major mission objectives are:

- Collect and archive medium-resolution (circa 30-meter (m) spatial resolution) multispectral image data affording seasonal coverage of the global land mass for a period of no less than five years, with no credible single-point failures.
- Collect and archive moderate-resolution (circa 120 m ground-sample distance) thermal image data affording seasonal coverage of the global land mass for a continuous period of no less than five years, with no credible single-point failures.
- Ensure that L9 data are sufficiently consistent with data from the earlier Landsat missions, in terms of acquisition geometry, calibration, coverage characteristics,

spectral characteristics, output product quality, and data availability to permit studies of land surface change over multidecadal periods.
- Distribute L9 data products to the public on a nondiscriminatory basis.

1.2.1 Landsat Missions Overview

Landsat satellites have provided multispectral images of the Earth continuously since 1972, creating a unique data record of the Earth's land masses. This unique retrospective of the Earth's surface has been used across several disciplines to achieve an improved understanding of the Earth's land surfaces and the impact of humans on the environment.

Landsat data have been used in a variety of government, public, private, and national security applications. Examples include land and water management, global change research, oil and mineral exploration, agricultural yield forecasting, pollution monitoring, land surface change detection, and cartographic mapping.

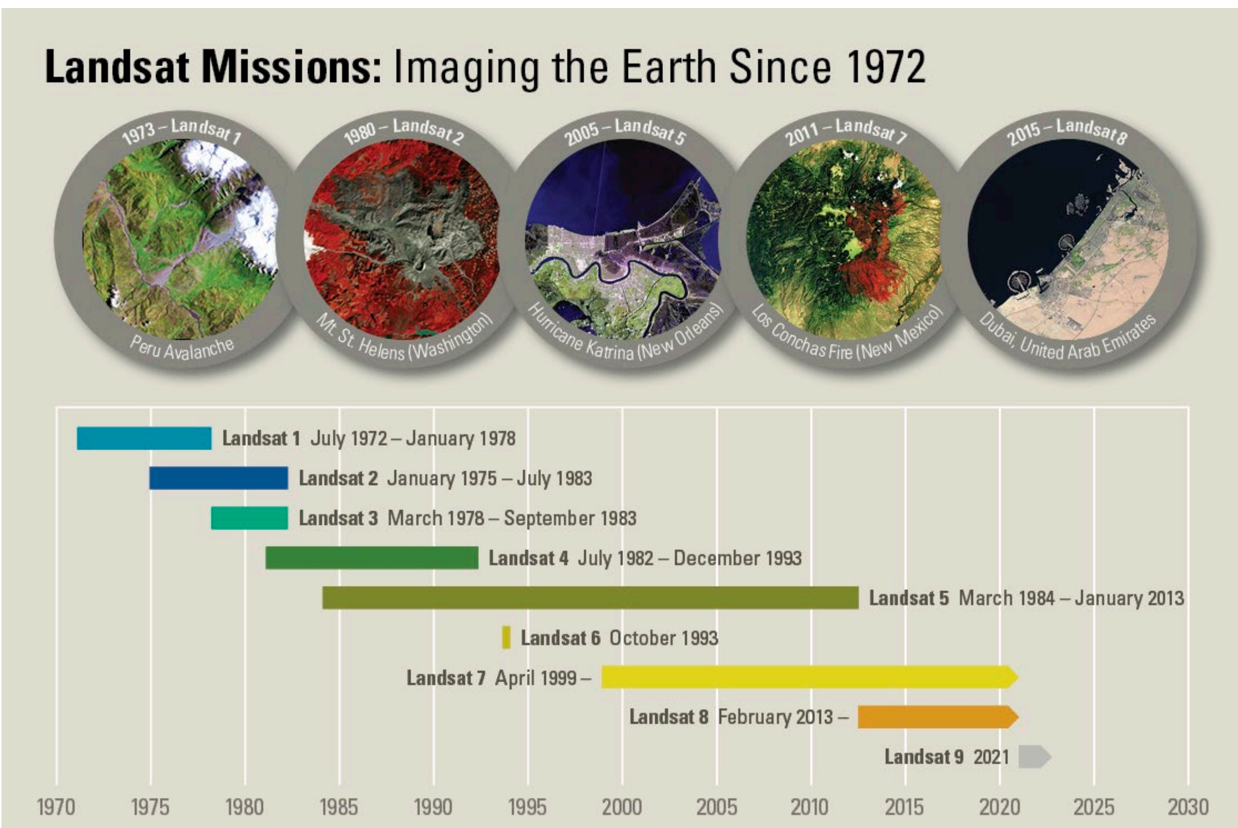

Figure 1-1. Landsat Missions Timeline

Landsat 1, originally known as ERTS-1 was launched July 23, 1972, with two Earth-viewing imagers – a Return Beam Vidicon (RBV) and an 80-m, 4-band Multispectral Scanner (MSS). Landsat 2 and Landsat 3, launched January 22, 1975, and March 5,1978, respectively, were configured similarly. On July 16, 1982, Landsat 4 was launched with the MSS and the new Thematic Mapper (TM) instrument, which included improved ground resolution at 30-m and better defined spectral characteristics. In addition to using an updated instrument, Landsat 4 made use of the Multi-Mission Modular Spacecraft (MMS), which replaced the Nimbus-based spacecraft design employed for Landsat 1 – Landsat 3.

Landsat 5 (L5), launched March 1,1984, also carried the TM and MSS sensors. The satellite long outlived its original three-year design life, delivering Earth imaging data for nearly 29 years – setting a Guinness World Record For 'Longest Operating Earth Observation Satellite’. The L5 TM sensor collected over 2.9 million scenes that are held within in the USGS Landsat archive.

Landsat 6, carried the Enhanced Thematic Mapper (ETM) that included a 15-m panchromatic (Pan) band, failed to achieve orbit on October 5, 1993.

Landsat 7 (L7) was launched April 15,1999, and performed nominally until the ETM Plus (ETM+) sensor’s Scan Line Corrector (SLC) failed in May 2003, which led to about 22 percent data loss in each scene. Since that time, L7 has acquired data in the “SLC-off” mode. All L7 SLC-off data are of the same high radiometric and geometric quality as data collected prior to the SLC failure.

Landsat 8, launched February 11, 2013, represented an evolutionary advance in technology. The Operational Land Imager (OLI), a push-broom sensor with a four-mirror telescope and 12-bit quantization, collects data for visible, near infrared, and short wave infrared spectral bands as well as a panchromatic band, while providing data in two additional spectral bands — one tailored especially for detecting cirrus clouds and the other for coastal zone observations. The Thermal Infrared Sensor (TIRS) collects data for two more narrow spectral bands in the thermal region formerly covered by one wide spectral band on Landsats 4–7.

Landsat 9, launched September 27, 2021, carries nearly identical sensors as L8 — the OLI-2, and the TIRS-2. The OLI-2 data has 14-bit quantization, and improvements to the TIRS-2 increases the quality of split-window thermal data usability.

Figure 1-2 displays the bandpass wavelengths of the sensors for all Landsat satellites. Table 5-4 displays the wavelength ranges for L9 OLI-2 and TIRS-2 bands. Wavelength ranges for all Landsat sensors can be found at https://www.usgs.gov/faqs/what-are-band-designations-landsat-satellites.

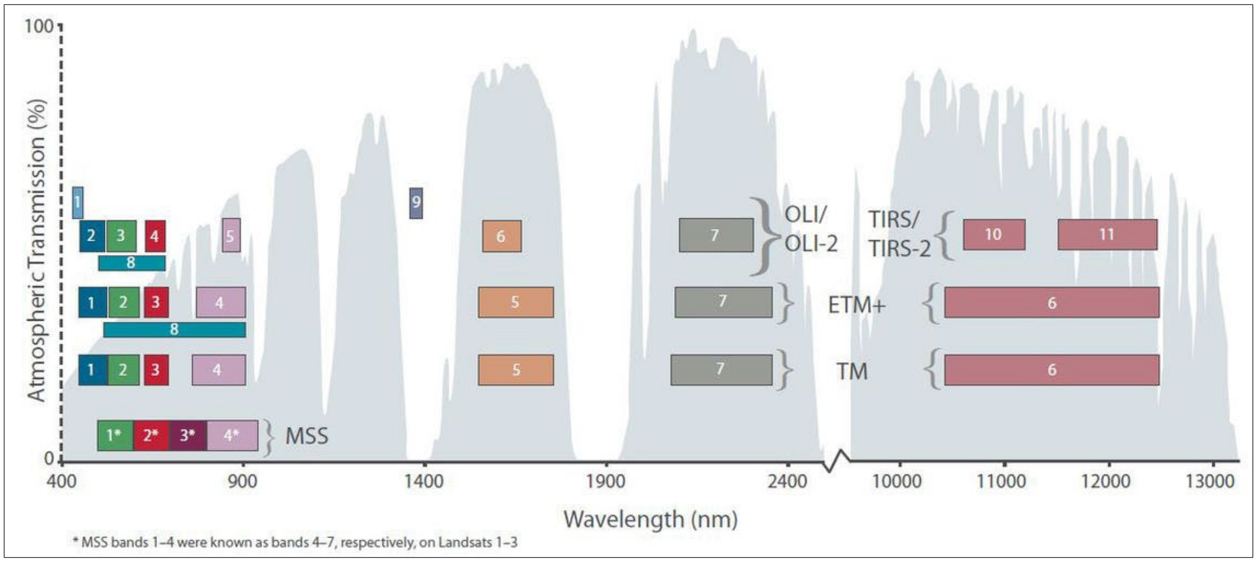

Figure 1-2. Spectral Bandpasses for all Landsat Sensors

1.3 Purpose and Scope

The primary purpose of this document is to provide a basic understanding and associated reference material for the L9 Observatory and its science data products.

This **Landsat 9 Data Users Handbook** is prepared by the USGS Landsat Project Science Office at the EROS Center in Sioux Falls, South Dakota.

1.4 Document Organization

This document contains the following sections:

- Section 1 describes the background for the L9 mission as well as previous Landsat missions
- Section 2 describes the Space and Ground Segments of the L9 Mission
- Section 3 provides a comprehensive overview of the current L9 Observatory, including the spacecraft, the Operational Land Imager 2 (OLI-2) and Thermal Infrared Sensor 2 (TIRS-2) instruments, and the L9 concept of operations
- Section 4 contains an overview of radiometric and geometric instrument Calibration/Validation activities
- Section 5 describes Level 1 (L1) products and product generation
- Section 6 describes the Level 2 (L2) products and product generation
- Section 7 describes the atmospheric auxiliary data products
- Section 8 describes the Full Resolution Browse (FRB) images
- Section 9 provides an overview of data search and access using the various online tools
- Appendix A provides details about L9 postlaunch calibration images
- Appendix B contains an example of L9 L1 product Object Description Language (ODL) MTL metadata

- Appendix C contains an example of L9 L1 product Extensible Markup Language (XML) metadata
- Appendix D describes the observatory component systems used by L9 geometric algorithms
- Appendix E provides a listing of the acronyms used in this document
- The References section contains a list of documents, publications, and webpages referred to in this document

Section 2 Landsat 9 Mission

The L9 management structure is composed of an ongoing partnership between NASA and USGS for sustainable land imaging.

The L9 system entails three major mission components:

- The Space Segment
    - Includes the spacecraft bus, the OLI-2 instrument, and the TIRS-2 instrument
- The Launch Services Segment
    - Comprised of the launch vehicle (LV), launch site, and launch preparation facilities
- The Ground Segment
    - Made up of the Landsat Ground System, Landsat Multi-Satellite Operations Center (LMOC), and Data Processing and Archive System (DPAS)

NASA contracted with Ball Aerospace to develop the OLI-2 sensor and with Northrop Grumman (formerly Orbital ATK) to build the spacecraft; NASA Goddard Space Flight Center (GSFC) built the TIRS-2 instrument.

NASA is responsible for the satellite launch and completion of the on-orbit checkout before handing operations to the USGS, which is typically +/- 100 days (see Figure 2-1). The USGS is responsible for the development of the Ground System and is responsible for operation and maintenance of the Observatory and the Ground System for the life of the mission. In this role, the USGS captures, processes, and distributes L9 data and maintains the L9 data archive.

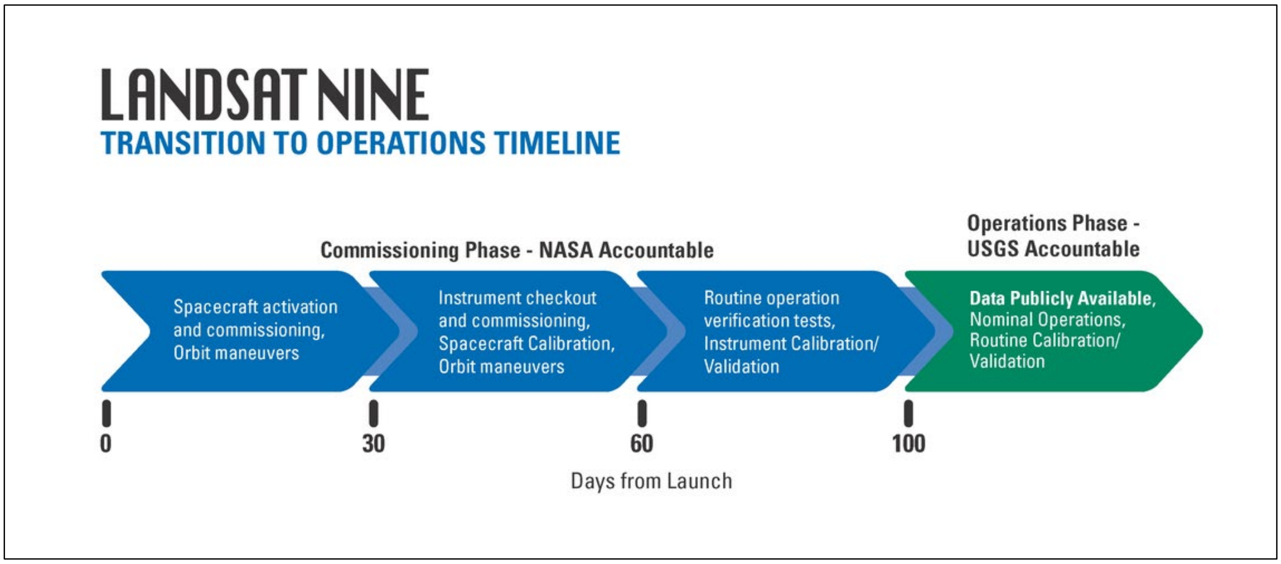

Figure 2-1. Landsat 9 Typical Transition to Operations Timeline

The Landsat Project at the USGS EROS Center manages the overall L9 mission operations. In this capacity, USGS EROS directs on-orbit flight operations, implements mission policies, directs acquisition strategy, and interacts with International Ground Stations (IGSs). USGS EROS captures L9 data and performs preprocessing, archiving, product generation, and distribution functions. USGS EROS also provides a public interface into the archive for data search and ordering. Figure 2-2 displays the locations of all companies and agencies involved with L9.

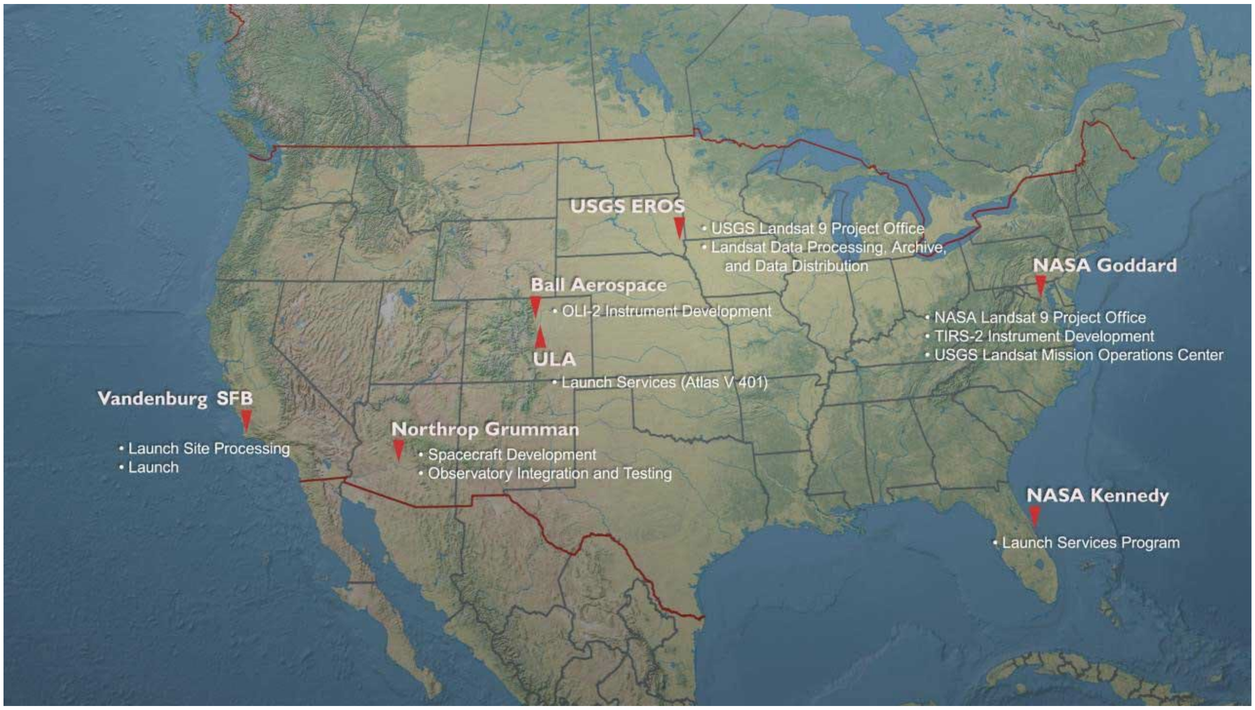

Figure 2-2. Landsat 9 Mission Team Member Locations

2.1 Space Segment

The Space Segment includes the L9 Observatory and associated Ground Support Equipment (GSE). The GSE provides the functionality to perform ground-based integration and testing of the Observatory before launch. The Observatory consists of the spacecraft and OLI-2 and TIRS-2 sensors. Northrop Grumman provides the spacecraft and Observatory integration support.

The overall objectives of the L9 mission are as follows:

- Offer 16-day repetitive Earth coverage, and an 8-day offset with L8.
- Build and periodically refresh a global archive of sunlit, substantially cloud-free land images
- Acquire more than 700 scenes per day

L9 Mission data, which consist of image data and ancillary data, are collected, and downlinked to the Landsat Ground Network (LGN) via the X-Band communications link.

Mission data are always stored for subsequent playback; data acquired during LGN contacts are also transmitted to ground in real-time. This link, using separate Virtual Channels (VCs), includes stored housekeeping telemetry data, real-time, and playback Mission data to LGN. Similarly, real-time only Mission data are downlinked to International Cooperators (ICs) equipped to receive L9 data.

The L9 Observatory also receives and executes commands and transmits real-time and stored housekeeping telemetry to Ground Stations within the Ground Network Element (GNE), NASA Space Network (SN), and NASA Near Earth Network (NEN) via the S-Band link.

2.2 Launch Services Segment

The Launch Services Segment provides the assets and services associated with the LV and the Observatory-to-LV integration. Included with the LV is all LV GSE, property, and facilities to integrate the Observatory to the LV, verify their integration, and conduct prelaunch testing with ground-based functions. The launch site is located at Vandenberg Space Force Base (VSFB) in California.

2.3 Ground Segment

The L9 Ground Segment comprises the Ground System, and Operations.

2.3.1 Ground System

The Ground System is composed of the GNE, the LGN, LMOC, and DPAS.

2.3.1.1 Ground Network Element (GNE)

The GNE includes the Landsat Ground Network (LGN) and Data Collection and Routing System (DCRS). The objective of the GNE is to provide highly reliable S-Band and X-Band communication services with the Observatory and route the data appropriately within the Ground System.

2.3.1.1.1 Landsat Ground Network (LGN)

The five ground receiving stations that make up the Landsat 9 USGS Ground Network are in Sioux Falls, South Dakota; Alice Springs, Australia; Neustrelitz, Germany; Gilmore Creek, Alaska; and Svalbard, Norway. These receiving stations are responsible for downlinking the satellite telemetry (via S-Band Radio Frequency (RF) link) and science data (via X-Band RF link) that feeds the USGS Landsat data archive. The stations can also uplink commands to the satellite. More information about LGN can be found at https://www.usgs.gov/landsat-missions/usgs-landsat-ground-stations.

2.3.1.1.2 Landsat International Cooperators (IC)

Landsat's longstanding network of cooperators around the world embodies the United States' policy of peaceful use of outer space and the worldwide sharing of civil space technology for public benefit. Outside of the U.S., there are nearly 30 actively operating ground stations in 16 countries around the world; three of the stations have been involved for nearly 50 years – seeing the advancement throughout all Landsat Missions.

Data acquired by L9 are stored on the satellite's Solid State Recorder (SSR) and downlinked to USGS EROS for inclusion in the USGS Landsat archive when the satellite comes in contact with the LGN (See Section 2.3.1.1.1). For updated information and a map displaying the IGSs, please visit https://landsat.usgs.gov/igs-network.

2.3.1.2 Landsat Multi-Satellite Operations Center (LMOC)

The LMOC includes all the ground-based assets needed to operate the L9 Observatory, excluding the ground network. The LMOC plans and schedules all flight operations resources and spacecraft contact activities and supports prelaunch readiness, launch, commission, and operations. The LMOC monitors and controls the L9 Observatory and provides a full suite of attitude and orbit determination capabilities within flight dynamics. The LMOC handles all of the science, calibration, and Observatory activity planning through the generation and verification of stored command loads for the L9 Observatory. Data exchanged with LMOC includes telemetry, command and control, collection requests, plans, and schedules, trending and analysis summaries, logs, and additional associated interaction.

L9 also includes a fully capable Backup Multi-Satellite Operations Center (bLMOC), which is physically separate from and synchronized with the primary LMOC. The bLMOC will become active if the primary LMOC experiences a critical failure.

2.3.1.3 Data Processing and Archive System (DPAS)

The DPAS ingests and processes mission data to produce interval files and subset interval files and generates Landsat data products for distribution to the public. The DPAS also contains functionality used for the calibration and validation of Landsat data and products.

2.3.2 Operations

The Operations component of the Ground Segment includes ground network operations, data operations, and flight operations. Ground network operations include the daily operations of the Ground Stations to ensure successful contact with the Observatory. The ground network operations consist of the personnel required to operate and maintain the LGN stations and equipment.

Data operations include the daily processing and distribution of Landsat data products. This consists of ingesting, processing, monitoring, characterizing, calibrating, validating, collecting metrics, preserving data, etc., thus enabling the detection and quantitative characterization of changes in the Earth's land surface.

The Flight Operations Team (FOT) is the organization responsible for conducting daily Landsat operations. The main duties include orbit maintenance and monitoring, conducting mission planning activities, monitoring real-time telemetry, and uplinking daily command products. These duties are conducted using the LMOC systems and tools.

2.4 Landsat 9 Long Term Acquisition Plan (LTAP-9)

The primary objective of the L9 mission is to generate a global high-quality observational record of land image data in continuity with the Landsat satellite series. The basic premise of the LTAP-9 is to acquire all defined, sunlit, collection sites as defined in the LTAP-9 Collection Request (LCR) that includes a table of path/row-based information, as well as all land, coastal/littoral regions, islands, reefs, atolls, and shallow water ecosystems where the sensors provide useful measurements. In addition, a variety of acquisitions (such as night scenes, off-nadir scenes, science campaigns, etc.) are incorporated through the Special Collection Requests (SCRs) process, and calibration acquisitions (such as solar, lunar, side slither, etc.) are incorporated through the Calibration Collection Requests (CalCRs) process. Due to the distribution of candidate scenes and the annual change in solar illumination, portions of time exist where the candidates may exceed the system capacity. The LTAP-9 addresses methods to select how candidate scenes are rejected when optimizing the schedule to meet resource constraints.

All interfaces related to Earth image scheduling use the Worldwide Reference System-2 (WRS-2) path/row coordinate system convention, including target path/row or orbital path/row and roll angle for off-nadir, even when the Observatory orbit is not compliant with the system. This includes the imaging intervals collected by the instruments, with each scene or imaging sensor activity within the interval being assigned a unique identifier (e.g., path, row, and date). The unique identifiers are shared within the system so that every individual scene requested can be tracked throughout the entire planning, collection, and production process.

The size of a L9 scene measures 185-kilometer (km) cross-track by 180 km along-track and includes a five percent overlap of the preceding and subsequent scenes. L9 is available to collect at least 838 WRS-2 scenes per 24-hour period, over a 16-day repeat cycle. Instrument Field of Views (IFOVs) are sufficient to cover the 185 km cross-track area of a scene when in the nominal mission orbit and the Observatory is pointing the instruments at nadir. Image data are collected on the spacecraft's 3.14 terabit Solid State Recorder (SSR) and transmitted to the LGNs in real-time, playback, or both. Image data are then transferred via a high-speed Wide Area Network (WAN) to USGS EROS for ingest, processing, archive, and distribution.

Off-nadir SCRs are made on a scene (or set of scenes) up to one WRS-2 path to the east or west of a possible near-term nadir path. To image scenes along one of these paths, the Observatory must perform up to a ±15-degree roll from nadir to align the boresights of the instruments along the targeted path. Once the offset is achieved, the instruments begin capturing the off-nadir image data. At the completion of the off-nadir imaging, the Observatory performs a reverse roll and resumes on-nadir imaging. This capability potentially allows a single scene to be imaged up to three times during the 16-day ground track repeat cycle.

All viable image data are processed by USGS EROS. This results in L1 and L2 data products that are made available via the web for the science and user community.

These data products are available for search and distribution within 12 hours of observations for 85 percent of the data received by the Ground System.

LSDS-1724 Landsat 9 Long-Term Acquisition Plan describes how L9 collects science data.

Section 3 Observatory Overview

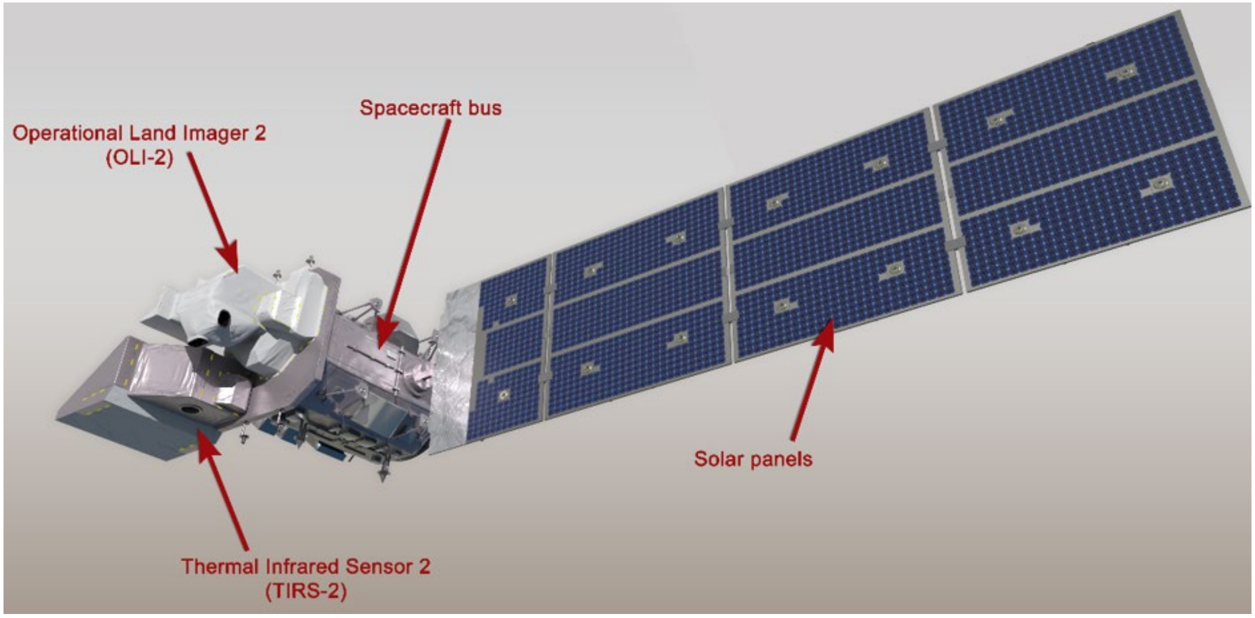

Figure 3-1. Illustration of Landsat 9 Observatory with bus and solar panels

The L9 spacecraft, with its two integrated imaging sensors, is referred to the L9 Observatory. The OLI-2, built by Ball, and the TIRS-2, built by NASA GSFC, both simultaneously image every scene but are capable of independent use if a problem in either sensor arises. In normal operation, the sensors view the Earth at-nadir on the sun-synchronous WRS-2 orbital path/row coordinate system, but special collections may be scheduled off-nadir.

The L9 Observatory operates in a 705 ±1-km near-polar, sun-synchronous orbit, completely orbiting the Earth every 98.9 minutes, with a 16-day ground track repeat cycle, and a Mean Local Time (MLT) equatorial crossing of the descending node within required 10:00 a.m. ±15 minutes. This allows imaging sensor data to be referenced to the WRS-2 path/row coordinate system convention as part of ground processing. L9 acquires data at an 8-day offset from L8 for each WRS-2 path. L9 has a design life of 5 years and carries 10 years of fuel consumables.

3.1 Concept of Operations

The fundamental L9 operations concept is to collect, archive, process, and distribute science data to continue to update the global archive.

The Landsat Mission Operation Center (LMOC) sends commands to the satellite once every 24 hours via S-Band communications from the Ground System to schedule daily data collections. LTAP-9 sets priorities for collecting data along the WRS-2 ground paths. LTAP-9 is modeled on the systematic data acquisition plan originally developed for L7 (Arvidson et al., 2006), and used for L8 also. OLI-2 and TIRS-2 collect data jointly to provide coincident images of the same surface areas. The MOC nominally schedules the collection of up to 750 OLI-2 and TIRS-2 scenes per day, where each scene covers a 185-by-180 km surface area. The objective of scheduling and data collection is to provide near cloud-free coverage of the global landmass for each season of the year.

The L9 Observatory initially stores OLI-2 and TIRS-2 data on board in an SSR. The LMOC commands the Observatory to transmit the stored data to the ground via an X-Band data stream from an all-Earth omni antenna. X-Band data are used for instrument data downlink, while S-Band is used for commanding and housekeeping telemetry operations.

The L9 Ground Network receives the data at several stations, and these stations forward the data to the EROS Center. The ground network also includes IGSs through ICs operated under the sponsorship of foreign governments. Data management and distribution by the ICs is in accordance with bilateral agreements between each IC and the U.S. Government. No unique data are held at the IGSs.

The data received from the ground network are stored and archived at the EROS Center. The OLI-2 and TIRS-2 data for each WRS-2 scene are merged to create a single file containing the data from both sensors. The data from both sensors are radiometrically corrected and co-registered to a cartographic projection, with corrections for terrain displacement resulting in a standard orthorectified digital image called the Level 1 product. Data processed to Level 1 are used as inputs to Level 2 and Level 3 science products.

3.2 Operational Land Imager 2 (OLI-2)

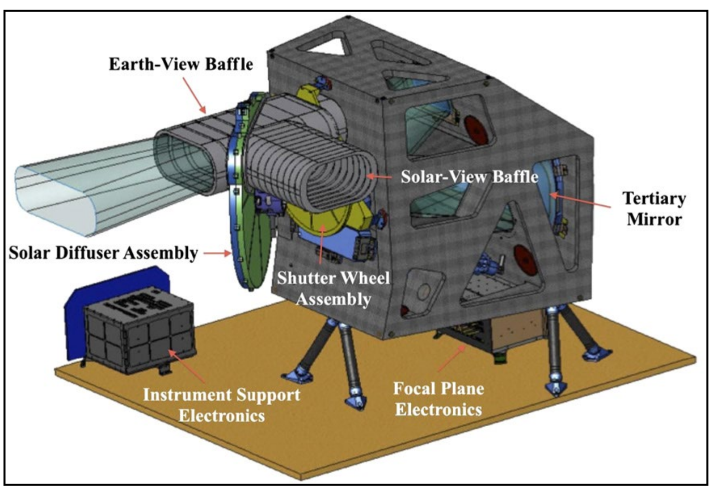

Figure 3-2. Illustration of the OLI-2 Sensor

The OLI-2 sensor collects image data in nine spectral bands over a 185 km swath with a maximum ground sampling distance (GSD), both in-track and cross track, of 30-meters(m) (98 feet) for all bands except the panchromatic band, which has a 15-meters

(49 feet) GSD. Like Landsat 8's OLI sensor, the widths of several OLI-2 bands were refined to avoid atmospheric absorption features that were apparent within earlier Landsat sensors. The band passes for all Landsat sensors can be found at https://www.usgs.gov/faqs/what-are-band-designations-landsat-satellites.

The OLI-2 is a push-broom sensor that employs a four-mirror anastigmatic telescope that focuses incident radiation onto the focal plane while providing a 15-degree FOV covering the 185 km across-track ground swath from the nominal L9 Observatory altitude. Periodic sampling of the across-track detectors as the Observatory flies forward along a ground track forms the multispectral digital images. The detectors are divided into 14 identical Sensor Chip Assemblies (SCAs) arranged in an alternating pattern along the centerline of the focal plane (Figure 3-3).

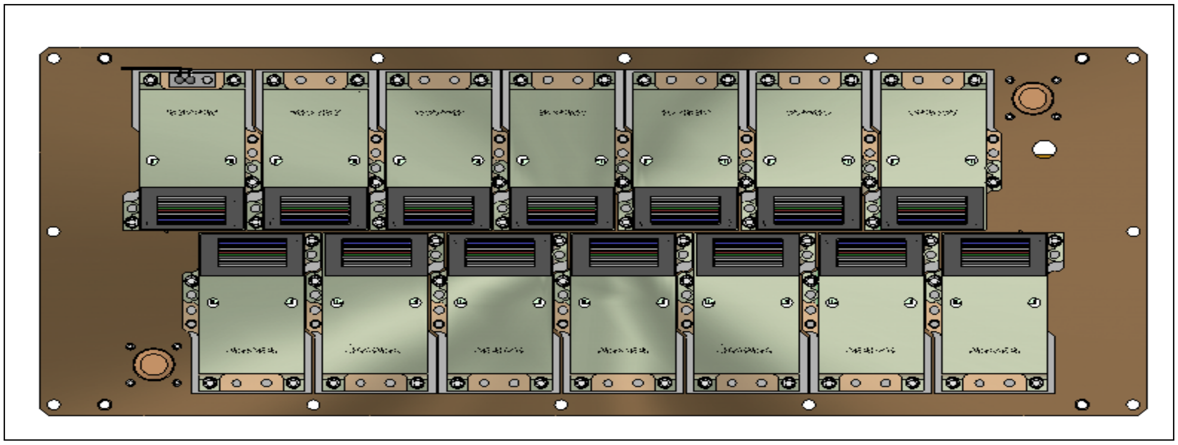

Figure 3-3. OLI-2 Focal Plane

Each SCA consists of rows of detectors, a Read-Out Integrated Circuit (ROIC), and a nine-band filter assembly. Data are acquired from 6,916 across-track detectors for each spectral band (494 detectors per SCA), except for the 15 m Pan band, which contains 13,832 detectors. The spectral differentiation is achieved by interference filters arranged in a "butcher-block" pattern over the detector arrays in each module. Even- and odd-numbered detector columns are staggered and aligned with the satellite's flight track. Even-numbered SCAs are the same as odd-numbered SCAs, however even-numbered SCAs are rotated 180 degrees from the odd-numbered SCAs (See Figure 3-4). The detectors on the odd and even SCAs are oriented such that they look slightly off-nadir in the forward and aft viewing directions. This arrangement allows for a contiguous swath of imagery as the push-broom sensor flies over the Earth, with no moving parts. One redundant detector per pixel is in each Visible and Near Infrared (VNIR) band, and two redundant detectors per pixel are in each Short Wavelength Infrared (SWIR) band. The spectral response from each unique detector corresponds to an individual column of pixels within the Level 0 product.

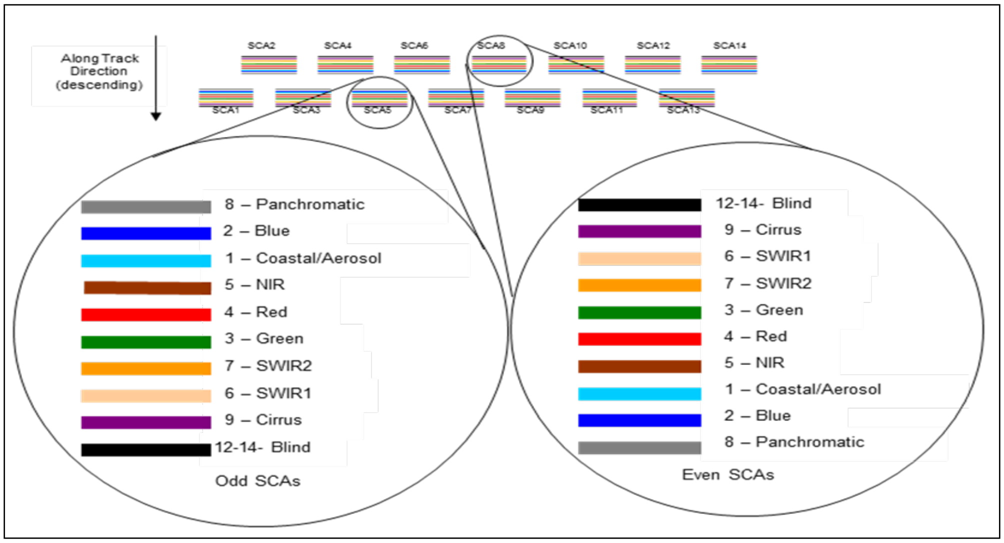

Figure 3-4. Odd/Even SCA Band Arrangement

Silicon PIN (SiPIN) detectors collect the data for the visible and near-infrared spectral bands (Bands 1 to 5 and 8). Mercury–Cadmium–Telluride (HgCdTe) detectors are used for the shortwave infrared bands (Bands 6, 7, and 9). An additional ‘blind’ band is shielded from incoming light and used to track small electronic drifts. There are 494 illuminated detectors per SCA, per band (988 for the Pan band); therefore, 70,672 operating detectors must be characterized and calibrated during nominal operations.

Data generated by OLI-2 are quantized to 14 bits, which improves the Signal-to-Noise Ratio (SNR) of transmitted OLI-2 data up to 25 percent at typical radiances, compared to L8’s 12-bit data transmission.

OLI-2 also contains internal calibration sources consisting of two solar diffusers, three pairs of stim lamps and a dark shutter to ensure radiometric accuracy and stability and has the ability to perform lunar calibrations.

3.3 Thermal Infrared Sensor 2 (TIRS-2)

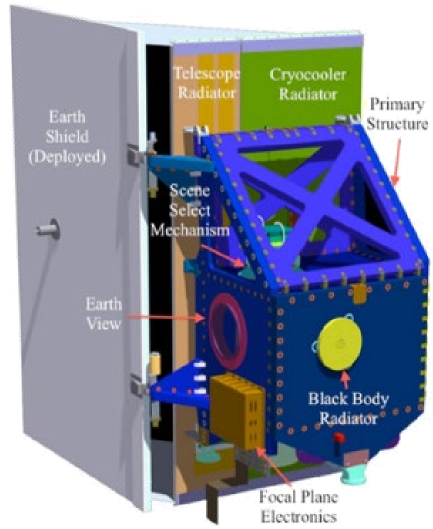

Figure 3-5. TIRS-2 Instrument with Earth shield Deployed

The TIRS-2 sensor has a 5-year design life and collects image data for two thermal bands with a 100 m spatial resolution over a 185-km swath.

TIRS-2 is a push-broom sensor employing a focal plane with long arrays of photosensitive detectors. TIRS-2 uses Quantum Well Infrared Photodetectors (QWIPs) to measure longwave thermal infrared energy emitted by the Earth's surface, the intensity of which is a function of surface temperature. The TIRS-2 QWIPs are sensitive to two thermal infrared wavelength bands, enabling separation of the temperature of the Earth's surface from that of the atmosphere. QWIPs' design operates on the complex principles of quantum mechanics. Gallium arsenide semiconductor chips trap electrons in an energy state 'well' until the electrons are elevated to a higher state by thermal infrared light of a certain wavelength. The elevated electrons create an electrical signal that can be read out, recorded, translated to physical units, and used to create a digital image.

The TIRS-2 instrument, while a rebuild of the L8 TIRS, has improvements that allowed the instrument to be upgraded from Risk Class C to a Risk Class B, which indicates that higher (5-year) reliability standards have been met. Stray light performance has also been improved through improved telescope baffling, and improvements were made to the position encoder for the Scene Select Mirror (SSM) to address problematic encoder behavior observed in L8 TIRS.

Like OLI-2, the TIRS-2 requirements also specify cross-track spectral uniformity; radiometric performance, including absolute calibration uncertainty, polarization sensitivity, and stability; ground sample distance and edge response; and image geometry and geolocation, including spectral band co-registration. The TIRS-2 prelaunch noise estimates are measured in terms of Noise Equivalent Change in Temperature (NEΔT) rather than the signal-to-noise ratios used for OLI-2 specifications (see Table 3-1). Final on-orbit results will be published and updated here in the future. The radiometric calibration uncertainty is specified to be less than 2 percent in terms of absolute, at-aperture spectral radiance for targets between 260 Kelvin (K) and 330 K (less than 4 percent for targets between 240 K and 260 K and for targets between 330 K and 360 K).

	NEΔT, 10.8 µm				NEΔT, 12.0 µm			
Source [K]	Mean	St.Dev.	Min	Max	Mean	St.Dev.	Min	Max
240	0.069	0.004	0.059	0.103	0.096	0.005	0.087	0.149
260	0.058	0.003	0.051	0.090	0.081	0.004	0.071	0.125
270	0.054	0.003	0.048	0.084	0.076	0.004	0.069	0.122
280	0.051	0.003	0.045	0.082	0.072	0.004	0.065	0.117
290	0.048	0.002	0.043	0.078	0.069	0.003	0.062	0.112
300	0.047	0.002	0.042	0.075	0.066	0.003	0.060	0.111
310	0.047	0.002	0.042	0.075	0.066	0.003	0.060	0.111
320	0.045	0.002	0.041	0.073	0.063	0.003	0.058	0.116
330	0.044	0.002	0.040	0.073	0.061	0.003	0.056	0.116
360	0.044	0.002	0.040	0.073	0.059	0.003	0.054	0.116

Table 3-1. TIRS-2 Noise Equivalent Change in Temperature (Prelaunch Measurements)

The TIRS-2 focal plane contains three identical SCAs, each with rows of QWIPs (Figure 3-6). The QWIP detectors sit between a ROIC and a two-band filter assembly. An additional masked or 'dark' band is used for calibration purposes. TIRS-2 has 640 illuminated detectors per SCA, with approximately 27-pixel overlap to ensure there are no spatial gaps. Each TIRS-2 SCA consists of a 640-column by 512-row grid of QWIP detectors. Almost all the detectors are obscured except for two slits that contain the spectral filters for the 12.0 µm and 10.8 µm bands. These filters provide unvignetted illumination for approximately 30 rows of detectors under each filtered region.

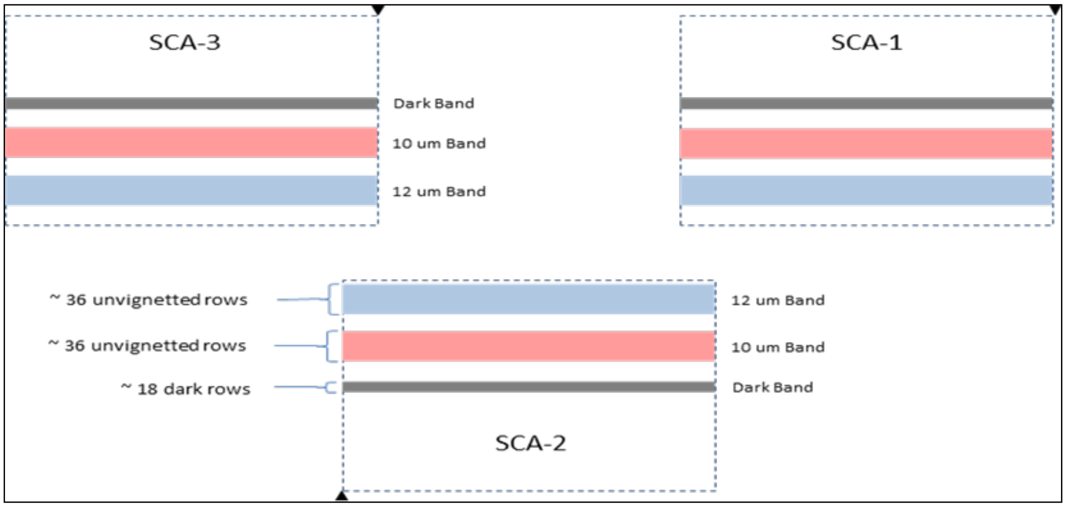

Figure 3-6. TIRS-2 Focal Plane

Thermal energy enters the TIRS-2 instrument through a scene select mirror and a series of four lenses before illuminating the QWIP detectors on the Focal Plane Array (FPA) (Figure 3-7). Two rows of detector data from each filtered region are collected, with pixels from the second row used only as substitutes for any inoperable or out-of-spec detectors in the primary row. The Calibration Parameter File (CPF) specifies these rows.

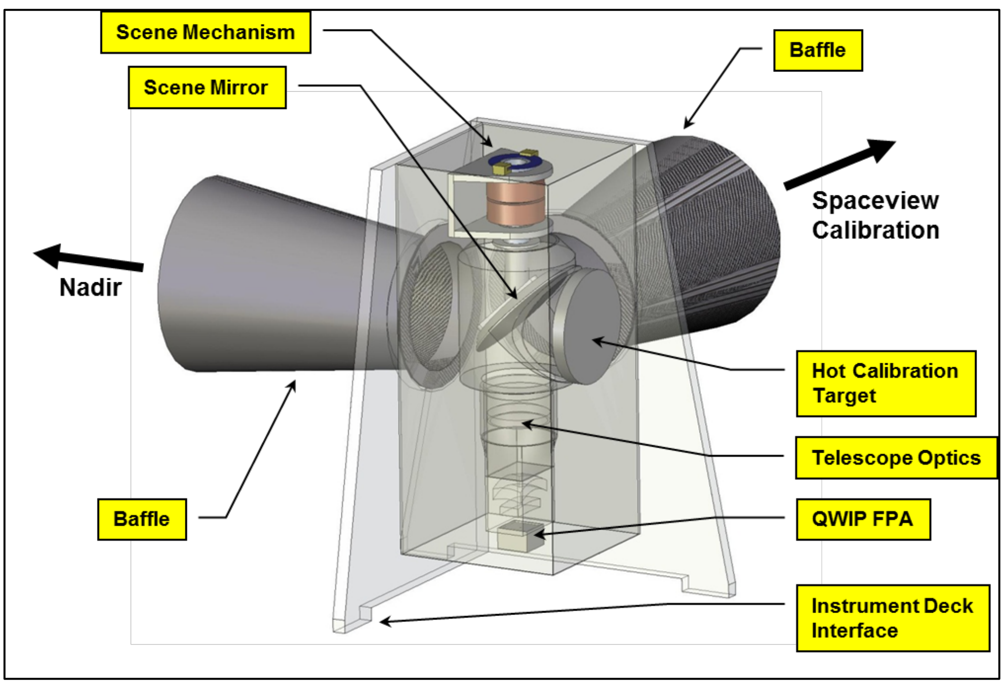

Figure 3-7. TIRS-2 Optical Sensor Unit

3.4 Spacecraft Overview

Northrop Grumman built the L9 spacecraft at its manufacturing facility in Gilbert, Arizona. Northrop Grumman is responsible for the design and fabrication of the L9 spacecraft bus, integration of the two sensors onto the bus, satellite level testing, on-orbit satellite checkout, and continuing on-orbit engineering support under GSFC contract management. The specified design life is 5 years, with an additional requirement to carry sufficient fuel to maintain the L9 orbit for 10 years. However, historically the operational lives of the Landsat sensors and spacecraft exceed the design lives and fuel should not limit extended operations.

The spacecraft supplies power, orbit and attitude control, communications, and data storage for OLI-2 and TIRS-2. The spacecraft consists of the mechanical subsystem (primary structure and deployable mechanisms), command and data handling subsystem, attitude control subsystem, electrical power subsystem, Radio Frequency (RF) communications subsystem, hydrazine propulsion subsystem, and thermal control subsystem. All the components, except for the propulsion module, are mounted on the exterior of the primary structure. A 9×0.4 m deployable sun-tracking solar array generates power that charges the spacecraft’s 125 amp-hour nickel–hydrogen (Ni–H2) battery. A 3.14-terabit solid-state data recorder provides data storage aboard the spacecraft, and an Earth-coverage X-Band antenna transmits data from the sensors either in real time or played back from the data recorder. The sensors are mounted on an optical bench at the forward end of the spacecraft. Fully assembled, the spacecraft, without the instruments, is approximately 3 m high and 2.4×2.4 m across, with a mass of 2071 kg fully loaded with fuel.

3.5 Spacecraft Data Flow Operations

The L9 Observatory receives a daily load of software commands transmitted from the ground. These command loads tell the Observatory when to capture, store, and transmit image data from the OLI-2 and TIRS-2. The daily command load covers the subsequent 72 hours of operations, with the commands for the overlapping 48 hours overwritten each day. This precaution is taken to ensure that sensor and spacecraft operations continue in the event of a one- or two-day failure to successfully transmit or receive commands. The Observatory's Payload Interface Electronics (PIE) ensures that image intervals are captured in accordance with the daily command loads. The OLI-2 and TIRS-2 are powered on continuously during nominal operations to maintain the thermal balance of the two instruments. The two sensors' detectors continuously produce signals that are digitized and sent to the PIE at an average rate of 265 megabits per second (Mbps) for the OLI-2 and 26.2 Mbps for TIRS-2.

Ancillary data, such as sensor and select spacecraft housekeeping telemetry, calibration data, and other data necessary for image processing, are also sent to the PIE. The PIE receives the OLI-2, TIRS-2, and ancillary data, merges these data into a Mission Data stream, identifies the Mission Data intervals scheduled for collection, and performs a lossless compression of the OLI-2 data (TIRS-2 data are not compressed) using the Rice algorithm (Rice et al., 1993). The PIE then sends the compressed OLI data and the uncompressed TIRS-2 data to the 3.14 terabit SSR. The PIE also identifies the image intervals scheduled for real-time transmission and sends those data directly to the Observatory's X-Band transmitter. The IC receiving stations only receive real-time transmissions, and the PIE also sends a copy of these data to the onboard SSR for playback and transmission to the L9 Ground Network Element (GNE) receiving stations (USGS captures all of the data transmitted to ICs). OLI-2 and TIRS-2 collect data coincidently; therefore, the Mission Data streaming from the PIE contain both OLI-2 and TIRS-2 data as well as ancillary data.

The Observatory broadcasts Mission Data files from its X-Band, Earth-coverage antenna. The transmitter sends data to the antenna on multiple virtual channels, providing for a total data rate of 384 Mbps. The Observatory transmits real-time data, SSR playback data, or both real-time data and SSR data, depending on the time of day and the Ground Stations within view of the satellite. Transmissions from the Earth coverage antenna allow a Ground Station to receive Mission Data as long as the Observatory is within view of the station antenna. OLI-2 and TIRS-2 collect the L9 science data. The spacecraft bus stores the OLI-2 and TIRS-2 data on an onboard SSR and then transmits the data to ground receiving stations.

Section 4 Instrument Calibration

Calibration and validation of the OLI-2 and TIRS-2 instruments are a key component of proper operations. Operational calibration sequences (shutter, lamp, blackbody, and deep space) and key calibration events (lunar and solar) offer a known source for calibration and on-orbit absolute radiance. These calibration data collections are performed at various frequencies to support the instrument calibration needs. Periodically, OLI-2 shutter and TIRS-2 deep space collects are acquired and used to determine bias values to apply to the imagery. A variety of other calibration types (lamp, integration time sweeps, etc.) occur less frequently and are used to validate the calibration of the instruments. The lunar calibration is nominally performed once every 28 days and solar calibration is performed approximately once per week (seven to nine days) for radiometric and geometric calibration of the instruments.

4.1 Radiometric Characterization and Calibration Overview

The L9 calibration activities begin early in the instrument development phases, continue through On-orbit Initialization and Verification (OIV), and go on continually throughout mission operations. This section describes the instrument calibration activities for the OLI-2 and TIRS-2 from development and preflight testing, through OIV, and into nominal mission operations, as this is how the verification of instrument performance requirements proceeded. Table 4-1 provides a summary of the various calibration measurements.

	Purpose	**How This is Used to Develop Calibration Parameters**
OLI-2 Preflight Activity		
Radiance of integrating sphere measured at multiple illumination levels	Establish linearity of detectors and focal plane electronics	Known radiance levels of the integrating sphere allow for linearity coefficients to be determined
Integration time sweeps of integrating sphere	Establish linearity of detectors and focal plane electronics	Known effective radiance levels allow for linearity coefficients to be determined and compared to multiple illumination levels of the integrating sphere; these measurements can be repeated on-orbit
Heliostat illumination of the solar diffusers	Derive a measure of the transmission of the heliostat and the reflectance of the solar diffuser panels	Verify effectiveness of the solar diffuser panels on-orbit
Measurement of the spectral reflectance of the solar diffuser panels	Determine in-band spectral reflectance of the solar diffuser panels	With the known spectral reflectance of the solar diffuser panels, coefficients are determined to convert the OLI-2 response, in DNs, to spectral reflectance

	Purpose	How This is Used to Develop Calibration Parameters
Measurement of the Bi-directional Reflectance Distribution Function (BRDF) of the solar diffuser panels	Determine the reflectance of the solar diffuser panels in on-orbit orientation	Determine the coefficients to convert the OLI-2 response to spectral reflectance
Transfer radiometer measurements of the integrating sphere and solar diffuser panels at the same illumination levels as measured by the OLI-2	Ensure traceability of the measurements compared to those made from the solar diffuser panels	Changes to the spectral response of the instrument are determined by inflight measurements of the solar diffuser panels, and coefficients used to scale the digital numbers of the instrument response to calibrated radiances can be adjusted
Measurement of in-band and out-of-band spectral response using Goddard Laser for Absolute Measurement of Radiance (GLAMR)	Spectral response requirements verification and the Relative Spectral Response (RSR) characterization	
SNR measured at multiple radiance levels from the integrating sphere (or solar diffuser panel)	Requirement verification and characterization of radiometric performance	
Wide-field collimator measurements of fixed geometric test patterns	To build an optical map of the detectors	Enables construction of a Line of Sight (LOS) model from the focal plane to the Earth
Wide-field collimator measurements of fixed geometric test patterns with different reticle plates	To derive line spread functions, edge response, and modulation transfer function	
TIRS-2 Preflight Activity		
Flood source-controlled heating of louvered plate	Temperatures across the surface of the plate are analyzed to characterize the uniformity of the radiometric response across the detectors within the focal plane and across the multiple SCAs	Known radiance levels of the flood source at different temperatures allow for linearity coefficients to be determined
Integration time sweeps of flood source	Establish linearity of detectors and focal plane electronics	Known effective radiance levels allow for linearity coefficient to be determined and compared to multiple flood source temperatures; these can be repeated on-orbit
A wide-field collimator and a set of fixed geometric patterns are scanned across the focal plane	To build an optical map of the detectors	Enables construction of a LOS model from the focal plane to the Earth
A wide-field collimator and a set of fixed geometric patterns are scanned across the focal plane at multiple temperature settings	To derive line spread functions, edge response, and modulation transfer function	

	Purpose	How This is Used to Develop Calibration Parameters
OLI-2 On-Orbit Activities		
Integration time sweeps of solar diffuser	Characterize detector linearity	Potentially update linearization coefficients
Integration time sweeps of stim lamps	Characterize detector linearity at low signals	Potentially update linearization coefficients
Solar diffuser collects	Noise characterization including SNR, absolute radiometric accuracy characterization, uniformity characterization, radiometric stability characterization, relative gain calibration, absolute calibration (both radiance and reflectance)	The known reflectance of the diffuser panel is used to derive updated relative and absolute calibration coefficients
Long dark collects	Radiometric stability and noise (impulse noise, white noise, coherent noise, and 1/f noise) characterization	
Extended solar diffuser collects	Monitor the detector stability (within-scene)	
Stimulation lamps data collects	Monitor the detector stability over days	
Side-slither maneuver	Characterize detector relative gains, in order to improve uniformity by reducing striping	Scanning the same target with detectors in line enables updated relative gains to be calculated
Focal Plane Module (FPM) overlap statistics	Normalize the gain of all the SCAs, to improve uniformity	Relative gain characterization
Cumulative histograms	Characterize striping in imagery	Relative gain characterization
Lunar data collection	Characterize stray light and characterize the absolute radiometric accuracy	
Characterization of Pseudo-Invariant Calibration Sites	Monitoring of temporal stability	Monitoring trends in Pseudo-Invariant Calibration Site (PICS) responses indicates a need for absolute radiometric calibration updates
OLI detector aging characterization	Characterize detector select map	Potentially update flight detector select map
TIRS-2 On-Orbit Activities		
Integration time sweeps with black body and deep space	Monitor linearity of detectors and focal plane electronics	Determine calibration need to update linearity coefficients
Varying black body temperature over multiple orbits	Characterize detector linearity	
Black body and deep space collects	Noise (Noise Equivalent Delta Radiance ((NEdL))	Relative gain characterization
Long collects (over ocean)	Coherent noise, 1/f	Relative gain characterization
Vicarious calibration		Absolute radiometric calibration

Table 4-1. Summary and Purpose of Calibration Activities Pertaining to CPFs

4.1.1 Description of Calibration Data Collections

A distinction is made between the calibration activities that measure, characterize, and evaluate instrument and system radiometric performance and those that are used to derive improved radiometric processing parameters contained in the L9 CPF for use by the Landsat Product Generation System (LPGS). The measurement and evaluation activities are referred to as characterization operations, while the parameter estimation activities are referred to as calibration. Although both types of activities contribute to the "radiometric calibration" of the L9 OLI-2 and TIRS-2 instruments, the remainder of this document uses the term "characterization" to refer to radiometric assessment and evaluation operations and the term "calibration" to refer to those associated with estimating radiometric processing parameters.

Shutter Collects

Shutter collects provide the individual detector dark levels or biases, which are subtracted during ground processing from each detector's response in Earth images. This removes variations in detector dark current levels, reducing striping and other detector-to-detector uniformity issues in the imagery. These normal shutter collects are acquired before daylight imaging begins and after daylight imaging ends. An extended shutter collect is acquired about every six months and is about 36 minutes in duration. These longer shutter collects provide a measure of stability over typical Earth imaging intervals.

Stimulation Lamp Collects

The stimulation lamps are used to monitor the detector stability over days. While incandescent lamps tend to be poor absolute calibration sources, they excel at showing changes in detector response over relatively short periods. Three sets of stimulation lamps get used at three different frequencies: daily, bimonthly, and every six months. These different usages enable differentiation between detector changes and lamp changes.

Solar Diffuser Collects

The solar diffuser panels provide reflective references that were characterized prior to launch. The regular use of the primary diffuser enables detector stability to be monitored and potential changes in calibration to be fed back into the ground processing system to maintain radiometric accuracy of the Earth imagery products. The second solar diffuser panel is used every six months as a check on stability of the primary (working) diffuser. Longer, 60-second collects of the working solar diffuser are used to monitor the within-scene detector response stability. Diffuser collects are also used to characterize the system noise, SNR performance, absolute radiometric accuracy, uniformity, and relative detector gains.

In an additional solar diffuser data collect, the integration time sweep, a series of collects at different detector integration times, is performed at a constant signal level. These collects allow an on-orbit assessment of the OLI detector electronics' linearity.

Lunar Collects
Imaging the Moon approximately every 28 days enables an independent measure of the OLI radiometric stability, as the Moon is an extremely stable source. While the lunar surface is very stable, the viewing geometry can vary dramatically, so the lunar irradiance-based model, Robotic Lunar Observatory, is used to consider the viewing geometry. The lunar collects are also used to evaluate stray light effects and to find any other artifacts that might be visible. The Moon is a good source for these artifacts because it is bright compared to the surrounding space.

Side Slither Collects
During a side slither data collect, the spacecraft is yawed 90 degrees, so that the normally cross-track direction of the focal plane is turned along track. Here, each detector in an SCA tracks over nearly identical spots on the ground. By performing these side slither maneuvers over uniform regions of the Earth, individual detector calibration coefficients can be generated to improve the pixel-to-pixel uniformity. These maneuvers are performed over desert or snow/ice regions about every three months to monitor and potentially improve the detector-to-detector uniformity.

Examples of characterization activities include assessments of the following:

- The detector's response to the solar diffusers and radiometric accuracy
- The 60-second radiometric stability, to evaluate the absolute radiometric uncertainty and detect changes in detector response
- The detector response to stimulation lamp, to evaluate and detect changes in gain
- Radiometric uniformity (Full Field of View (FOV), banding 1, banding 2, and streaking as defined in the OLI-2 Requirements Document), all artifacts affecting the radiometric accuracy of the data, and SCA discontinuity differences characterized by gathering statistics information in the overlap areas between the SCAs
- Deep space data and blackbody data to evaluate the absolute radiometric uncertainty of the TIRS-2 instrument and detect changes in gains and biases to determine radiometric stability
- Dropped frames per interval, for trending the total number detected, excluding flagged dropped frames in all characterization algorithms

Examples of calibration activities include derivation of the following:

- Bias model parameters for each detector. The bias model for OLI-2 is constructed using data from associated shutter images, video reference pixels, dark (masked) detectors, and associated telemetry (e.g., temperatures). The bias model for TIRS-2 uses data from deep space images, dark (masked) detectors, and associated telemetry (e.g., temperatures). These bias model coefficients are used to derive the bias that needs to be subtracted from the detector during product generation.

- The relative gains for all active detectors, to correct the detector responses for "striping" artifacts.
- Gain determination to enable the conversion from DN to radiance and determine the accuracy of the radiometric product.
- The TIRS-2 background response determination.

4.1.2 Prelaunch

OLI-2

Preflight instrument performance and data characterization proceeded from the subsystem level (e.g., focal plane module and electronics) to fully integrated instrument and Observatory testing and analysis. Instrument testing and performance requirements verification were performed at multiple stages of development to ensure the integrity of performance at the component, subsystem, and system levels.

For radiometric calibration of the OLI-2, an integrating sphere was used as the National Institute for Standards and Technology (NIST) traceable radiance source. The OLI-2 was connected to the integrating sphere in a configuration that enabled the instrument to measure the output radiances from a prescribed set of illumination levels from xenon and halogen lamps. In addition, integration time sweeps of full illumination at successively shorter detector exposure times were used to establish the linearity of the detectors and focal plane module electronics. Measurements of the integrating sphere at various radiance levels were also used to characterize the linearity. These and the integration time sweeps are used to determine the reciprocity between the two.

Ball, the manufacturer of the OLI-2, used a heliostat to facilitate the Sun as a calibration source for prelaunch testing. The heliostat captured and directed sunlight from the rooftop of the Ball facility to the solar diffuser panels of the instrument placed in a thermal vacuum chamber inside the facility.

The spectral reflectance and BRDF of the panels were characterized at the University of Arizona. A transfer spectroradiometer was used to measure the radiances from the integrating sphere and the solar diffuser panels at the same illumination levels as measured by the OLI-2 to ensure traceability of the measurements compared to those made from the solar diffuser panels. On orbit, any changes to the spectral response of the instrument are determined by inflight measurements of the solar diffuser panels, and coefficients are used to scale the DNs of the instrument response so calibrated radiances can be adjusted.

The SNR for each of the OLI-2 spectral bands is characterized at a prescribed radiance level, referred to as $L_{typical}$. The SNR is defined as the mean of the measured radiances divided by their standard deviation. A curve is fit to the SNR at the measured radiance levels and is evaluated at the prescribed $L_{typical}$. The SNR is measured at multiple stages of the instrument build, culminating the testing of the fully integrated instrument. The high SNR combined with the 14-bit quantization of the OLI-2 radiometric response provides data that enhance our ability to measure and monitor subtle changes in the state and condition of the Earth’s surface.

The prelaunch verification of instrument and spacecraft radiometric performance specifications was carried out as part of the instrument and spacecraft manufacturers' development, integration, and test programs. The radiometric characteristics of the OLI instrument were measured during instrument fabrication and testing at the Ball facility.

TIRS-2

The TIRS-2 instrument is a NASA in-house development, so prelaunch characterization and testing was carried out at the NASA GSFC. A louvered plate with stringently controlled heating was used as a flood source and placed within the TIRS-2 FOV so that temperatures across the surface of the plate could be analyzed to characterize the uniformity of the radiometric response across the detectors within the focal plane and across the multiple SCAs. The flood source was measured at multiple temperature levels and at multiple integration time sweeps, in order to characterize the linearity of the detector responses.

A blackbody of known temperature was used as a calibration source to provide radiance to the detectors from which output voltages were converted to DNs. TIRS-2 also measured a space-view port with a cold plate set at 170 K mounted on it, and the DNs output from the instrument were converted to radiance. The blackbody radiances were scaled by a "view factor" that was determined by viewing through the Earth-view (nadir) port.

Earth-view measurements were made at several temperature settings in order to establish a relationship among the temperature, DN levels, and radiance. These measurements were then combined with the blackbody and space-view measurements to derive a final set of coefficients for scaling DNs to radiances. Detector linearization was performed prior to the bias removal for TIRS-2 because temperature contributions from instrument components were also being captured.

Additional measurements and tests were performed at Northrop Grumman as the L9 spacecraft was being fabricated and integrated with the OLI-2 and TIRS-2 payloads.

4.1.3 Postlaunch

Radiometric characterization and calibration will be performed over the life of the mission using the software tools developed as part of the L9 Image Assessment System (IAS). The IAS provides the capability to perform radiometric characterization routinely, to verify and monitor system radiometric performance and estimate improved values for key radiometric calibration coefficients. On-orbit activities include those that occur during the OIV period characterization and calibration and post-OIV nominal operations.

Characterization activities include the following:

- Noise – characterizing the OLI-2 response to shutter, lamp, diffuser, and lunar acquisitions, and the TIRS-2 response to deep space views, On-Board Calibrator

(OBC) collects, and lunar acquisitions are used to assess various detector noise characteristics, including coherent, impulse, SNR, NEdL, and ghosting.
- Stability - characterizing the response of OLI-2 to the solar diffusers, stim lamps, and lunar acquisition, and TIRS-2 to the OBC for assessing the transfer-to-orbit response, the short-term (within-orbit) and long-term stability, diffuser and lunar acquisition reproducibility for OLI-2, and post-maneuver recovery reproducibility for TIRS-2.

Calibration activities include the following:

- Absolute Radiometric Response – characterizing the OLI-2 solar diffuser, lunar irradiance, TIRS-2 OBC, PICS, vicarious data collects, and underfly acquisitions with L8 to assess the absolute radiometric response and derive the initial on-orbit absolute gain CPF values. Appendix A includes scenes collected for Calibration and underfly activities.
- Relative Radiometric Response – characterizing the OLI-2 diffuser, yaw, and PICS and TIRS-2 OBC, yaw, and PICS sites for assessing the SCA-to-SCA and pixel-to-pixel relative response/uniformity. Special OLI-2 diffuser and TIRS-2 OBC integration time sweep collects are characterized to assess detector linearity and possible updates to the CPF linearity calibration coefficients.

Key radiometric CPF parameters that may need updates include absolute gains, relative gains, bias (default values), linearity Lookup Tables (LUTs), diffuser and/or lamp radiances and diffuser non-uniformity (OLI-2), OBC LUTs and/or non-uniformity (TIRS-2), inoperable detectors, out-of-spec detectors, and detector select masks.

4.1.4 Operational Radiometric Tasks

The goals of these tasks are as follows:

- To demonstrate that the L9 mission meets or exceeds all radiometric requirements, particularly those that were deferred for formal verification on-orbit
- To perform an initial on-orbit radiometric calibration (relative and absolute) that makes it possible to achieve the previous goal and prepares the mission for routine operations
- To trend radiometric characterization parameters throughout the mission

4.1.4.1 OLI-2 Characterization Tasks

Several OLI-2 characterizations and requirements verifications relate strictly to whether the instrument performance meets specifications, and therefore are not strongly tied to the coefficients stored in the CPF that require on-orbit updates. These requirements include stability (60-second, 16-day), noise (overall, impulse, coherent, 1/f), stray light, ghosting, bright target recovery, detector operability, and detectors out-of-specification.

Several lunar calibration acquisitions are made during the commissioning period; each acquisition comprises 15 individual image scans, performed over two consecutive orbits. Each OLI-2 and TIRS-2 SCA is scanned across the Moon, with one scan repeated in both orbits to provide a check on continuity of the observations. Lunar acquisitions are performed when the Earth-Sun-Moon configuration provides lunar phase angles in the degree ranges of -9 to -5 or +5 to +9. The Moon traverses each phase angle range once per month, with the positive and negative angle ranges occurring approximately one day apart. In routine operations, one phase angle range is selected for all lunar acquisitions; during commissioning, both cases are collected.

4.1.4.2 OLI-2 Calibration Tasks

The OLI-2 instrument was radiometrically calibrated before launch. The sensor viewed an integrating sphere monitored by a spectrometer that had been calibrated relative to a source that is traceable to a reference in the NIST Facility for Spectroradiometric Calibrations (FASCAL). The gains (DN/radiance) from this calibration were stored in the CPF. The sensor's response to the diffuser panels was measured using the Sun as the source through a heliostat. Using the OLI-2 gains, the radiance of the diffuser was measured and was corrected for the heliostat and the atmospheric transmittance to obtain a "predicted" Top of Atmosphere (TOA) radiance for the diffuser. Additionally, the sensor diffuser's directional reflectance factors for the on-orbit illumination and view geometries were measured in the laboratory before launch, giving the diffuser a reflectance calibration. These data were used to derive "prelaunch" TOA radiance calibration coefficients. The first on-orbit measurements of the solar diffuser panel were compared to the "predicted" and "prelaunch" values to perform the transfer to orbit analysis.

A fundamental requirement of the Landsat Project is to provide a record of consistently calibrated image data. Therefore, OLI-2 data need to be consistent with data from the previous Landsat sensors. Although the instruments are calibrated consistently before launch and monitored before launch through on-orbit commissioning, there is still a need to check the calibration relative to previous Landsat instruments and update the calibration parameters as necessary.

Procedures were developed to characterize any shift in calibration that may occur through launch and into orbit. Three methods of validating the absolute radiometric calibration include: (1) cross-calibration with L8 OLI via simultaneous observations, (2) vicarious calibration, and (3) use of the PICS.

Although one of the goals of the Ground System is to generate OLI-2 images as free of striping and banding as is practicable, it cannot be expected that images over uniform areas will be completely free of banding or striping, especially when extreme contrast stretches are applied. There are several contributors to banding and striping: inadequately characterized differential non-linear responses among detectors; inadequately characterized relative gain and bias parameters; instability in gain, bias, or non-linearity; and spectral differences across or between SCAs.

4.1.4.3 TIRS-2 Characterization Tasks

Several TIRS-2 characterizations and requirements verifications relate strictly to whether the instrument meets performance specifications, and therefore are not strongly tied to the coefficients stored in the CPF that require on-orbit updates. These requirements include stability (60 second, 16-day), noise (overall, impulse, coherent, 1/f), stray light, ghosting, bright target recovery, detector operability, and detectors out-of-specification.

Several lunar acquisitions are performed during the commissioning period. Each acquisition comprises 15 individual image scans, performed over two consecutive orbits. Each TIRS-2 SCA is scanned across the Moon, with one scan repeated in both orbits to provide a check on continuity of the observations. As with OLI-2, the TIRS-2 lunar acquisitions are performed when the Earth-Sun-Moon configuration provides lunar phase angles in the degree ranges of -9 to -5 or +5 to +9. During the operational mission lifetime, lunar acquisitions will be performed monthly as defined for the OLI-2.

4.1.4.4 TIRS-2 Calibration Tasks

TIRS-2 data need to be consistent with data from the previous sensors, so the sensor's data need to be cross-calibrated with L8 TIRS. At least two techniques will be used for this comparison and calibration (i.e., simultaneous data acquisitions collected during the underfly of L8 and non-simultaneous observation of well-characterized targets). TIRS-2 was carefully characterized and calibrated before launch, and procedures were developed to be able to characterize any shift in calibration that may occur during launch and insertion into orbit.

As with the OLI-2, several factors may contribute to banding and striping in TIRS-2 imagery: inadequately characterized differential non-linearity among detectors; inadequately characterized relative gain and bias; instability in gain, bias, or non-linearity; and spectral differences across or between SCAs.

4.2 Geometric Calibration Overview

This subsection describes the geometric characterization and calibration activities performed over the life of the L9 mission, using the software tools developed as part of the L9 IAS. The IAS provides the capability to perform four types of geometric characterization routinely to verify and monitor system geometric performance, and four types of geometric calibration to estimate improved values for key system geometric parameters. L9 IAS geometry algorithms use ten coordinate systems. These coordinate systems are referred to frequently in this document and are briefly defined in Appendix D.

These are the parameters contained in the CPF for use in the L1 product generation. The measurement and evaluation activities are referred to as characterization operations, while the parameter estimation activities are referred to as calibration.

The geometric characterizations include the following:

1. Assessment of the absolute and relative geodetic accuracy of L1 data (Geodetic Characterization)

2. Assessment of the geometric accuracy of L1 products (Geometric Characterization)
3. Assessment of the accuracy of multi-temporal OLI-2 image-to-image registration (Image-to-Image Registration Characterization)
4. Assessment the accuracy of OLI-2 and TIRS-2 band-to-band registration (Band-to-Band Registration Characterization)

A fifth characterization algorithm will be used to evaluate OLI-2 spatial performance on-orbit. This Modulation Transfer Function (MTF) bridge characterization algorithm uses images of selected ground targets (e.g., the Lake Pontchartrain Causeway) to estimate the OLI-2 sensor edge response.

The geometric calibrations include the following:

1. Determination of the alignment between the spacecraft navigation reference frame and the OLI-2 payload LOS (Sensor Alignment Calibration)
2. Determination of corrections to the prelaunch OLI-2 Pan band lines of sight, including relative alignment of the OLI-2 sensor chip assemblies (OLI-2 Focal Plane Calibration)
3. Determination of the alignment between the TIRS-2 and OLI-2 sensors, including the relative alignment of the TIRS-2 sensor chip assemblies (TIRS Alignment Calibration)
4. Determination of corrections to the band location field angles for both OLI-2 and TIRS-2 (Band Alignment Calibration)

The most critical geometric calibration activities are to measure and verify the L9 spacecraft, OLI-2, and TIRS-2 system performance using the geodetic, geometric, band-to-band, image-to-image, and spatial characterization capabilities; to monitor the OLI-2 sensor-to-spacecraft attitude control system alignment calibration; and to monitor the TIRS-2-to-OLI-2 alignment calibration. This includes verifying and, if necessary, updating the OLI-2 and TIRS-2 focal plane (SCA-to-SCA) and band alignment calibrations. Monitoring and refining the OLI-2-to-spacecraft and TIRS-2-to-OLI-2 alignment knowledge is critical to ensure that the L1 product accuracy specifications can be met. These calibration parameters were not expected to change greatly through launch, but they may require minor refinement on-orbit. The results of these calibration activities are used to verify that the system is performing within specifications and to create the CPFs used by the IAS and the LPGS to create L1 products that meet the L9 accuracy requirements. The calibration activities will continue throughout the life of the mission to monitor the stability of the system’s geometric and spatial performance and to identify and characterize any systematic variations in the system’s geometric parameters as a function of time, temperature, and location. A longer sequence of calibration observations over a range of conditions will be needed to isolate, model, and characterize these higher-order behaviors. Table 4-2 summarizes these activities, along with the prelaunch activities.

	Purpose	How This is Used to Develop Calibration Parameters
OLI-2 Preflight Activity		
Initial LOS directions for detectors using design locations	Establish nominal focal plane locations for individual detectors, bands, and SCAs	Gives nominal detector focal plane locations that can then be adjusted
Edge and line target analysis through thermal vacuum testing	Provide prelaunch adjustment to initial LOS of individual detectors	Allows refinement to initial LOS design model for detectors
TIRS-2 Preflight Activity		
Initial LOS directions for detectors using design locations	Establish nominal focal plane locations for individual detectors, bands, and SCAs	Gives nominal detector focal plane locations that can then be adjusted
Edge and line target analysis through thermal vacuum testing	Provide prelaunch adjustment to initial LOS of individual detectors	Allows refinement to initial LOS design model for detectors
OLI-2 On-Orbit Activities		
OLI Geodetic Accuracy Assessment	Ensure L1 Systematic imagery meets horizontal accuracy requirements and measures product accuracy prior to application of ground control	Folds into the OLI instrument to Attitude Control System alignment parameters
OLI-2 to Attitude Control System Alignment	Improves in-flight knowledge of OLI-2 to the Attitude Control System	OLI instrument to Attitude Control System alignment parameters
Geometric Accuracy Assessment	Evaluates the accuracy of the L1 Terrain-Precision corrected imagery and measures product accuracy after application of ground control	
Image-to-Image Registration Assessment	Ensures ability to co-register L1T imagery and measures OLI-2-to-OLI-2 and OLI-2-to-reference ability	
OLI-2 Focal Plane Calibration	Ensures accuracy between and within SCA geometry of the OLI-2 Pan imagery and corrects for SCA-to-SCA misalignment	Allows for adjustment to OLI-2 LOS parameters
Band-to-Band Registration Assessment	Measures the ability to align OLI-2 and TIRS-2 bands within a L1T image	Folds into the updating of the LOS parameters
Band Alignment Calibration	Adjusts OLI-2 LOS parameters based on band-to-band registration assessment	Allows for adjustment of the OLI-2 LOS parameters
OLI-2 Spatial Characterization	Characterizes OLI-2 system transfer function on orbit	
TIRS-2 On-Orbit Activities		
TIRS-2 Internal Geometric Characterization	Measures the ability to align the two TIRS-2 bands within a L1T	Folds into updating of the TIRS-2 LOS parameters
TIRS-2 Internal Geometric Calibration	Adjusts TIRS-2 LOS parameters based on TIRS-2 internal geometric characterization	Allows for adjustment of the TIRS-2 LOS parameters

	Purpose	How This is Used to Develop Calibration Parameters
TIRS-2 Alignment Calibration	Measures the ability to align 3 SCAs of TIRS-2 to the OLI-2 instrument	Allows for adjustment of TIRS-2 to OLI-2 alignment parameters

Table 4-2. Summary of Geometric Characterization and Calibration Activities

4.2.1 Collection Types

Lunar Collects

Due to differences in the viewing geometry between lunar collects and nominal Earth collects, lunar collects are used only for measuring the alignment of the cirrus band with the other OLI bands.

Earth Collects

Geometric characterization and calibration are performed on nominal nadir-viewing Earth collects. The major difference associated with these collects and the type of characterization or calibration that is performed depends on the reference imagery for which it is characterized, and in some cases, eventually calibrated against. Three types of reference imagery are used for geometric characterization and calibration, including the Global Land Survey (GLS), Digital Orthophoto Quadrangle (DOQ) mosaics, and Satellite Pour l'Observation de la Terre (SPOT) mosaics.

4.2.2 Prelaunch

OLI-2 Prelaunch

An initial OLI-2 geometric model that defined the LOS for the detectors on the focal plane was calculated using the nominal design locations of the detectors and telescope optical system. This initial or nominal design was then updated using edge and line targets that were projected on to the focal plane through the optical system during prelaunch thermal vacuum testing. This model was then considered an as-built prelaunch set of LOSs for each detector for which each band for each SCA could be adjusted postlaunch using the IAS geometric characterization and calibration processes.

A Horizontal Collimator Assembly (HCA) and a set of fixed geometric patterns are scanned across the focal plane to build an optical map of the detectors that enables construction of an LOS model from the focal plane to the Earth. A similar process is used with a different reticle plate to derive line spread functions. These measurements assist with characterizing the alignment of detectors within a given SCA as well as with aligning adjacent SCAs. These are fundamental parameters required for constructing the geometric models to achieve many of the geometric requirements.

A wide-field collimator and a set of fixed geometric patterns were scanned across the focal plane to build an optical map of the OLI-2 detectors that enabled construction of an LOS model from the focal plane to the Earth. Instead of these targets being viewed under fixed illumination settings, these targets were presented and contrasted by controlled temperature settings. These measurements assisted with characterizing the alignment of detectors within a given SCA as well as with aligning adjacent SCAs. These were fundamental parameters required for constructing the geometric models to achieve many of the geometric requirements

<u>TIRS-2 Prelaunch</u>
An initial TIRS-2 geometric model, consisting of a detector and sensor chip assembly within the focal plane along with the optics of the telescope, was determined based on its assembly through instrument and component design and final integration to the spacecraft. This included the focal plane and detector placement, the telescope and optical components, and the TIRS-2-to-spacecraft alignment measurements. These components were then updated during prelaunch using measurements taken during thermal vacuum testing. Targets were projected into the TIRS-2 FOV at operator-selectable locations, allowing for careful identification of both the target within the focal plane and the origination of the target itself. This model was then considered an as-built prelaunch set of LOSs for each detector for which each band for each SCA could be adjusted postlaunch using the IAS geometric characterization and calibration processes.

4.2.3 OLI-2 Geodetic Accuracy Assessment

The purpose of the geodetic accuracy assessment is to ensure that the L9 L0R data can be successfully processed into L1 systematic products that meet the system requirement of 65 meters at a circular error with 90 percent confidence (Circular Error 90 (CE90)) horizontal accuracy.

Predefined Ground Control Points (GCPs) (consisting of image chips with known geodetic positions) are automatically correlated with data from the OLI-2 SWIR1 or Pan bands (for DOQ control) to measure the discrepancy between the known ground location and the position predicted by the OLI-2 geometric model.

The results of the control point mensuration are used for analysis by the IAS geodetic characterization software. The precision-correction software also combines the estimated attitude error from the precision solution with the current best estimate of OLI-2-to-spacecraft alignment from the CPF, to compute the adjusted alignment that would make the resulting attitude error zero. This apparent alignment is stored in the geometric trending database for subsequent use by the sensor alignment calibration procedures.

The geodetic accuracy characterization software processes the control point residuals (deleting those identified as outliers) to generate summary statistics and a geodetic accuracy analysis report each time the precision correction solution process is successfully completed. The geodetic accuracy results are stored in the geometric characterization trending database, with a flag to indicate the control type used (GLS or DOQ).

4.2.4 OLI-2 Sensor Alignment Calibration

The goal of the sensor alignment calibration is to improve the in-flight knowledge of the relationship between the OLI-2 instrument and the spacecraft attitude control system reference frame. Sensor alignment calibration uses the results of the GCP processing conducted both as part of routine L1 product generation (using GLS control) and as part of calibration/validation analysis activities over geometric calibration sites (using DOQ control). The end-to-end OLI-2 geolocation accuracy error budget assumes that the IAS can estimate this alignment to an accuracy of 33 microradians (3-sigma) over periods as short as one 16-day WRS-2 cycle.

The potential need for sensor alignment calibration updates will be identified by monitoring the geodetic accuracy characterization results. If persistent geolocation accuracy biases are observed, then that would suggest the need for generating an updated sensor alignment matrix for inclusion in the CPF. Automated software tools are used to detect the existence of a new alignment calibration solution and to perform automated testing of the new and old calibration solutions against a set of test scenes extracted from the list of retrieved alignment calibration scenes. A new alignment matrix will be generated whenever a new version of the CPF is scheduled for release, nominally on a quarterly basis; therefore, any slowly varying seasonal alignment variations will be accounted for.

4.2.5 OLI-2 Geometric Accuracy Assessment

The purpose of the geometric accuracy assessment is to evaluate the accuracy of L1T image products using an independent set of GCPs. Although the geodetic accuracy characterization results report both the pre- and post-GCP correction scene accuracy statistics, the post-fit statistics are not an unbiased estimate of the actual accuracy of the corrected scene. An independent geometric accuracy assessment is performed by correlating the final L1 product with a separate set of GCPs that were withheld from the original precision correction solution. Scenes for which the number of available GCPs was too small to permit withholding some from the precision correction process do not have validation points. The geometric accuracy assessment procedure runs as a part of the standard L1 product generation flow.

4.2.6 OLI-2 Internal Geometric Characterization and Calibration

OLI-2 internal geometric accuracy refers to internal geometric distortions within the OLI-2 images due to errors in the relative alignment of the 14 SCAs, also known as Focal Plane Modules (FPMs), on the OLI-2 focal plane. If the OLI-2 LOS model knowledge of the pointing for each SCA is slightly inaccurate, this will result in internal geometric distortions in the L1T products and, potentially, visible image discontinuities at SCA boundaries. Although the OLI-2 LOS model is carefully characterized prelaunch, tools are available to detect and, if necessary, correct any SCA-to-SCA misalignment that may be observed by updating the OLI-2 LOS model calibration. These tools are implemented in the IAS as the image-to-image registration accuracy characterization and the OLI-2 focal plane calibration algorithms.

The OLI-2 Pan band is used as the geometric reference for the entire instrument.

The image-to-image registration accuracy and the pattern of registration errors may indicate the presence of unwanted internal distortions in the OLI-2 image that could be addressed by refining the OLI-2 focal plane calibration. The following subsections describe the details of the image-to-image registration assessment and OLI-2 focal plane calibration procedures individually.

4.2.6.1 OLI-2 Image-to-Image Registration Assessment

The goal of the image-to-image registration assessment is to verify the L9 requirement that multi-temporal images of the same WRS scene can be successfully co-registered to an accuracy of 0.4 Linear Error 90 Percent (LE90) multispectral pixels (i.e., 12 meters). The image-to-image assessment procedure uses GCPs that have been extracted from a previously generated L1 image, or that match the points used to correct the pre-existing L1 product, to perform precision and terrain correction of a new acquisition to Level 1. It then performs a point-by-point comparison of the two images using automated image correlation.

Image-to-image registration assessment using the Pan band demonstrates the accuracy of the overall precision correction solution as well as the internal geometric fidelity of the images.

4.2.6.2 OLI-2 Focal Plane Calibration

The OLI-2 focal plane calibration is intended to detect and measure systematic deviations of the OLI-2 LOS for each SCA from the model measured during prelaunch characterization. Any significant deviations detected will be folded back into the CPF as updates to the LOS model Legendre polynomial coefficients.

4.2.6.3 Band-to-Band Registration Assessment

The band-to-band registration assessment measures the relative alignment of the nine OLI-2 and two TIRS-2 spectral bands after processing to L1 to verify that the 4.5-m LE90 OLI-2, 18-m LE90 TIRS-2, and 30-meter LE90 OLI-2-to-TIRS-2 band-to-band registration requirements are met.

4.2.6.4 Band Alignment Calibration

The purpose of band placement calibration is to estimate improved values for the locations of the spectral bands on the OLI-2 and TIRS-2 focal planes for inclusion in the CPF. The band locations are embodied in the LOS model Legendre coefficients for each OLI-2 and TIRS-2 band/SCA. OLI-2 and TIRS-2 band alignment would use essentially the same algorithm but would process separately.

The Pan band is used as the reference for the OLI-2 solution because it is the band used to perform the sensor alignment and focal plane calibrations. TIRS-2 Band 10 is used as the reference for TIRS-2 band alignment since it is also used in TIRS-2 alignment calibration. The OLI-2 cirrus band is used only for lunar and high-altitude terrestrial targets.

4.2.7 TIRS-2 Internal Geometric Characterization and Calibration

The TIRS-2 geometric alignment calibration procedure accomplishes both internal and external geometric alignment calibration for the TIRS-2 instrument. TIRS-2 internal geometric accuracy can be degraded by internal geometric distortions within the TIRS-2 images due to errors in the relative alignment of the three SCAs on the TIRS-2 focal plane. If the TIRS-2 LOS model knowledge of the pointing for each SCA is slightly inaccurate, this will result in internal geometric distortions in the L1 product images and, potentially, visible image discontinuities at SCA boundaries.

TIRS-2 external geometric accuracy refers to the accuracy with which TIRS data can be registered to corresponding OLI-2 data and to an absolute ground coordinate system. This accuracy is dependent primarily on accurate knowledge of the alignment between the OLI-2 and TIRS-2 instruments.

The alignments of both the OLI-2 and TIRS-2 instruments relative to the spacecraft Attitude Control System (ACS) frame were measured during Observatory integration, but due to the accuracy limitations of these measurements and the likelihood of launch shift and zero-G release altering these alignments, on-orbit TIRS-2 alignment estimation was updated to achieve the TIRS-2 geometric accuracy requirements. Although the TIRS-2 LOS model was also carefully characterized prelaunch, TIRS-2 alignment calibration provides the tools needed to detect and, if necessary, correct any SCA-to-SCA misalignment that may be observed while updating the TIRS-2 LOS model calibration.

The TIRS-2 10.8-micron band (Band 10) is used as the geometric reference for aligning the TIRS-2 instrument to the OLI. Band 10 is also used as the reference band in TIRS-2 band alignment calibration. As the TIRS-2 geometric reference, internal SCA-to-SCA focal plane alignment is also performed using Band 10.

The following subsection describes the details of the TIRS-2 alignment calibration procedure.

4.2.7.1 TIRS-2 Alignment Calibration

The TIRS-2 alignment calibration measures systematic deviations of the TIRS-2 lines-of-sight for each SCA from the model measured during prelaunch characterization while simultaneously measuring the global misalignment of all three TIRS-2 SCAs relative to the OLI. These measurements are used to compute updates to the TIRS-2-to-OLI-2 and, indirectly, TIRS-2-to-ACS alignment matrices as well as updates to the TIRS-2 LOS model Legendre polynomial coefficients, with the results being folded back into the CPF.

A control reference image of coincident OLI-2 SWIR bands with good emissive-to-reflective band correlation is used for calibration. The TIRS-2 alignment calibration procedure compares a precision- and terrain-corrected TIRS-2 Band 10 SCA-separated image with a coincident OLI-2 SWIR1 band SCA-combined reference image processed with the same spacecraft geometric model and scene-framing parameters. This enables measurement of the overall TIRS-2-to-OLI alignment, as well as the relative alignment of the individual TIRS-2 SCAs.

4.2.8 OLI-2 Spatial Performance Characterization

OLI-2 spatial performance, expressed as the slope and width of the instrument's response to a unit edge/step function, was carefully characterized during prelaunch testing. The experience of the L7 ETM+, which suffered from gradually degrading spatial fidelity over the first several years of on-orbit operations, led to the development of an algorithm to measure and track on-orbit spatial performance. This was done by using long bridge targets to characterize the ETM+ MTF, which is the frequency domain representation of the instrument's spatial response. This algorithm was subsequently adapted for use with push-broom sensors using Earth Observing -1's Advanced Land Imager (ALI) data, and a variant of this adapted algorithm is used for OLI-2 spatial characterization. A method for using lunar scans to characterize ALI spatial performance was also developed, but the results were not sufficiently reliable for use in operational performance characterization.

No calibration activities are associated with spatial performance, although the OLI-2 does have ground-commandable focus mechanisms, and TIRS-2 focus can be adjusted by changing telescope temperatures. To support on-orbit focus verification, additional focus test sites have been identified to provide qualitative information about the state of OLI-2 and TIRS-2 focus during the commissioning period. These sites, listed in Appendix A, were selected to contain distinct targets that could be used for visual assessment as well as additional sites for quantitative analysis using the enhanced version of the spatial performance characterization algorithm. Combined with the quantitative results of the spatial performance characterization algorithm, visual inspection of the focus sites adds confidence that the OLI-2 and TIRS-2 are in proper focus. The derivation of any adjustments to the focus mechanism positions or TIRS-2 telescope temperatures that may be required to improve on-orbit spatial performance would require additional analysis that is beyond the scope of this algorithm.

4.2.8.1 OLI-2 Bridge Target MTF Estimation

The purpose of the OLI-2 bridge target MTF estimation procedure is to use OLI-2 acquisitions of prescribed bridge targets to derive on-orbit estimates of the OLI-2 System Transfer Function (STF) for each OLI-2 spectral band other than the cirrus band. The STF estimates are then used to compute the corresponding point spread function and edge response slope performance for each spectral band. The OLI-2 bridge target MTF estimation procedure applies a model of the OLI-2 spatial response (in the form of the system transfer function) to predefined models of two bridges, shown in Figure 4-1, in the Lake Pontchartrain, Louisiana area, to simulate the OLI-2's response to each bridge in the direction transverse to the bridge. Comparing these models to oversampled bridge profiles constructed from actual OLI-2 image data by interleaving samples from different points along the bridge allows for adjusted OLI-2 STF parameters to be estimated.

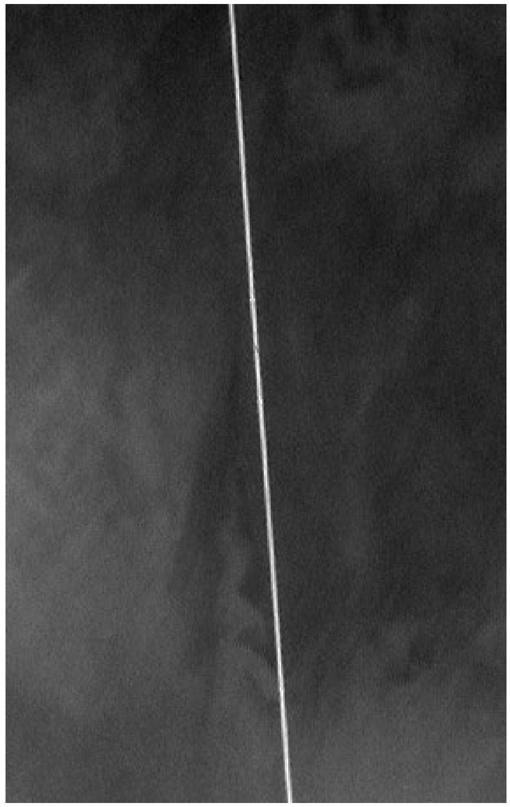

Figure 4-1. Simulated OLI-2 Image of the Lake Pontchartrain Causeway

4.2.9 Geometric Calibration Data Requirements

The geometric characterization and calibration operations require three primary types of supporting information: GCPs, reference images, and digital terrain data. The following subsections describe the required characteristics, potential sources, and preprocessing requirements for each of these support data types.

4.2.9.1 Ground Control Points (GCPs)

The IAS uses GCPs for all geometric characterization and calibration activities. In all cases, the GCPs are used to perform a precision correction solution that will ensure accurate registration of the image data to a cartographic projection and use digital elevation data to correct for relief displacement in the process. The IAS and LPGS both access a database of GCPs.

In 2020, the GCPs were updated for Landsat Collection 2 (C2) data processing. Landsat 8 Operational Land Imager (OLI) Ground Control Points (GCPs) were re-baselined to the European Space Agency Sentinel-2 Global Reference Image (GRI). This effort updated over 5.1 million GCPs as well as the extraction of 2.5 million new Landsat 8 GCPs globally for inclusion in Collection 2 L1 product generation. This update improved the per-pixel geodetic accuracy and interoperability of the global Landsat archive spatially, temporally, and with Sentinel-2. (Storey JC, Rengarajan R, Choate MJ. Bundle Adjustment Using Space-Based Triangulation Method for Improving the Landsat Global Ground Reference. *Remote Sensing*. 2019)

The GLS control database covers essentially every land scene observed from the WRS-2 orbit. The control derived from the GLS is accurate to approximately 20 meters Root Mean Square Error (RMSE) absolute, but since the goal is to make data products that are consistent with those generated from the archive of historical data, GLS GCPs include image chips extracted from the ETM+ Band 5 at 30-meter GSD. These have been automatically subdivided into separate CONTROL and VALIDATION subsets in scenes where a sufficient number of points were available.

The DOQ control database only covers scenes designated as geometric calibration sites. There are two main clusters of these sites. The first set is in the United States and was selected to provide at least one acquisition opportunity on every WRS-2 cycle day, including a group in the southwestern U.S. that is at approximately the same latitude to provide consistent acquisition conditions (position in orbit, ETM+ time-on). These contain control extracted from reduced-resolution DOQ data (panchromatic, 15-meter GSD). A second group of control scenes is in the eastern half of Australia. This control set is based on mosaics of SPOT panchromatic data provided by Geoscience Australia's National Earth Observation Group (NEOG). Being in the southern hemisphere, this set provides somewhat different orbital geometry and thermal conditions than the U.S. set. One of the primary purposes of the DOQ control set is to ensure accurate registration between L1T products and the DOQ- and SPOT-derived reference imagery used for focal plane calibration.

The original GLS control points were extracted from the GLS ETM+ images using an automated interest operator technique that selected points based on a local spatial operator that identified "interesting" points, and a spatial distribution test that decided which points provided the best distribution of control across the scene. A subsequent test was added to weed out points that contained only water. The GLS control has been in routine operational use for generating Landsat 5 and L7 standard L1T data products. An important note is that the GLS images themselves were generated based on a global block triangulation of L7 scenes with a sparse set of ground control provide by the National Geospatial Intelligence Agency (NGA). The scenes that contain NGA control are more accurate than those that were positioned solely through triangulation. The NGA-controlled scene subset will therefore be given special attention when mining the geodetic accuracy and sensor alignment data for systematic within-orbit effects.

The DOQ control points were extracted from the DOQ mosaic reference images (U.S. set) and the SPOT mosaic reference image (Australia). Therefore, they inherit the accuracy of those products. Because the primary purpose of these points is to ensure good OLI-to-reference image registration, the absolute accuracy of these points, though believed to be better than the GLS control, is of less interest.

4.2.9.2 Reference Images

Two types of reference images are used by the geometric super-site calibration operations described above. The first type includes previously generated L9 L1 products used in the image-to-image registration assessment process. These reference images were generated by processing L0R data through the IAS L1 processing software after launch and are not discussed further here. The second type of reference images were constructed prelaunch using a high-resolution image source. These images are used to provide the reference for OLI focal plane calibration as described above. These reference images are the subject of the remainder of this section.

The key characteristics of the focal plane calibration reference images are as follows:

1. High absolute geodetic accuracy (including removal of any terrain displacement effects)
2. Internal geometric integrity (no systematic internal distortions that could be confounded with OLI focal plane alignment effects)
3. Spectral similarity to the OLI Pan band
4. Resolution as good as or better than the OLI Pan band
5. Availability in areas of minimal seasonal change and low average cloud cover

Geodetic accuracy of one-half of a panchromatic pixel (7.5 meters) should be sufficient, although higher accuracy is desirable. The internal geometric accuracy requirement disqualifies ETM+ data as a source of reference imagery, although in an emergency, ETM+ reference data (e.g., GLS) would be better than no data.

High-resolution panchromatic imagery from aerial photographs that meet the geodetic accuracy requirement have been available for years. Panchromatic satellite imagery is available from SPOT and several high-resolution commercial missions, but the cost associated with acquiring the volume of data required to cover a Landsat scene has limited the application of these sources to a set of sites in Australia where Geoscience Australia's NEOG have provided full WRS-2 scene SPOT data coverage.

The preferred source of high-resolution reference imagery based on availability and cost are the DOQ produced under contract to the USGS. The DOQs are created by digitizing and orthorectifying panchromatic aerial photography. The DOQ products are distributed as 3.75 arc-minute quarter quads at 1-meter resolution. The DOQ geodetic accuracy is specified to meet National Map Accuracy Standards (NMAS) for 1:24,000-scale maps. This standard calls for a Circular Error (CE) of 40 feet at the 90 percent confidence level, which converts to approximately 6 meters CE one sigma and meets the one-half OLI pixel requirement. DOQ data coverage has improved since the launch of L7, to the point where it is now possible to generate a DOQ reference image nearly everywhere in the conterminous U.S. Though still time-consuming to construct, this has made it possible to assemble sufficient DOQ reference sites to provide at least one acquisition opportunity on every WRS-2 cycle day.

SPOT data, though not quite as accurate as the DOQ data, are available globally. The primary drawback of using SPOT data is the cost. Fortunately, our colleagues at Geoscience Australia were good enough to provide several Landsat scene-sized mosaics of SPOT data in Australia for use in Landsat 5 and 7 bumper-mode calibrations. These reference images will continue to be used for OLI focal plane calibration, though they can be expected to become less useful over time as the imagery becomes outdated.

4.2.9.3 Terrain Data

Digital terrain data are needed to provide the elevation information used by the IAS and LPGS in the L1 terrain-correction process. Terrain-corrected images are used in all geometric calibration operations described in the previous subsections. The elevation information must completely cover the geometric calibration sites to support the terrain-correction process. The height values must be referenced to the World Geodetic System 1984 (WGS84) ellipsoid rather than mean sea level to be consistent with the ground control height values. Vertical accuracy better than 15 meters (one sigma) is desirable. This keeps terrain-induced errors below 0.1 panchromatic pixels at the edges of the OLI-2 FOV. An accuracy of 30 meters (one sigma) is acceptable. For product generation purposes, it is also desirable that the elevation data used be consistent with the GLS 2000 reference dataset. The Digital Elevation Model (DEM) data used to generate the GLS datasets meet these requirements.

Assembling a global elevation dataset suitable for generating a global Landsat image base was a primary objective of the GeoCover (which evolved into the Global Land Survey) project. This resulted in a global DEM constructed from the best available source data, including the USGS Natural Elevation Data (NED) DEM data, the Canadian Digital Elevation Dataset (CDED), the NASA/NGA Shuttle Radar Topography Mission (SRTM) data, and NGA Digital Terrain Elevation Data (DTED) products. The GLS DEM provides a globally (mostly) consistent elevation dataset that corresponds to the GLS imagery that defines the L9 geometric reference. Tools were developed to retrieve any specified land area from the global DEM, so the elevation datasets required to process any given scene (nadir-viewing or off-nadir) are extracted and assembled on demand from the GLS archive. The digital terrain data for the desired output product area are extracted from the GLS DEM archive, as noted above, and then preprocessed into the output space used for the calibration test scene. This DEM resampling step is part of the normal L1 processing sequence.

4.3 Calibration Parameters

The Calibration and Validation Team (CVT) is responsible for the sustained radiometric and geometric calibration of the L9 satellite and the TIRS-2 and OLI-2 sensors. To achieve this, the team assesses new imagery daily, performs both radiometric and geometric calibration when needed, and develops new processing parameters for creating L1 products. Processing parameters are stored in the CPF, the Response Linearity Look-Up Table (RLUT), and the Bias Parameter File (BPF), which are stamped with effectivity dates and bundled with L0R products.

4.3.1 Calibration Parameter File

The CVT updates the CPF at least every three months. Updates were more frequent during early orbit checkout and will occur between the regular three-month cycles whenever necessary. Irregular updates will not affect the regular schedule. The timed release of a new CPF must be maintained because of the Universal Time Code (UTC)

Corrected (UT1) time corrections and pole wander predictions included in the file. These parameters span 180 days and include approximately 45 days before and 45 days after the effective start date of each CPF. The IAS maintains an archive of CPFs, which can be accessed at https://www.usgs.gov/landsat-missions/calibration-validation.

The CPF is time-stamped with an effective date range. The parameters in the file—Effective_Date_Begin and Effective_Date_End—designate the range of valid acquisition dates and are in YYYY-MM-DDThh:mm:ss format (ISO 8601). The parameter file used in processing an image requires an effective date range that includes the acquisition date of the ordered image.

Through the course of the mission, a serial collection of CPFs is generated and made available for download. CPFs are replaced when improved calibration parameters for a given period are developed. The need for unique file sequence numbers becomes necessary as file contents change. Version numbers for all effective date ranges after the launch begin with 01.

Table 4-3 shows the CPF file naming convention.

LCNNCPF_YYYYMMDD_yyyymmdd_cc.nn	
L	Constant for Landsat
C	Sensor (C = combined for OLI-2 and TIRS-2)
NN	Satellite numerical representation (09 = Landsat 9)
CPF	Three-letter CPF designator
YYYY	Four-digit effective starting year
MM	Two-digit effective starting month
DD	Two-digit effective starting day
yyyy	Four-digit effective ending year
mm	Two-digit effective ending month
dd	Two-digit effective ending day
cc	Collection number (“02” = Collection 2)
nn	Version number for this file (starts with 00)

Table 4-3. Calibration Parameter File Naming Convention

Refer to LSDS-1834 Landsat 8-9 OLI/TIRS Calibration Parameter File (CPF) Data Format Control Book (DFCB) for more details about the CPF parameter descriptions.

4.3.2 Response Linearization Lookup Table (RLUT) File

The RLUT file provides the parameters used to linearize the detector response for the OLI-2 and TIRS-2 instruments. Multiple methods of linearizing the response are supported. The parameters are organized into groups of detectors for each band/SCA. The file is very large and stored in Hierarchical Data Format (HDF). This document provides a high-level overview of how the RLUT is applied to linearize the detector response, but for full details, refer to the Calibration and Validation (Cal/Val) Algorithm Description Document (ADD).

Each RLUT file covers an effective date range. The parameters in the file, “Effective Begin Date” and “Effective End Date”, designate the range of valid acquisition dates and are in YYYY-MM-DDThh:mm:ss format (ISO 8601). The parameter file used in processing an image should have an effective date range that includes the acquisition date of the ordered image. The detector linearity is not expected to change often; therefore, the effective date range is typically very large.

Throughout the mission, the file change history is maintained by means of effective begin and end dates plus the assignment of a version number to deal with changes that occur during the effective date period.

The file name contains the file identifier, sensor identifier, satellite number, effective date range, and version number. Table 4-4 shows the RLUT file naming convention.

LCNNRLUT_YYYYMMDD_yyyymmdd_CC_NN.h5	
L	Constant representing Landsat
C	Sensor (C = Combined OLI and TIRS)
NN	Satellite numerical representation (“09” = Landsat 9)
RLUT	Response Linearization Look Up Table
YYYY	Four-digit effective starting year
MM	Two-digit effective starting month
DD	Two-digit effective starting day
yyyy	Four-digit effective ending year
mm	Two-digit effective ending month
dd	Two-digit effective ending day
cc	Collection number (“02”)
nn	Version number for this file (“stars with 00”)
h5	HDF file extension

Table 4-4. Response Linearization Lookup Table File Naming Convention

Refer to LSDS-1834 Landsat 8-9 OLI/TIRS Calibration Parameter File (CPF) Data Format Control Book (DFCB) for more information about how RLUT files are updated.

4.3.3 Bias Parameter Files

Bias Parameter Files (BPFs) are used by the IAS and LPGS in L1 processing. BPFs are created both for the OLI-2 sensor, and the TIRS-2 sensor.

The nominal OLI-2 / TIRS-2 acquisition sequence occurs in the following order:

- TIRS-2 deep-space collect
- OLI shutter collect

- Earth image / calibration collect(s)
- OLI-2 shutter collect
- TIRS-2 deep-space collect

The OLI-2 bias model calibration algorithm generates a BPF when a normal shutter collect is received. The effective date range of the new BPF spans the period between the acquisition date of the previous closest-in-time shutter collect and the acquisition date of the newly received shutter collect. It applies to the Earth image / calibration data collect(s) acquired within that effective date range.

Similarly, the TIRS-2 bias model calibration algorithm generates a BPF when a normal deep-space collect is received. The effective date range of the new BPF spans the period between the acquisition date of the previous closest-in-time deep-space collect and the acquisition date of the newly received deep-space collect. It applies to the Earth image / calibration data collect(s) acquired within that effective date range.

The OLI-2 shutter and TIRS-2 deep-space collects are not always collected in the sequence shown. There are times when only the OLI-2 shutter or TIRS-2 deep-space collects are obtained.

The file name contains the file identifier, sensor, effective date range, and version number. Table 4-5 shows the BPF naming convention.

LCNNBPFYYYYMMDDHHMMSS_yyyymmddhhmmss.nn	
L	Constant representing Landsat
C	Sensor (O for OLI or T for TIRS)
NN	Satellite numerical representation (09 = Landsat 9)
BPF	Bias Parameter File
YYYY	Four-digit effective starting year
MM	Two-digit effective starting month
DD	Two-digit effective starting day
HH	Two-digit effective starting hours
MM	Two-digit effective starting minutes
SS	Two-digit effective starting seconds
yyyy	Four-digit effective ending year
mm	Two-digit effective ending month
dd	Two-digit effective ending day
hh	Two-digit effective ending hours
mm	Two-digit effective ending minutes
ss	Two-digit effective ending seconds
nn	Version Number for this file (starts with 01)

Table 4-5. Bias Parameter File Naming Convention

Refer to LSDS-1835 Landsat 8-9 OLI/TIRS BIAS Parameter File (BPF) Data Format Control Book (DFCB) for more technical information about BPFs.

Section 5 Level 1 Products

5.1 Level 1 Product Generation

The LPGS generates standard L1 data products, which include a 16-bit Quality Band (QB) and an angle coefficient file for distribution. Along with the L1 product, the LPGS also generates a Full-Resolution Browse (FRB) and an 8-bit Quality Image. The LPGS uses the same algorithms to generate L1 products that the IAS uses within its L1 processor. This method allows the LPGS to provide identically calculated characterization data to the IAS for trending and analysis.

Level 1 Precision Terrain (Corrected) (L1TP) product — Includes radiometric, geometric, and precision correction, and uses a DEM to correct parallax errors due to local topographic relief; the accuracy of the precision/terrain-corrected product depends on the availability of GCPs, as well as the resolution of the best available DEM.

Level 1 Systematic Terrain (Corrected) (L1GT) product — Includes radiometric and geometric corrections, and uses a DEM to correct parallax error due to local topographic relief; the accuracy of the terrain-corrected product depends on the resolution of the best available DEM.

The geometric algorithms used by LPGS at EROS were originally developed for the L8 IAS. The overall purpose of the IAS geometric algorithms is to use Earth ellipsoid and terrain surface information in conjunction with spacecraft ephemeris and attitude data, in addition to knowledge of the OLI-2 and TIRS-2 instruments and L9 satellite geometry, to relate locations in image space (band, detector, sample) to geodetic object space (latitude, longitude, and elevation). These algorithms are used to create accurate L1 output products, characterize the sensors' absolute and relative geometric accuracy, and derive improved estimates of geometric calibration parameters, such as the sensor to spacecraft alignment.

5.1.1 Level 1 Processing System

The L1 processing algorithms include the following:

- Ancillary data processing
- Radiometric processing
- L9 sensor/platform geometric model creation
- Sensor LOS generation and projection
- Output space / input space correction grid generation
- Systematic, terrain-corrected image resampling
- Geometric model precision correction using ground control
- Precision, terrain-corrected image resampling

The LPGS is composed of seven major Subsystems: Process Control Subsystem (PCS), Data Management Subsystem (DMS), Radiometric Processing Subsystem (RPS), Geometric Processing Subsystem (GPS), Quality Assessment Subsystem

(QAS), Landsat Level 2 Processing Subsystem (L2PS), and User Interface (UI). The following describes the purpose and function of each major LPGS subsystem.

- PCS – Controls work order scheduling and processing. The PCS manages and monitor LPGS resources and provides processing status in response to operator requests.
- DMS – Provides data management services for the LPGS and handles the external interfaces for the system. It provides tools for formatting and packaging products. The DMS also maintains LPGS disk space and populates temporary storage with data from ingested files.
- RPS – Converts the brightness of the L0R image pixels to absolute radiance in preparation for geometric correction. The RPS performs radiometric characterization of L0R images by locating radiometric artifacts in images. The RPS provides the results of characterizations performed to the IAS characterization database. The RPS uses applicable algorithms to correct radiometric artifacts and convert the image to radiance.
- GPS –The GPS provides the results of characterizations performed to the IAS characterization database. The GPS processes the satellite ancillary data, generates a line-of-sight model, prepares a resampling grid, and resamples the data to create an L1GT or L1T product. The GPS performs sophisticated satellite geometric correction to create the image according the map projection and orientation specified for the L1 standard product. A terrain occlusion mask is also created for L8-9 products.
- QAS – Performs cloud cover assessment and generates the product quality band. For L1-7 products, QAS applications also perform automated quality checking of the L1R and L1G images.
- L2PS – Performs L2 processing, including calculations of TOA reflectance, surface reflectance, brightness temperature, and surface temperature. It also creates the L2 product.
- UI – Provides the Graphical User Interface (GUI) for the LPGS operator and the Anomaly Analysis Subsystem (AAS). It allows the operator to monitor the status of work orders and track processing anomalies.

Figure 5-1 shows the LPGS multi-mission Standard Level 1 Product Data Flow, which includes radiometric and geometric processing for all Landsat data; some items may not apply to L9.

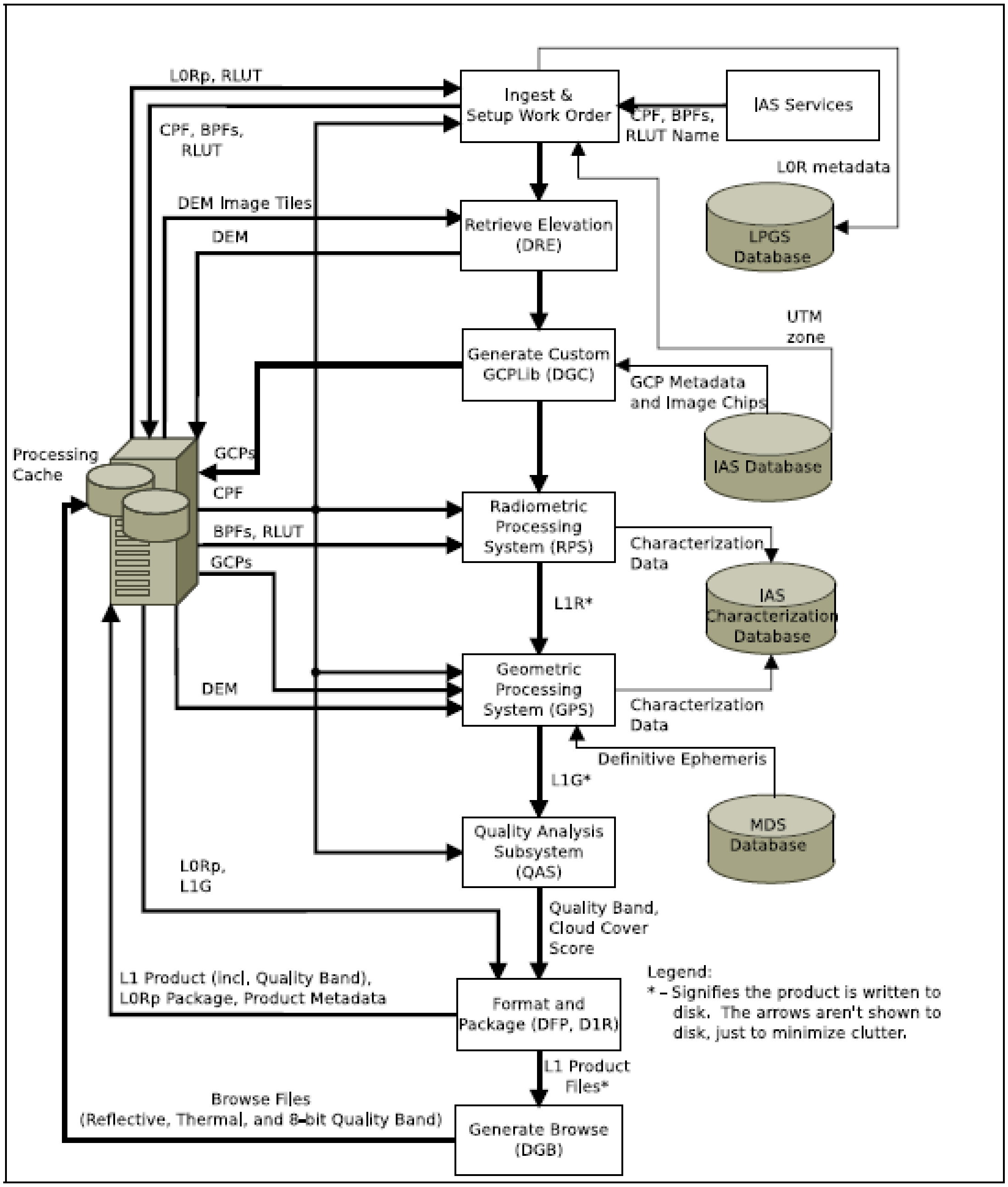

Figure 5-1. LPGS Multi-mission Level 1 Product Creation Data Flow Diagram

5.1.2 Ancillary Data

The L9 OLI-2 and TIRS-2 geometric correction algorithms are applied to the wideband (data contained in Level 0R (raw) or 1R (radiometrically corrected)) products. Some of these algorithms also require additional ancillary input datasets. These include the following:

- Ancillary data from the spacecraft and Scalable Inertial Reference Unit (SIRU) provides attitude information for the spacecraft.

- Ground control / reference images for geometric test sites - used in precision correction, geodetic accuracy assessment, and geometric calibration algorithms.
- Digital elevation data for geometric test sites - used in terrain correction and geometric calibration.
- Prelaunch ground calibration results, including band/detector placement and timing, and attitude sensor characteristics.
- Earth parameters, including static Earth model parameters (e.g., ellipsoid axes, gravity constants) and dynamic Earth model parameters (e.g., polar wander offsets, UT1-UTC time corrections) - used in systematic model creation and incorporated into the CPF.

5.1.3 Cloud Cover Assessment (CCA)

The L9 CCA system uses the C Function of Mask (CFMask) algorithm to identify fill, cloud, cloud confidence, and cloud shadow in Landsat 9 scenes for representation in the QA band as bit-mapped values. CFMask derives from the Function of Mask (FMask), an algorithm written at Boston University.

CFMask is a multi-pass algorithm that uses decision trees to prospectively label pixels in the scene; it then validates or discards those labels according to scene-wide statistics. It also creates a cloud shadow mask by iteratively estimating cloud heights and projecting them onto the ground.

Users should be aware that, like other cloud algorithms, CFMask may have difficulties over bright targets, such as building tops, beaches, snow/ice, sand dunes, and salt lakes. Optically, thin clouds will always be challenging to identify and have a higher probability of being omitted by the algorithm. In addition, the algorithm performance has only been validated for cloud detection, and to a lesser extent for cloud shadows. No rigorous evaluation of the snow/ice detection has been performed.

NOTE: Comparison of the various cloud detection algorithms used for Landsat data products has been performed. (Foga, S.) Landsat CCA validation data can be accessed from the Landsat Cloud Cover Assessment Validation Datasets webpage.

5.2 Level 1 Data Products

About 750 Landsat 9 scenes are imaged globally each day and archived at the USGS EROS Landsat Archive. L9 data are processed to a L1 standard scene product and made available for download at no cost to users. Each L1 scene is 190 km x 180 km, and each scene has a small overlap with the previous and following scene within the WRS-2 path it is collected. Figure 5-2 displays the dimensions for a single Landsat L1 scene.

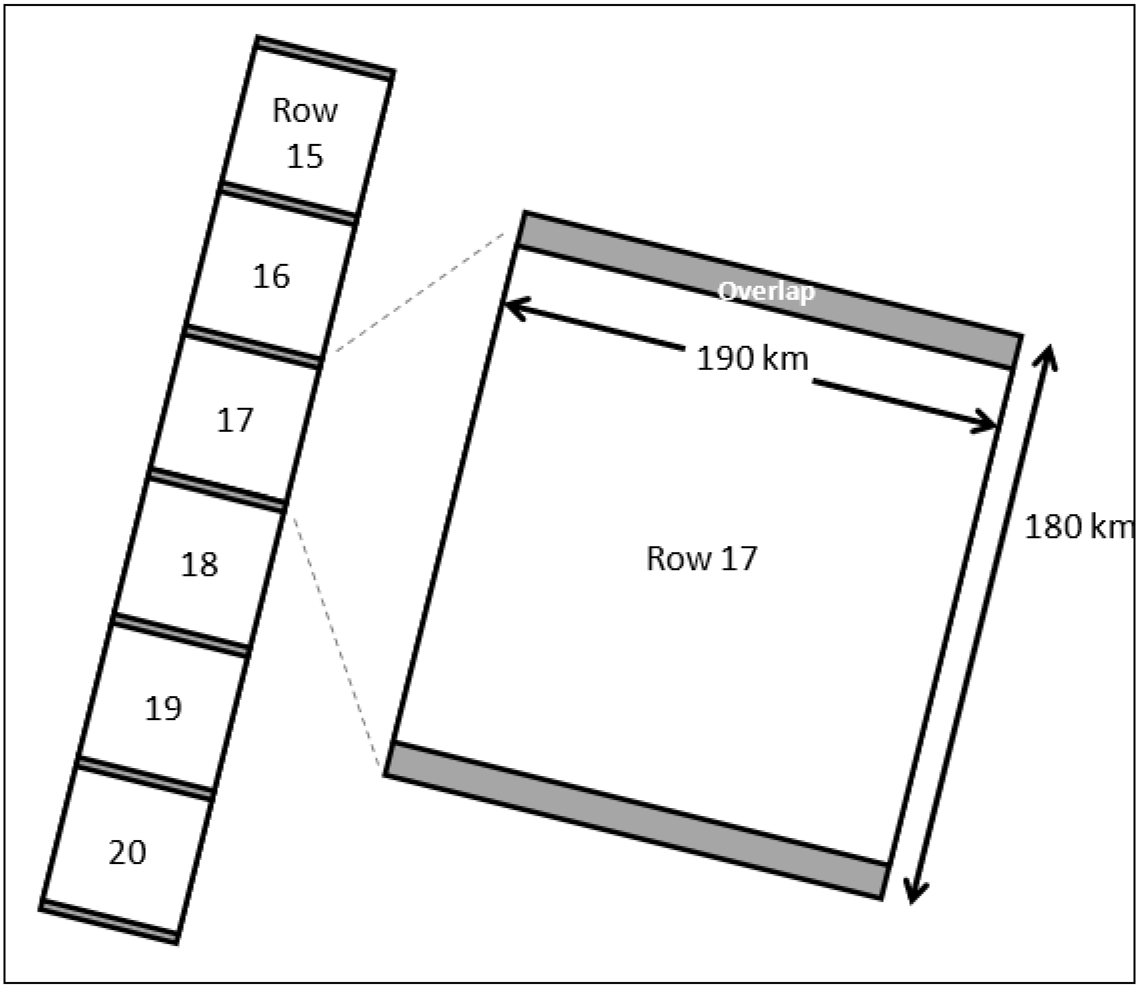

Figure 5-2. Level 1 Product Ground Swath and Scene Size

L9 L1 data are geometrically and radiometrically corrected, using inputs from each sensor and the spacecraft, as well as the applied GCPs and DEMs. The result is a geometrically rectified product free from distortions related to the sensor (e.g., view angle effects), satellite (e.g., attitude deviations from nominal), and Earth (e.g., rotation, curvature, relief). The image is also radiometrically corrected to remove relative detector differences, dark current bias, and some artifacts.

L9 L1 data are Digital Number (DN) products in an unsigned 16-bit integer format and can be converted to TOA reflectance (Bands 1–9) or radiance (Bands 1–11) using scaling factors provided in the product metadata. Refer to LSDS-1747 Landsat 8-9 Calibration and Validation (Cal/Val) Algorithm Description Document (ADD) for a description of the radiance calculations, reflectance calculations, and rescaling procedures used during processing. Refer to LSDS-1834 Landsat 8-9 Operational Land Imager (OLI) – Thermal Infrared Sensor (TIRS) Calibration Parameter File (CPF) Data Format Control Book (DFCB) for definitions of the reflectance conversion and the rescaling values used to process the L1 products. CPFs used to process specific scenes can be accessed on https://www.usgs.gov/landsat-missions/landsat-calibration-parameter-files.

5.2.1 Level 1 Output Product Format

L9 L1 data are delivered in a Cloud Optimized Georeferenced (COG) Tagged Image File Format. COGs are an extension of the current Geographic Tagged Image File Format (GeoTIFF) file format which improves access to Geospatial datasets in a cloud-based environment by allowing users to request only the bands that they need. Refer to LSDS-1388 Landsat Cloud Optimized GeoTIFF (COG) Data Format Control Book (DFCB) to learn more about the COG format.

In addition to COG format, the data incorporate cubic convolution (cc) resampling, North-up (Map) image orientation, and Universal Transverse Mercator (UTM) map projection (Polar Stereographic projection is used for scenes with a center latitude greater than or equal to -63.0 degrees) using the WGS84 datum.

5.2.2 Level 1 Output Product Files

Each L9 L1 scene contains a grayscale image file for each band (9 for OLI-2 and 2 for TIRS-2), along with two QA bands, 2 metadata files, and 5 files related to Angle Coefficients. Table 5-1 lists the L9 L1 output product files.

Landsat 9 Level 1 Product Files
L1GT/L1TP image files (11 total, one for each band)
QA_PIXEL file
QA_RADSAT file
L1GT/L1TP ODL (MTL) metadata file
L1GT/L1TP XML metadata file
Sun Azimuth Angle file
Sun Zenith Angle file
View (sensor) Azimuth Angle file
View (sensor) Zenith Angle file
Angle coefficient file

Table 5-1. L9 Level 1 Product Files

Each L9 L1 scene is named with a unique Product Identifier that includes the data processing level, Path/Row, acquisition, and data processing dates, as well as which Landsat Collections tier the data are processed are listed in Table 5-2.

LCNN_LLLL_PPPRRR_YYYYMMDD_yyyymmdd_CC_TX	
L	Landsat
C	Sensor (“C” = OLI/TIRS combined, “O” = OLI-only, “T” = TIRS-only)
NN	Satellite (“09” = Landsat 9)
LLLL	Processing correction level (L1TP/L1GT)
PPP	WRS path
RRR	WRS row
YYYYMMDD	Acquisition year (YYYY)/Month(MM)/Day(DD)
yyyymmdd	Processing year (yyyy)/ Month (mm)/ Day (dd)
CC	Collection number (02)
TX	Collection category (“T1” = Tier 1, “T2” = Tier 2)
Example:	**LC09_L1TP_029030_20190729_20200827_02_T1**

Table 5-2. Landsat 9 Level 1 Product Identifier

The Landsat Product ID displayed in Table 5-2 is the first part of the file name of the L1 product that is downloaded; the file type and extension components of the file name are described in Table 5-3. Example file names are shown in Section 5.2.3.

Identifier	Description
FT	File type, where FT equals one of the following: image band file number (B1–B11), VAA (Band 4 View (sensor) Azimuth Angle), VZA (Band 4 View (sensor) Zenith Angle), SAA (Band 4 Solar Azimuth Angle), SZA (Band 4 Solar Zenith Angle), MTL (metadata file), QA_PIXEL (QA Pixel-level Band file), QA_RADSAT (QA Radiometric Saturation and Terrain Occlusion Band), MD5 (checksum file), ANG (angle coefficient file)
ext	File extension, where .TIF equals COG file extension, .xml equals XML extension (metadata), and .txt equals text extension

Table 5-3. Landsat 9 File Types and Extensions

5.2.3 Example Level 1 File Names

Image Files

LC09_L1TP_097018_20211118_20211118_02_T2_B1.TIF
LC09_L1TP_097018_20211118_20211118_02_T2_B2.TIF
LC09_L1TP_097018_20211118_20211118_02_T2_B3.TIF
LC09_L1TP_097018_20211118_20211118_02_T2_B4.TIF
LC09_L1TP_097018_20211118_20211118_02_T2_B5.TIF
LC09_L1TP_097018_20211118_20211118_02_T2_B6.TIF
LC09_L1TP_097018_20211118_20211118_02_T2_B7.TIF
LC09_L1TP_097018_20211118_20211118_02_T2_B8.TIF
LC09_L1TP_097018_20211118_20211118_02_T2_B9.TIF
LC09_L1TP_097018_20211118_20211118_02_T2_B10.TIF

LC09_L1TP_097018_20211118_20211118_02_T2_B11.TIF

Band 4 Angle Files
LC09_L1TP_097018_20211118_20211118_02_T2_SAA.TIF
LC09_L1TP_097018_20211118_20211118_02_T2_SZA.TIF
LC09_L1TP_097018_20211118_20211118_02_T2_VAA.TIF
LC09_L1TP_097018_20211118_20211118_02_T2_VZA.TIF

Pixel QA Band
LC09_L1TP_097018_20211118_20211118_02_T2_QA_PIXEL.TIF

Radiometric Saturation and Terrain Occlusion QA Band
LC09_L1TP_097018_20211118_20211118_02_T2_QA_RADSAT.TIF

Metadata
LC09_L1TP_097018_20211118_20211118_02_T2_MTL.txt
LC09_L1TP_097018_20211118_20211118_02_T2_MTL.xml

Angle Coefficient File
LC09_L1TP_097018_20211118_20211118_02_T2_ANG.txt

Checksum
LC09_L1TP_097018_20211118_20211118_02_T2_MD5.txt

Table 5-4 displays the bands of the L9 OLI-2 and TIRS-2 instruments and provides the wavelength range for each. These wavelength ranges are visualized in Figure 1-2.

Band Number	Band Description	Band Range (nm)
OLI-2 Sensors		
1	Coastal Aerosol	435-451
2	Blue	452-512
3	Green	533-590
4	Red	636-673
5	Near-Infrared (NIR)	851-879
6	Short Wavelength Infrared (SWIR) 1	1566-1651
7	SWIR 2	2107-2294
8	Panchromatic	503-676
9	Cirrus	1363-1384
TIRS-2 Sensors		
10	Thermal Infrared Sensor 1	10600-11190
11	Thermal Infrared Sensor 2	11500-12510

Table 5-4. Landsat 9 OLI-2 and TIRS-2 Bands

Refer to LSDS-1822 Landsat 8-9 OLI/TIRS Collection 2 Level 1 Data Format Control Book (DFCB) for details about L9 L1 specifications (Data Type, Units, Fill Values and Value Ranges).

5.2.4 Level 1 Quality Assessment Bands

Landsat 9 L1 products include two Quality Assessment bands: The Quality Assessment Pixel-level Band (QA_PIXEL) and the Quality Assessment Radiometric Saturation and Terrain Occlusion Band (QA_RADSAT). Refer to LSDS-1822 Landsat 8-9 OLI/TIRS Collection 2 Level 1 Data Format Control Book (DFCB) for details about L9 QA band specifications (Data Type, Units, and Range Values).

5.2.4.1 Quality Assessment Pixel-level Band (QA_PIXEL)

The output from the CFMask algorithm is used as an input for the QA Application, which calculates values for all fields in the QA band file. The QA band file contains quality statistics gathered from the cloud mask and statistics information for the scene.

The QA band file is an unsigned 16-bit COG image with the same dimensions as the L1 scene. Refer to LSDS-1388 Landsat Cloud Optimized GeoTIFF (COG) Data Format Control Book (DFCB) for more details on COG.

For some artifacts, bits that are distinguishable at the L1 stage of processing are allocated. Bit 0 is the least significant. As several pixel quality classification types exist, a range of confidence levels is provided for each classification type. A 3x3 pixel window is used for setting cloud dilation. Table 5-5 shows the bits being set to artifact mapping.

Bit	Flag Description	Values
0	Fill	0 for image data 1 for fill data
1	Dilated Cloud	0 for cloud is not dilated or no cloud 1 for cloud dilation
2	Cirrus	0 for Cirrus Confidence: no confidence level set or Low Confidence 1 for high confidence cirrus
3	Cloud	0 for cloud confidence is not high 1 for high confidence cloud
4	Cloud Shadow	0 for Cloud Shadow Confidence is not high 1 for high confidence cloud shadow
5	Snow	0 for Snow/Ice Confidence is not high 1 for high confidence snow cover
6	Clear	0 if Cloud or Dilated Cloud bits are set 1 if Cloud and Dilated Cloud bits are not set
7	Water	0 for land or cloud 1 for water

Bit	Flag Description	Values
8-9	Cloud Confidence	00 for no confidence level set 01 Low confidence 10 Medium confidence 11 High confidence
10-11	Cloud Shadow Confidence	00 for no confidence level set 01 Low confidence 10 Reserved 11 High confidence
12-13	Snow/Ice Confidence	00 for no confidence level set 01 Low confidence 10 Reserved 11 High confidence
14-15	Cirrus Confidence	00 for no confidence level set 01 Low confidence 10 Reserved 11 High confidence

Table 5-5. Quality Assessment Pixel-Level Band Bit Description

5.2.4.2 Radiometric Saturation and Terrain Occlusion QA Band File

The radiometric saturation QA band indicates which sensor band(s) are saturated. Radiometric saturation is not common for OLI-2; it typically happens because of clouds and bright targets. While the TIRS-2 sensor is not usually affected by radiometric saturation, however volcanos and fires can saturate the sensor.

Radiometric saturation can occur under two situations:

1. When processed L1 product's saturated pixels have the maximum unsigned 16-bit value of 65535
2. When a sensor is saturated during data capture

The terrain occlusion bit is set when the desired terrain is not visible from the sensor due to intervening terrain. Table 5-6 shows which bits are for band data saturation and which bit is for terrain occlusion.

Bit	Flag Description	Values
0	Band 1 Data Saturation	0 no saturation 1 saturated data
1	Band 2 Data Saturation	0 no saturation 1 saturated data
2	Band 3 Data Saturation	0 no saturation 1 saturated data
3	Band 4 Data Saturation	0 no saturation 1 saturated data
4	Band 5 Data Saturation	0 no saturation 1 saturated data
5	Band 6 Data Saturation	0 no saturation 1 saturated data
6	Band 7 Data Saturation	0 no saturation 1 saturated data
7	Unused	0 not checked
8	Band 9 Data Saturation	0 no saturation 1 saturated data
9	Unused	0
10	Unused	0
11	Terrain occlusion	0 no terrain occlusion 1 terrain occlusion
12	Unused	0
13	Unused	0
14	Unused	0
15	Unused	0

Table 5-6. Radiometric Saturation and Terrain Occlusion QA Band Bit Description

5.2.5 Angle Coefficient File

L9 L1 products include an angle coefficient file (ANG.txt). This file contains coefficients that are used in the calculation of per-pixel solar (sun) and sensor (satellite, view) azimuth and zenith values. The ANG.txt file is used as input into tools that allow users to generate sensor and sun viewing angles, which are described in Section 5.2.6.

5.2.6 Solar Illumination and Sensor Viewing Angle Coefficient Files

L9 L1 products include Band 4 angle bands, which are used in conjunction with the pixel values for each of the Landsat bands in the L1 product. All the angle band files have units of hundredths of degrees.

Zenith and azimuth angles for solar illumination are calculated, and each is output to a separate band file. Zenith and azimuth angles for sensor viewing are also calculated, each is output to a separate band file. Table 5-7 displays the angle band files. Visit https://www.usgs.gov/landsat-missions/solar-illumination-and-sensor-viewing-angle-coefficient-files for technical details in utilizing these files.

File Abbreviation	File Description
SAA	Solar Azimuth Angle
SZA	Solar Zenith Angle
VAA	Sensor Azimuth Angle
VZA	Sensor Zenith Angle

Table 5-7. Solar Illumination and Sensor Viewing Angle Files

5.2.7 Level 1 Metadata Files

The L1 metadata files are created during product generation and contain information regarding the product ordered. The XML metadata file and ODL (MTL) metadata file have comparable fields. The LANDSAT_METADATA_FILE group for ODL is synonymous to the root element LANDSAT_METADATA_FILE for XML. The LANDSAT_METADATA_FILE group for ODL contains nested groups, synonymously, the LANDSAT_METADATA_FILE root element for XML has child elements. In the XML metadata file, the ODL parameter name is used in the start-tag and end-tag for elements. All parameters listed in the metadata file using ODL format are also in a separate metadata file using the XML format.

The XML metadata file and ODL metadata file have some contrasts. The ODL file distinguishes between strings and numerical values through the presence or absence of quotes around a value. The XML file does not make that distinction. The ODL file has an END statement signifying the end of the file. The XML file does not have a comparable entity.

An example of an ODL file is listed in Appendix B. An example of an XML file is listed in Appendix C.

5.2.8 Checksum File

A single checksum file is created for all the files in the product. The checksum file contains a Message-Digest Algorithm 5 (MD5) checksum for every file. The file is in plain text format and contains the output from md5sum for each file. The checksum file is not distributed with the final product.

Refer to LSDS-1822 Landsat 8-9 OLI/TIRS Collection 2 Level 1 Data Format Control Book for more information about L9 L1 products.

Section 6 Level 2 Products

6.1 Level 2 Product Generation

The Landsat Product Generation System (LPGS) generates standard L2 data products. Figure 6-1 shows the LPGS L2 Product Data Flow.

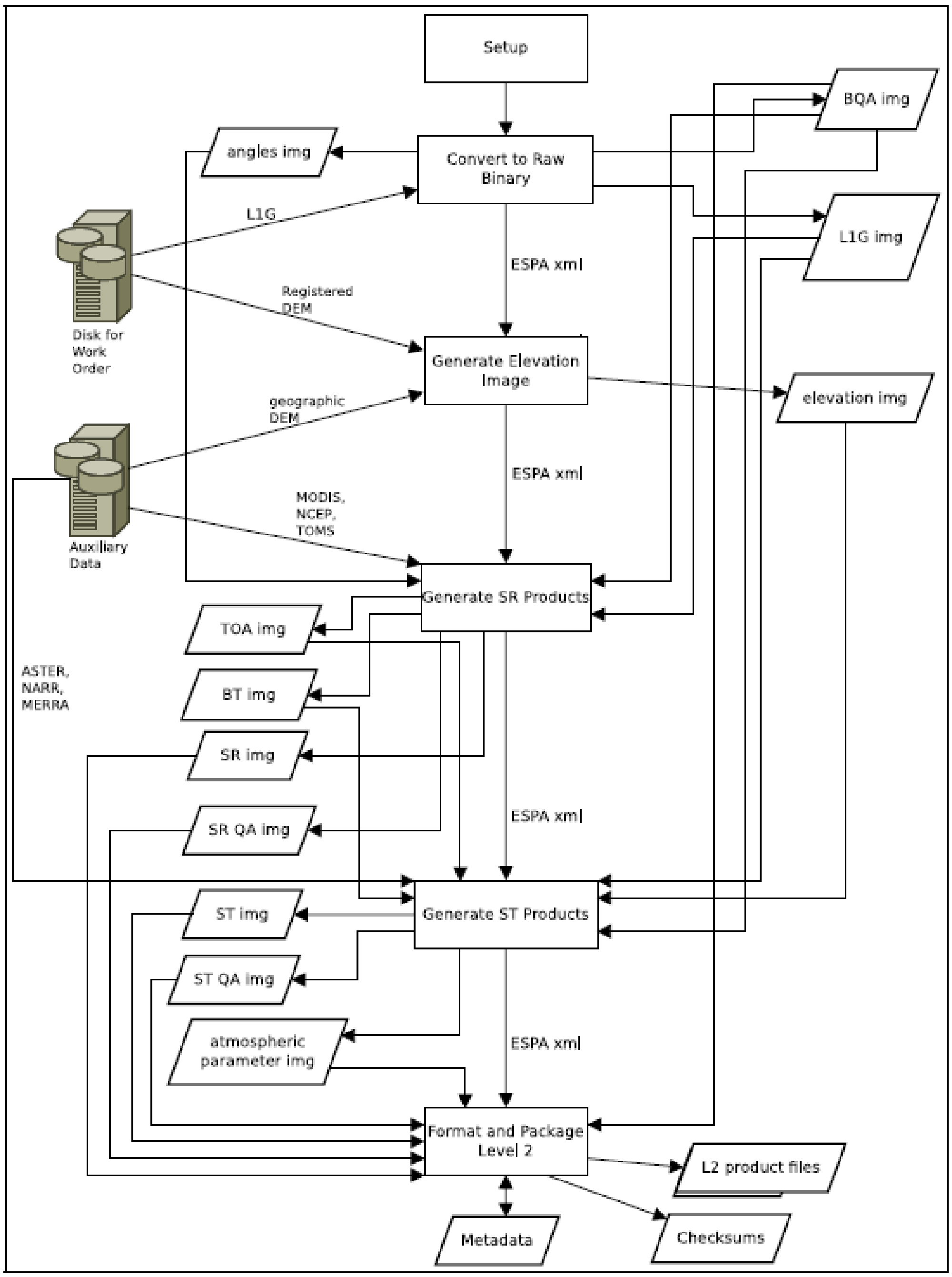

Figure 6-1. LPGS Level 2 Product Creation Data Flow Diagram

6.2 Level 2 Products

Landsat 9 L2 Science Products (L2SP) include Surface Reflectance (SR) and Surface Temperature (ST) data, along with intermediate bands, an angle coefficients file, and Quality Assessment (QA) Bands. (In cases where no ST can be created, an SR-only product is made - L2SR). L2SP are created by correcting a L1 Systematic Terrain (Corrected) (L1GT) or L1 Precision Terrain (Corrected) (L1TP) product for atmospheric effects.

The standard L2SP is a Digital Number (DN) product stored in a 16-bit unsigned integer format. Refer to LSDS-1747 Landsat 8-9 Calibration and Validation (Cal/Val) Algorithm Description Document (ADD) for a description of the atmospheric auxiliary data preprocessing, the SR algorithm, and the Single Channel algorithm for ST. SR bands approximate what a field spectroradiometer sensor held just above the Earth's surface would measure. The ST band provides the temperature of the Earth's surface in Kelvin (K). Refer to LSDS-1328 Landsat 8-9 OLI/TIRS Collection 2 Level 2 Data Format Control Book (DFCB) for more details about the calculation of SR and ST for inclusion into L2SP.

6.2.1 Level 2 Output Product Format

L2 data products are atmospherically corrected, and each image band in the L2SP is in a separate file. Each band is a grayscale COG file, which contains unsigned 16-bit integers. L2 products retain the processing qualities of the L1 data used to create them: CC resampling, North-up (Map) image orientation, and Universal Transverse Mercator (UTM) map projection (Polar Stereographic projection is used for scenes with a center latitude greater than or equal to -63.0 degrees) using the WGS84 datum.

6.2.2 Level 2 Output Files

Each L9 L2 product contains the SR, and where possible, the ST data files. (When ST cannot be processed, the SR product is delivered with its angle coefficients file, and SR specific QA bands). Table 6-1 lists the L9 L2 output product files.

Landsat 9 Level 2 Product Files
L2SP/L2SR image files
ST Intermediate Band files
QA_PIXEL file
QA_RADSAT file
SR_QA_AEROSOL file
ST_QA file
Angle Coefficient file
L2SP/L2SR metadata files

Table 6-1. L9 Level 2 Product Files

Each L9 L2 product is named with a unique Product Identifier that includes the L2 processing level, Path/Row, acquisition, and data processing dates, as well as which Landsat Collections tier the data are processed are listed in Table 6-2.

Landsat 9 Level 2 Product Identifier	
	LCNN_LLLL_PPPRRR_YYYYMMDD_yyyymmdd_CC_TX
Identifier	**Description**
L	Landsat
C	Indicates which sensor collected data for this product “C” = Combined OLI-2/TIRS-2
NN	Landsat satellite (“09” = Landsat 9)
LLLL	Processing level (L2SP, L2SR)
PPP	WRS-2 path
RRR	WRS-2 row
YYYYMMDD	Acquisition year (YYYY)/month(MM)/day(DD)
yyyymmdd	Processing year (yyyy/month(mm)/day(dd)
CC	Collection number (“02”)
TX	Collection category: "T1" for Tier 1, "T2" for Tier 2
Example:	**LC09_L2SP_029030_20190729_20200827_02_T1**

Table 6-2. L9 Level 2 Product Identifier

The Landsat Product ID described in Table 6-2 is the first part of the file name; the file type and extension components of the file name are described in Table 6-3. Example file names are shown in Section 6.2.3.

Landsat 9 File Types and Extensions	
Identifier	**Description**
FT	File type, where FT equals one of the following: MTL (metadata file), MD5 (checksum file), (SR_B1-7) (Surface Reflectance Bands), (ST_B10) (Surface Temperature Band), SR_QA_AEROSOL (Aerosol retrieval per pixel), QA_PIXEL (Quality Assessment Pixel-level Band), QA_RADSAT (QA Radiometric Saturation and Terrain Occlusion Band), ST_QA (Surface Temperature QA), ST_TRAD (Thermal band converted to radiance), ST_URAD (Upwelled Radiance), ST_DRAD (Downwelled Radiance), ST_ATRAN (Atmospheric Transmittance), ST_EMIS (Emissivity estimated from ASTER GED Band 10), ST_EMSD (Emissivity standard deviation), ST_CDIST (Pixel distance to cloud), ANG (angle coefficient file)
.ext	File extension, where .TIF equals COG file extension, .xml equals XML extension (metadata), and .txt equals text extension

Table 6-3. L9 Level 2 File Types and Extensions

6.2.3 Example L2 File Names

SR Image Files
LC09_L2TP_097018_20211118_20211118_02_T2_SR_B1.TIF
LC09_L2TP_097018_20211118_20211118_02_T2_SR_B2.TIF
LC09_L2TP_097018_20211118_20211118_02_T2_SR_B3.TIF
LC09_L2TP_097018_20211118_20211118_02_T2_SR_B4.TIF
LC09_L2TP_097018_20211118_20211118_02_T2_SR_B5.TIF
LC09_L2TP_097018_20211118_20211118_02_T2_SR_B6.TIF
LC09_L2TP_097018_20211118_20211118_02_T2_SR_B7.TIF

ST Image Files
LC09_L2TP_097018_20211118_20211118_02_T2_ST_B10.TIF

QA Band
LC09_L2TP_097018_20211118_20211118_02_T2_QA_PIXEL.TIF

Radiometric Saturation and Terrain Occlusion QA Band
LC09_L2TP_097018_20211118_20211118_02_T2_QA_RADSAT.TIF

SR Aerosol QA
LC09_L2TP_097018_20211118_20211118_02_T2_SR_QA_AEROSOL.TIF

ST QA
LC09_L2TP_097018_20211118_20211118_02_T2_ST_QA.TIF

Metadata
LC09_L2TP_097018_20211118_20211118_02_T2_MTL.txt
LC09_L2TP_097018_20211118_20211118_02_T2_MTL.xml

Angle Coefficient File
LC09_L2TP_097018_20211118_20211118_02_T2_ANG.txt

ST Intermediate Band Files
LC09_L2TP_097018_20211118_20211118_02_T2_ST_TRAD.TIF
LC09_L2TP_097018_20211118_20211118_02_T2_ST_URAD.TIF
LC09_L2TP_097018_20211118_20211118_02_T2_ST_DRAD.TIF
LC09_L2TP_097018_20211118_20211118_02_T2_ST_ATRAN.TIF
LC09_L2TP_097018_20211118_20211118_02_T2_ST_EMIS.TIF
LC09_L2TP_097018_20211118_20211118_02_T2_ST_EMSD.TIF
LC09_L2TP_097018_20211118_20211118_02_T2_ST_CDIST.TIF

Checksum
LC09_L2TP_097018_20211118_20211118_02_T2_MD5.txt

Refer to LSDS-1328 Landsat 8-9 OLI/TIRS Collection 2 Level 2 Data Format Control Book (DFCB) for details about L9 L2 SR and ST data specifications (Data Type, Units, Fill Values and Value Ranges).

6.2.4 Surface Temperature Intermediate Bands

Seven ST intermediate bands are included in the L2SP when the Single Channel algorithm is used to generate ST:

- **Atmospheric Transmittance layer (ATRAN):** Indicates the ratio of the transmitted radiation to the total radiation incident upon the medium (atmosphere).

- **Distance to Cloud (CDIST):** Indicates the distance, in kilometers, that a pixel is from the nearest cloud pixel. Infrequently, the pixel distance to cloud will be greater than the maximum allowed value. This layer is used with emissivity standard deviation to create surface temperature QA.

- **Downwelled Radiance layer (DRAD):** This indicates the thermal energy emitted by the atmosphere that reaches the Earth's surface and is then reflected toward the sensor.

- **Emissivity layer (EMIS):** This indicates the ratio of the energy radiated from a material’s surface to the energy radiated from a blackbody. Landsat emissivity values greater than the water emissivity constant are adjusted to be the water constant (0.988). Negative values for emissivity are replaced with the fill value instead.

- **Emissivity Standard Deviation (EMSD):** This indicates the extent of variation for the emissivity product. This layer is used with CDIST to create ST_QA.

- **Thermal Radiance layer (TRAD):** This displays the values produced when L1’s TIRS-2 Band 10 is converted to radiance. The maximum value for thermal radiance, 25 $Wm^{-2}sr^{-1}\mu m^{-1}$, may be exceeded (e.g., over volcanoes and fires). TRAD is generated so all the radiance layers share the same units.

- **Upwelled Radiance layer (URAD):** This indicates the amount of energy emitted from the atmosphere and scattered toward the sensor.

Refer to LSDS-1328 Landsat 8-9 OLI/TIRS Collection 2 Level 2 Data Format Control Book (DFCB for details about the ST intermediate bands (Data Type, Units, Fill Values and Value Ranges).

6.2.5 Level 2 Quality Assessment Bands

Four QA bands are included in the L9 L2 product. These QA bands consist of the L1 Pixel (see Table 5-5), L1 Radiometric Saturation (see Table 5-6), the SR Aerosol (Section 6.2.5.1), and ST Uncertainty.

Refer to LSDS-1328 Landsat 8-9 OLI/TIRS Collection 2 Level 2 Data Format Control Book (DFCB) for details about L9 L2 QA band specifications (Data Type, Units, and Range and Fill Values, and Scale Factors).

6.2.5.1 SR Aerosol QA File

The SR Aerosol QA file provides low-level details about factors that may have influenced the final product. Table 6-4 lists the description of bits and values in the SR Aerosol QA File. Refer to LSDS-1328 Landsat 8-9 OLI/TIRS Collection 2 Level 2 Data Format Control Book (DFCB) to view the SR Aerosol QA Value Interpretations.

Bit	Flag Description	Values
0	Fill	0 Pixel is not fill 1 Pixel is fill
1	Valid aerosol retrieval	0 Pixel retrieval is not valid 1 Pixel retrieval is valid
2	Water	0 Pixel is not water 1 Pixel is water
3	Unused	0
4	Unused	0
5	Interpolated Aerosol	0 Pixel is not aerosol interpolated 1 Pixel is aerosol interpolated
6 7	Aerosol Level	00 Climatology 01 Low 10 Medium 11 High
(0 is Least Significant Bit, 7 is Most Significant Bit)		

Table 6-4. SR Aerosol QA File

6.2.5.2 Surface Temperature QA File

The ST QA file indicates uncertainty of the temperatures given in the ST band file. The ST QA file is generated using uncertainty values and distance to cloud values. Higher numbers indicate greater uncertainty. This file is not included in the product when an SR-only product is generated. The GDAL_NODATA tag defines the value of -9999 to be the no data value for this band.

6.2.6 Angle Coefficient Files

The angle coefficients file contains coefficients used for calculating solar and satellite viewing angles. While the file name is changed to indicate a part of L2 product, the contents of the angle coefficients file are copied verbatim from the L1 angle coefficients file, as described in Section 5.2.5.

6.2.7 Level 2 Metadata Files

The L2 metadata files are created during product generation and contain information regarding both the SR and ST products (SR alone if the product is L2SR). The L1 metadata is encapsulated in the L2 metadata. Some files listed in the L1 metadata are not contained in the L2 product. Some of the fields listed in the L1 metadata do not apply to the files in the L2 product.

The XML metadata file and ODL metadata file have comparable fields. The LANDSAT_METADATA_FILE group for ODL is synonymous to the root element LANDSAT_METADATA_FILE for XML. The LANDSAT_METADATA_FILE group for ODL contains nested groups, synonymously, the LANDSAT_METADATA_FILE root element for XML has child elements. In the XML metadata file, the ODL parameter name is used in the start-tag and end-tag for elements. All parameters listed in the metadata file using ODL format are also in a separate metadata file using the XML format.

The XML metadata file and ODL metadata file have some contrasts. The ODL file distinguishes between strings and numerical values through the presence or absence of quotes around a value. The XML file does not make that distinction. The ODL file has an END statement signifying the end of the file. The XML file does not have a comparable entity.

Due to many variabilities displayed in the L2 Metadata files, examples are not included in this document – instead, please refer to the Level 2 Metadata Files section of LSDS-1328 Landsat 8-9 OLI/TIRS Collection 2 Level 2 Data Format Control Book (DFCB).

6.2.8 Checksum File

A single checksum file is created for all the files in the product. The checksum file contains a Message-Digest Algorithm 5 (MD5) checksum for every file. The file is in plain text format and contains the output from md5sum for each file. The checksum file is not distributed with the final product.

6.3 Additional Level-2 and Level 3 Science Products

Higher-level science products are created from Landsat standard Level-1 and Level-2 data; products currently produced at USGS EROS are listed below. The availability of Landsat 9 products may vary and is dependent on software and algorithm updates. Visit https://www.usgs.gov/landsat-missions/product-information for updates on L9 availability.

- Landsat Collection 2 U.S. Analysis Ready Data (ARD)
- Landsat Collection 2 Level-2 Aquatic Reflectance
- Landsat Collection 2 Level-3 Actual Evapotranspiration
- Landsat Collection 2 Level-3 Burned Area
- Landsat Collection 2 Level-3 Dynamic Surface Water Extent
- Landsat Collection 2 Level-3 Fractional Snow Covered Area

Section 7 Atmospheric Auxiliary Data

Landsat C2 L2 surface reflectance and surface temperature data processing requires atmospheric auxiliary data from multiple external sources. The required data are extracted from the source and the components specific to generating a C2 L2 product are repackaged and are available to download. These data are available for users wanting to generate custom L2 products using the C2 surface reflectance and surface temperature algorithms. **It is not necessary for users to download the atmospheric auxiliary data for use with C2 L2 products.**

L9 OLI-2 surface reflectance products are generated using the Land Surface Reflectance Code (LaSRC), which uses the coastal aerosol band for aerosol inversion tests, uses auxiliary climate data from Moderate Resolution Imaging Spectroradiometer (MODIS), and uses a radiative transfer model. (Vermote et al., 2016).

L9 surface temperature products are generated from Landsat C2 L1 thermal infrared bands, TOA reflectance, TOA Brightness Temperature, ASTER GED data, ASTER Normalized Difference Vegetation Index (NDVI) data, and atmospheric profiles of geopotential height, specific humidity, and air temperature extracted from Goddard Earth Observing System (GEOS) Model , Version 5, Forward Processing Instrument Teams (FP-IT) (for acquisitions from 2000 to present) or Modern Era Retrospective analysis for Research and Applications Version 2 (MERRA-2) (for acquisitions from 1982 to 1999).

Table 7-1 displays the C2 surface reflectance and surface temperature atmospheric auxiliary data inputs used for L9 L2 data generation. Refer to LSDS-1329 Landsat Atmospheric Auxiliary Data Data Format Control Book (DFCB) for details about the data utilized in the creation of these products.

Dataset Source	Purpose	Download Source
Earth Topography Five Minute Grid (ETOPO5) (File is named CMGDEM.hdf)	Calculate surface pressure	Landsat Web Site
Landsat 8-9 Ratio Map	Retrieve aerosol	Landsat Web Site
MODIS Fused: Daily Surface Reflectance and Daily Aerosol MODIS Climate Modeling Grids	Retrieve ozone and water vapor	EarthExplorer
Landsat Data Continuity Mission Look Up Tables (LDCMLUT)	Atmospheric correction of a Lambertian surface	Landsat Web Site
ASTER GED	Calculate emissivity	EarthExplorer
GEOS FP-IT	Retrieve atmospheric profiles of geopotential height, specific humidity, and air temperature	EarthExplorer

Table 7-1. Landsat 9 Level 2 Atmospheric Auxiliary Data Inputs

Section 8   Full Resolution Browse Images

Landsat 9 Full Resolution Browse (FRB) browse images are created for quick and efficient image selection and for visual interpretation. FRB files are created from Landsat L1 data products and distributed in Cloud Optimized Geographic Tagged Image File Format (COG) and Joint Photographic Experts Group (JPEG) formats. The examples in Figure 8-1 display the (left to right): Reflective browse image, Thermal browse image, and Quality Band browse image..

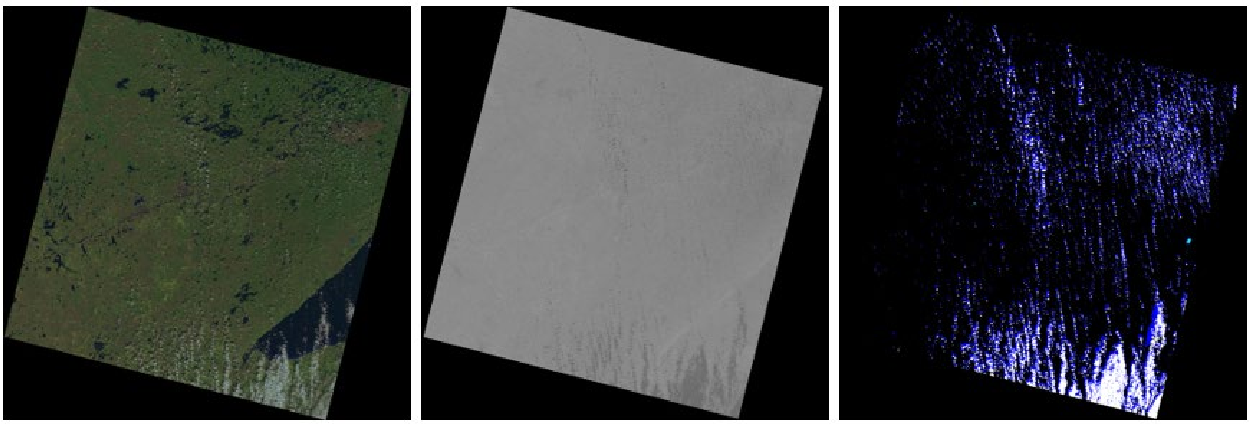

Figure 8-1. FRB Reflective, Thermal, and Quality Image Examples

The Landsat C2 Reflective FRB image is a composite of three bands to show a “natural” looking (false color) image. Reflectance values were calculated from the calibrated scaled digital number (DN) image data. The reflectance values were scaled to a 1-255 range using a gamma stretch with a gamma=2.0. This stretch was designed to emphasize vegetation without clipping the extreme values. The following bands for the L8-9 sensor were used to create the Reflective FRB:

- Landsat 9 OLI/OLI-2 = Bands 6,5,4

The Landsat C2 Thermal FRB is a one-band grayscale image that displays thermal properties of a Landsat scene. Image brightness temperature values were calculated from the calibrated scaled digital number (DN) image data. An image-specific 2 percent clip and a linear stretch to 1-255 were applied to the brightness temperature values. The following bands for each sensor were used to create the Thermal FRB:

- Landsat 9 TIRS/TIRS-2 = Band 10

The Landsat C2 Quality FRB images are 8-bit files generated from the Landsat L1 QA band to provide a quick view of the quality of the pixels within the scene to determine if a particular scene would work best for the user's application. This file includes values representing bit-packed combinations of surface, atmosphere, and sensor conditions that can affect the overall usefulness of a given pixel. The color-mapping assignments for the Quality FRB are displayed in Figure 8-2.

16-Bit Radiometric Saturation (RADSAT QA) Band		16-Bit Quality (QA) Band		8-Bit Quality File OLI / TIRS		8-Bit Quality File ETM+ / TM	8-Bit Quality File MSS	Color	Priority
Bit	**Description**	**Bit**	**Description**	**Bit**	**Description**	**Description**	**Description**		
		0	Designated Fill	**0**	Designated Fill	Designated Fill	Designated Fill		**Highest**
		1	Dilated Cloud						|
9	Dropped Pixel			**1**		Dropped Pixel	Dropped Pixel		|
11	Terrain occlusion				Occluded				|
0-6, 8*	Band 1-7, 9 Saturation			**2**	Radiometric Saturation	Radiometric Saturation	Radiometric Saturation		|
		3	Cloud	**3**	Cloud	Cloud	Cloud		|
		4	Cloud Shadow	**4**	Cloud Shadow	Cloud Shadow	**Unused**		|
		5	Snow	**5**	Snow/Ice	Snow/Ice	**Unused**		v
		2	Cirrus	**6**	Cirrus	**Unused**	**Unused**		**Lowest**
		6	Clear	**7**	**Unused**	**Unused**	**Unused**	**Unused**	
		7	Water						
		8-9	Cloud Confidence						
		10-11	Cloud Shadow Confidence						
		12-13	Snow/Ice Confidence						
7, 10, 12-15	**Unused**	14-15	Cirrus Confidence						

* For ETM, bit 8 in RADSAT QA indicates Band 6H data saturation. It indicates Band 8 data saturation in OLI / TIRS, and it is unused in TM and MSS. Saturation in any bands sets 8-bit QA file.

Figure 8-2. Landsat Quality Full Resolution Image Color Mapping Assignments

Landsat Collection 2 FRB Images can be downloaded as individual files for each Landsat scene from EarthExplorer. Refer to LSDS-1823 Landsat 1-9 Full Resolution Browse (FRB) Data Format Control Book (DFCB) for more details about FRB Images.

Section 9 Landsat 9 Data Access

The USGS archive holds data collected by the Landsat suite of satellites, beginning with Landsat 1 in 1972. Over 750 L9 scenes are added to the USGS archives each day and become available to all users for download at no charge using the access interfaces described in this section. Landsat data are in the public domain, which means there are no copyright or licensing restrictions on the use of Landsat products downloaded from the USGS. Visit https://www.usgs.gov/centers/eros/data-citation for more details on citing data from the USGS.

Note: Data acquired by previous sensors were initially processed into Collection 1 (C1) in 2016, and then into C2 in 2020. L9 data are processed only into the C2 archive.

Note: Any references to C2 currently pertain to all Landsat sensors, including L9. The Landsat Collection 2 webpage contains for more details about L9 data products: https://www.usgs.gov/landsat-missions/landsat-collection-2.

9.1 Commercial Cloud Data Access

L9 L1 and L2 products are processed and delivered from a commercial cloud environment. Leveraging the storage and processing that cloud services provide places the data next to the processing for the first time, offering new ways to explore the growing record of Landsat observations.

Refer to this webpage for more information about working with Landsat data within a cloud environment https://www.usgs.gov/landsat-missions/landsat-commercial-cloud-data-access. The LSDS-2032 Landsat Commercial Cloud Direct Access User Guide also contains basic information on how users leverage the Landsat data in the cloud to enhance existing workflows by utilizing common tools available in the commercial cloud environment.

While the ability to work with the data directly “in the cloud” is very beneficial, users can also utilize well-known data access interfaces to download L9 data products; these are listed in the following sections. The functionality of each interface differs, but the data products are all delivered from the same location. For a comprehensive view of all the Landsat data access portals and other tools available, visit https://www.usgs.gov/landsat-missions/landsat-data-access.

9.2 EarthExplorer (EE)

EarthExplorer (EE) is the primary search interface accessing aerial, mapping, elevation, and satellite data held in the USGS archives, including Landsat data products. Before downloading data products, users must access the USGS EROS Registration System (ERS),submit the user registration and receive confirmation of successful username creation. Some functions of EE will work only after a successful login.

https://earthexplorer.usgs.gov

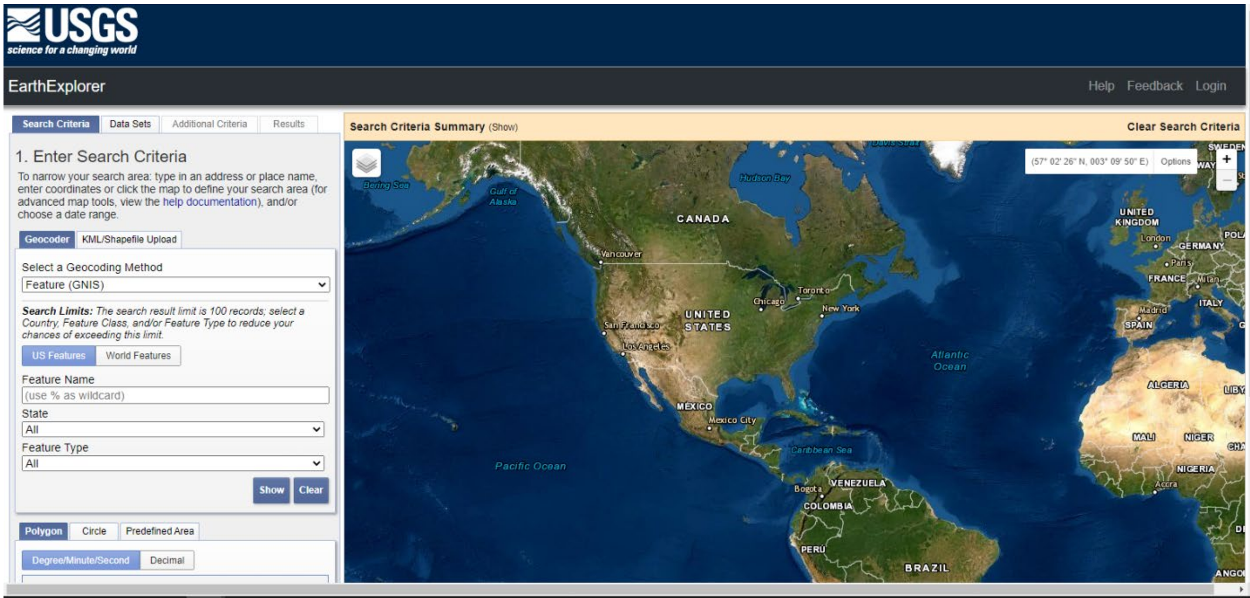

Figure 9-1. EarthExplorer Interface

The Search Criteria tab options allow users to select the geographic area of interest by typing a place name, latitude/longitude coordinates, path/row, a shape file, or a .kml file. The user can also specify the desired cloud cover limits, along with the date range for which results will be returned.

The Data Sets tab lists all categories of data held in the USGS EROS Archives. Figure 9-2 shows how the Landsat 8-9 OLI/TIRS C2 L2 and L1 datasets are displayed in the Landsat section on the Data Sets tab. Multiple datasets can be selected for comprehensive searching.

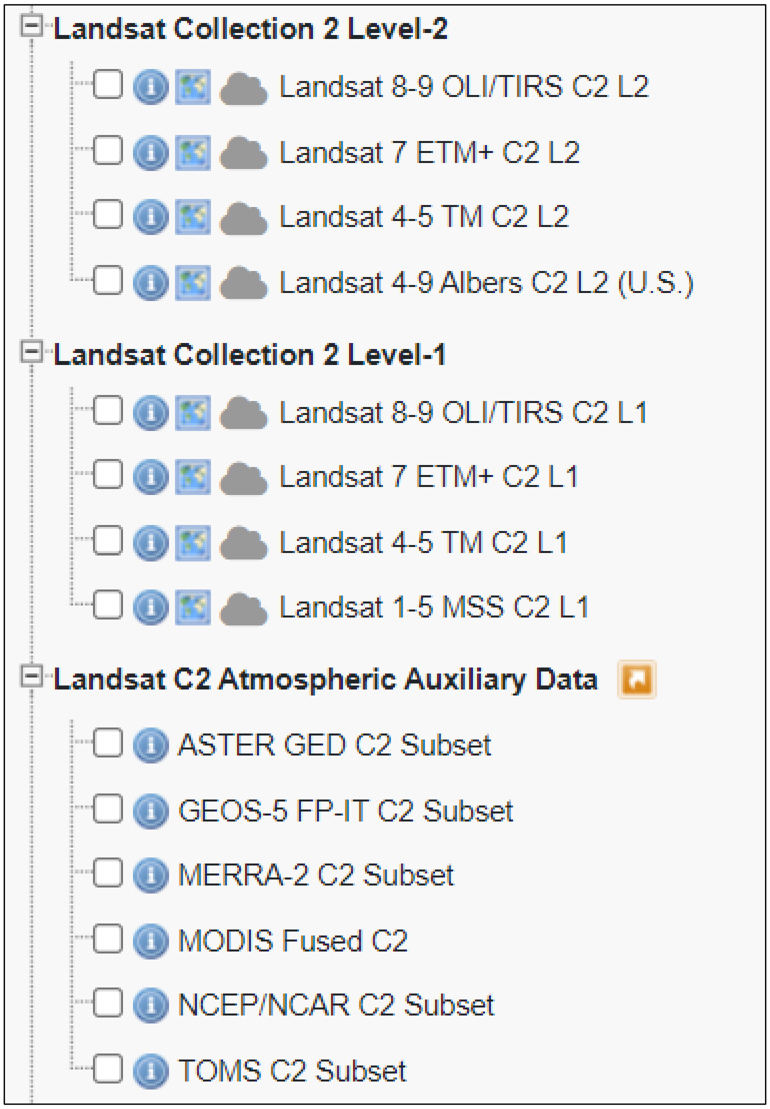

Figure 9-2. EarthExplorer Landsat Datasets

After selecting the Data Set(s), the Additional Criteria tab becomes available. This tab allows users to search by specific Landsat Produce Identifier, WRS Path/Row, Collection Category, and Land Cloud Cover, among others. Nighttime data can be specified on this tab as well.

After making the selection(s), clicking the Results button will conduct a search of the archives. After a successful search, scenes meeting the entered criteria are returned, with options to view a footprint and/or browse image of the scene on the map. A subset of the metadata file is also provided, along with download options. Download files for a single result using the green down arrow icon and selecting a product from the popup or add several results to a Bulk Order using the gold icon and select the products to download from the Item Basket. Refer to the EE Help Index for tutorials and additional information about bulk downloading data from EE: https://www.usgs.gov/centers/eros/science/earthexplorer-help-index.

9.2.1 L9 Level 2 Product Downloads

For L9 L2 scenes, a bundle containing all the files associated with a scene (surface reflectance and/or surface temperature – see Section 6.2.1) can be downloaded, or specific bands and files can be downloaded individually. See Figure 9-3 and Figure 9-4.

Figure 9-3. Landsat Level 2 scene data download box

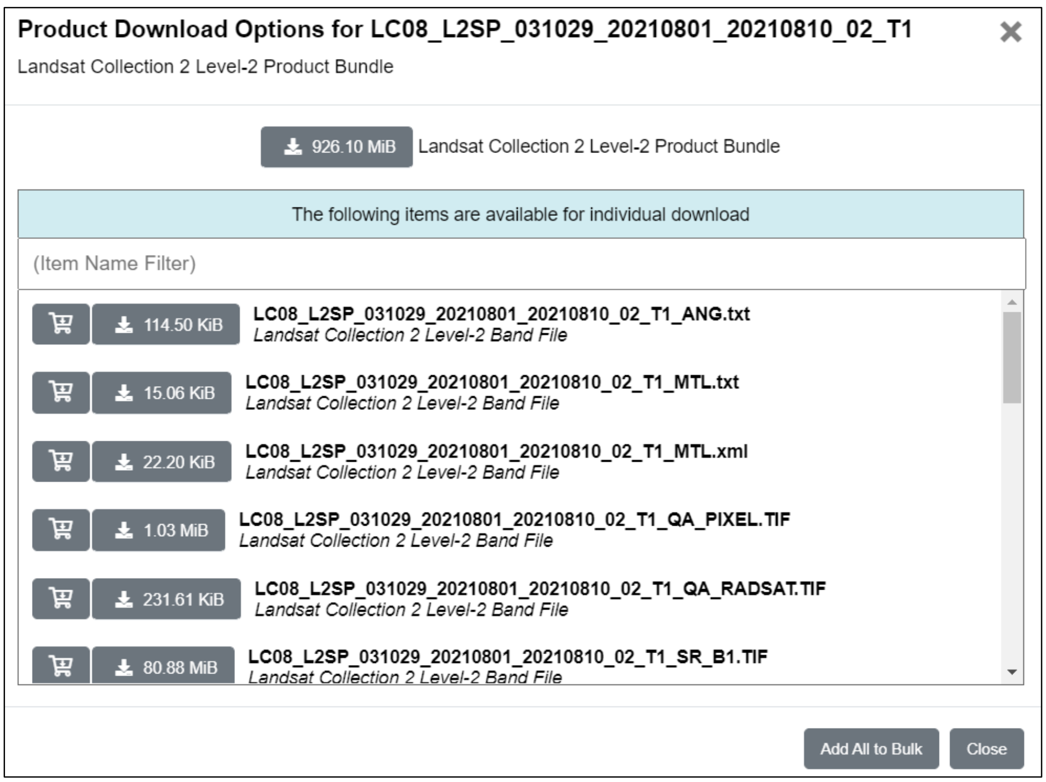

Figure 9-4. Example Level 2 scene download options from EarthExplorer

9.2.2 L9 Level 1 Product Downloads

For L9 L1 scenes, a bundle containing all the files associated with a scene (multispectral and thermal bands, ancillary and metadata files - see Section 5.2.1) can be downloaded, or specific bands can be downloaded individually. Full-resolution Browse images can also be downloaded for each scene. See Figure 9-5 and Figure 9-6.

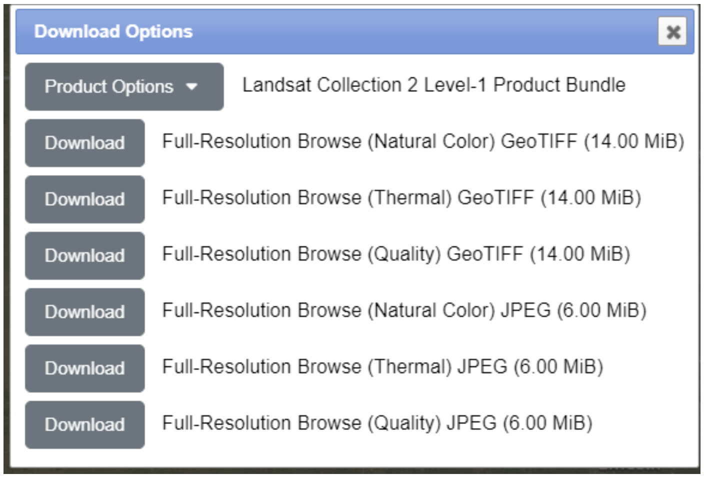

Figure 9-5. Landsat Level 1 scene data download box

9.3 LandsatLook

In 2020, the LandsatLook Viewer was redesigned to allow rapid viewing and access to Landsat C2 L2 data. The viewer leverages resources available via a commercial cloud environment including COG and Spatio-Temporal Asset Catalog (STAC) metadata. Landsat 1-5 MSS data are not displayed or available from this viewer. Before downloading data from LandsatLook, users must access the USGS ERS, submit the user registration and receive confirmation of successful username creation. Some functions of LandsatLook will work only after a successful login.

https://landsatlook.usgs.gov/

LandsatLook enables users to create dynamic custom mosaics from scenes within the Landsat archive for an area of interest and allows users to customize mosaic using three band combinations, select spectral indices and quality assessment band filtering.

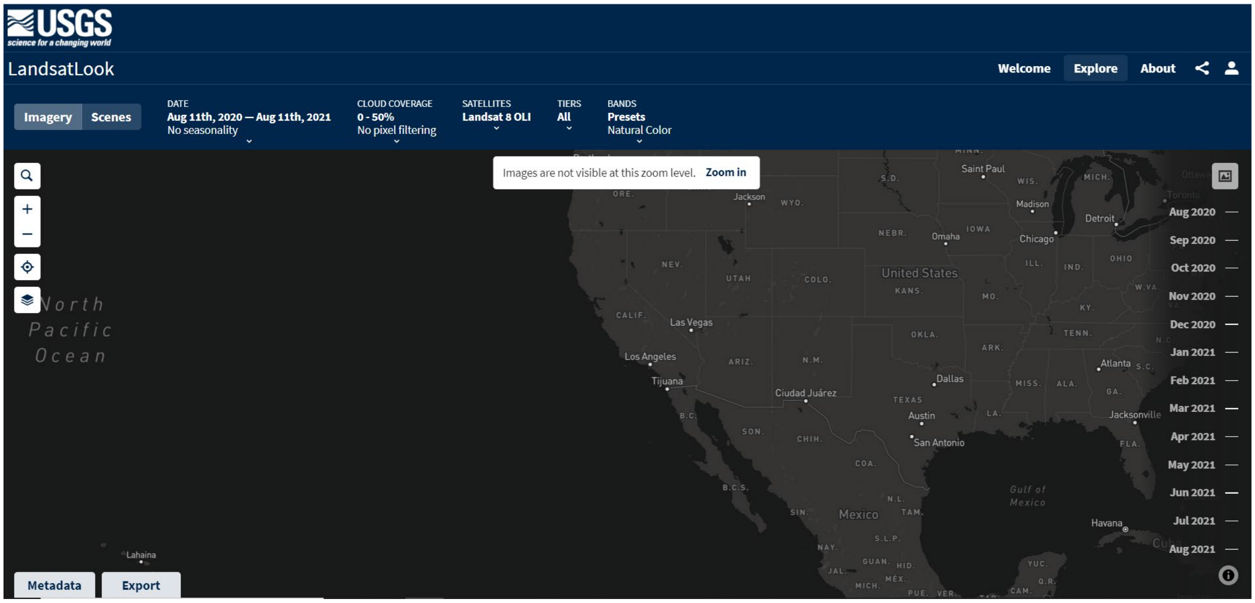

Figure 9-6. LandsatLook Viewer

The geographic area of interest can be selected by using the mouse — clicking and holding the right mouse button allows users to pan around the map while the scroll wheel controls the zoom. Alternatively, there are several icons on the left of the screen which can also control the map view. The magnifying glass allows users to type in an area of interest and search the whole globe while the "+" and "-" buttons control the zoom, additionally the target button will zoom the map to a user's location if they have allowed their web browser access to do so. Further search criteria can be added by adjusting the date and cloud coverage drop-down menus.

The satellites and menus allow users to select the Landsat satellites to search for display. LandsatLook displays Landsat C2 SR imagery.

The map view changes to reflect the results of the search criteria selected once it is zoomed in enough to display data. The time it takes to display imagery depends on how broad the submitted search is. Whenever search criteria is modified, the map will reload to display the best image possible.

9.3.1 Data Downloads

Download options for search results can be found in the Metadata or Export tabs found at the bottom right of the screen. LandsatLook provides single-band downloads; no bundles containing more than one file are available.

On the Metadata tab, the Product Identifiers of scenes are listed, along with some simple metadata that can be used to further refine the results. Figure 9-9 shows an example of the metadata listing, along with download options. Actions that can be done while viewing the Metadata tab include selecting and downloading the Metadata (See

Figure 9-10) selecting and downloading the SR-related bands (Figure 9-11) and selecting and downloading the ST-related bands (Figure 9-12).

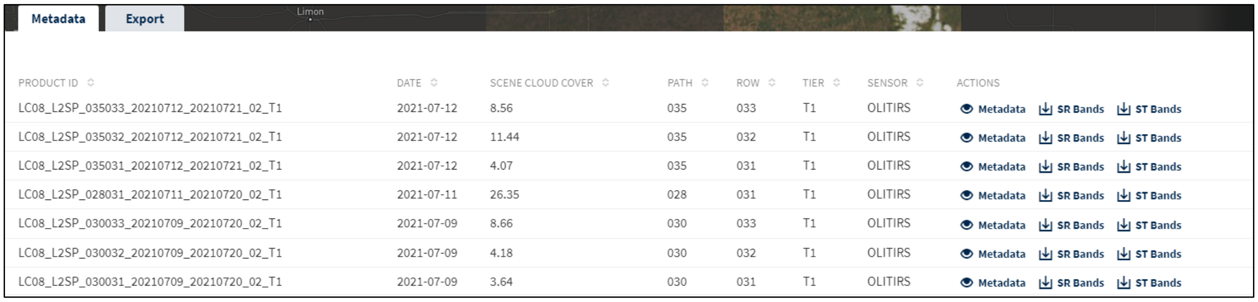

PRODUCT ID	DATE	SCENE CLOUD COVER	PATH	ROW	TIER	SENSOR	ACTIONS
LC08_L2SP_035033_20210712_20210721_02_T1	2021-07-12	8.56	035	033	T1	OLITIRS	Metadata SR Bands ST Bands
LC08_L2SP_035032_20210712_20210721_02_T1	2021-07-12	11.44	035	032	T1	OLITIRS	Metadata SR Bands ST Bands
LC08_L2SP_035031_20210712_20210721_02_T1	2021-07-12	4.07	035	031	T1	OLITIRS	Metadata SR Bands ST Bands
LC08_L2SP_028031_20210711_20210720_02_T1	2021-07-11	26.35	028	031	T1	OLITIRS	Metadata SR Bands ST Bands
LC08_L2SP_030033_20210709_20210720_02_T1	2021-07-09	8.66	030	033	T1	OLITIRS	Metadata SR Bands ST Bands
LC08_L2SP_030032_20210709_20210720_02_T1	2021-07-09	4.18	030	032	T1	OLITIRS	Metadata SR Bands ST Bands
LC08_L2SP_030031_20210709_20210720_02_T1	2021-07-09	3.64	030	031	T1	OLITIRS	Metadata SR Bands ST Bands

Figure 9-7. LandsatLook Metadata View

When the Metadata action is selected, the information for the specific scene is displayed, as shown in Figure 9-10. (This is the same metadata that is included in bundle downloads from EarthExplorer.) A .json file can be downloaded by clicking the arrow in the top-right corner of this view.

Figure 9-8. LandsatLook Metadata File

In the Metadata View, when the SR Bands download icon is selected, the following box appears. This displays the SR-related data files available to download.

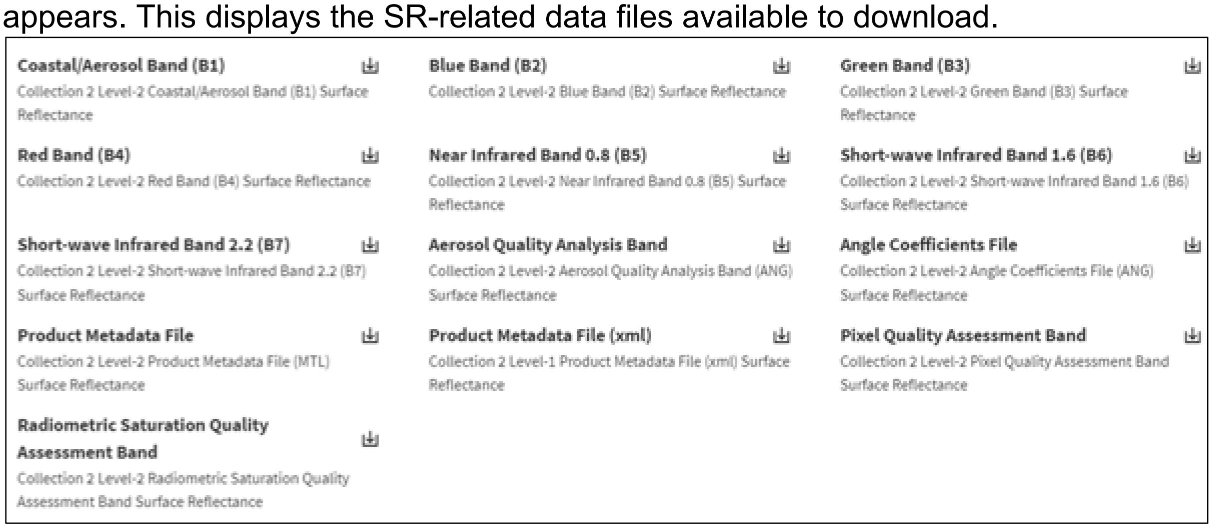

Figure 9-9. SR-related Band Downloads from LandsatLook

In the Metadata View, when the ST Bands download icon is selected, the following box appears. This displays the ST-related data files available to download.

Figure 9-10. ST-related Band Downloads from LandsatLook

9.3.2 Optional Animation, Map Image, and Metadata Exports

On the Export tab, options to download a Timelapse animated GIF of the current results displayed or download a .png image of the current Map View. The metadata for the current query can also be exported in a .json file. Sample code in Python (.py) format can also be copied to perform a metadata search matching the current query. Figure 9-13 displays the LandsatLook Export tab.

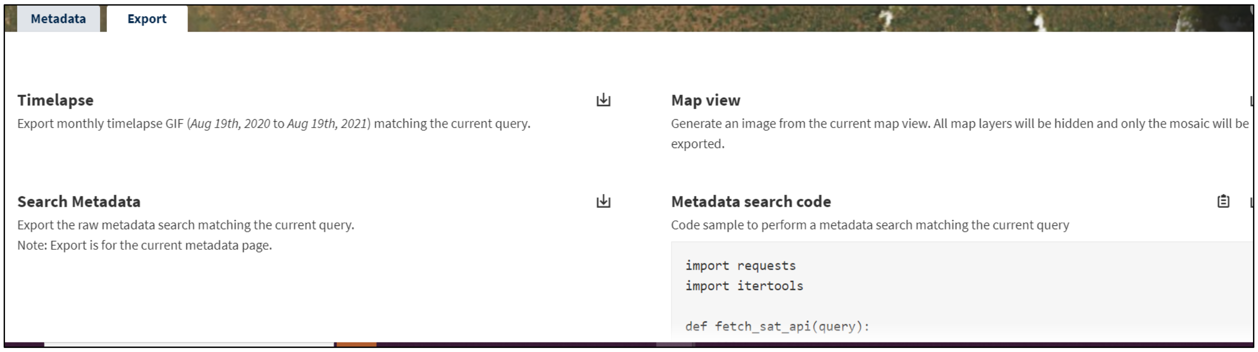

Figure 9-11. LandsatLook Export View

Appendix A Postlaunch Calibration Images

A.1 Landsat 9 First Light Images

From October 28-31, 2021, acquisitions were made to verify OLI-2 dark collects, OLI-2 stim lamp and solar diffuser calibrations, and TIRS-2 calibrations. On October 31, 2021, the "first light" Earth scenes were acquired over various areas of the world. These areas are listed in Table A-1 and can be seen on this NASA webpage: https://www.nasa.gov/press-release/nasa-usgs-release-first-landsat-9-images.

Location	WRS-2 Path	WRS-2 Rows
Australia	109	70-71, 75, 82-84
Himalaya	141	40-41
Italy	189	31-34
Ohio/Michigan	19	30-32
Florida	19	38-39
Yucatan	19	45-49
Colorado Rockies	35	32-34
Arizona	35	35-36

Table A-1. Landsat 9 'First Light' Images

A.2 L9 underfly with L8

From November 12-16, 2021, Landsat 9 was in orbit about 10 km below the Landsat 8 satellite, and an "underfly" was conducted to acquire data simultaneously over the WRS-2 paths listed in Table A-2. The underfly activity created an opportunity to cross-calibrate Landsat 9 data to data from Landsat 8, which is currently the accepted reference for calibration. More details about the benefits of the underfly activity can be found on this USGS webpage: https://www.usgs.gov/centers/eros/news/underfly-positions-landsat-9-below-landsat-8-simultaneous-scenes.

Landsat 8 Cycle Day	Date DOY	Landsat 8 Paths	Percent Path Overlap
14	Nov 12, 2021 316	105,121,137,153,169,185,201,217,233, 16,32,48,64,80,96	~10 percent western side
15	Nov 13, 2021 317	112,128,144,160,176,192,208,224, 7,23,39,55,71,87	~50 percent western side
16	Nov 14, 2021 318	103,119,135,151,167,183,199,215,231, 14,30,45,62,78,94	100 percent overlap
1	Nov 15, 2021 319	110,126,142,158,174,190,206,222, 5,21,37,53,69,85	~50 percent eastern side
2	Nov 16, 2021 320	101,117,133,149,165,181,197,213,229, 12,28,44,60,76,92	~10 percent eastern side

Table A-2. Landsat 9 Underfly Dates, Paths and Overlap with Landsat 8

Appendix B L9 Level 1 ODL (MTL) Metadata Example

An ODL (MTL) file is included with all L9 L1 data products. Landsat MTL files contain beneficial information for the systematic searching and archiving practices of data. Information about data processing and values important for enhancing Landsat data (such as conversion to reflectance and radiance) are also included in this file.

DFCBs define and describe the metadata files that are delivered with all Landsat data products. DFCBs for all sensors are located at https://www.usgs.gov/landsat-missions/landsat-project-documents.

```
GROUP = LANDSAT_METADATA_FILE
  GROUP = PRODUCT_CONTENTS
    ORIGIN = "Image courtesy of the U.S. Geological Survey"
    DIGITAL_OBJECT_IDENTIFIER = "https://doi.org/10.5066/P975CC9B"
    LANDSAT_PRODUCT_ID = "LC09_L1TP_097018_20211118_20211118_02_T2"
    PROCESSING_LEVEL = "L1TP"
    COLLECTION_NUMBER = 02
    COLLECTION_CATEGORY = "T2"
    OUTPUT_FORMAT = "GEOTIFF"
    FILE_NAME_BAND_1 = "LC09_L1TP_097018_20211118_20211118_02_T2_B1.TIF"
    FILE_NAME_BAND_2 = "LC09_L1TP_097018_20211118_20211118_02_T2_B2.TIF"
    FILE_NAME_BAND_3 = "LC09_L1TP_097018_20211118_20211118_02_T2_B3.TIF"
    FILE_NAME_BAND_4 = "LC09_L1TP_097018_20211118_20211118_02_T2_B4.TIF"
    FILE_NAME_BAND_5 = "LC09_L1TP_097018_20211118_20211118_02_T2_B5.TIF"
    FILE_NAME_BAND_6 = "LC09_L1TP_097018_20211118_20211118_02_T2_B6.TIF"
    FILE_NAME_BAND_7 = "LC09_L1TP_097018_20211118_20211118_02_T2_B7.TIF"
    FILE_NAME_BAND_8 = "LC09_L1TP_097018_20211118_20211118_02_T2_B8.TIF"
    FILE_NAME_BAND_9 = "LC09_L1TP_097018_20211118_20211118_02_T2_B9.TIF"
    FILE_NAME_BAND_10 = "LC09_L1TP_097018_20211118_20211118_02_T2_B10.TIF"
    FILE_NAME_BAND_11 = "LC09_L1TP_097018_20211118_20211118_02_T2_B11.TIF"
    FILE_NAME_QUALITY_L1_PIXEL = "LC09_L1TP_097018_20211118_20211118_02_T2_QA_PIXEL.TIF"
    FILE_NAME_QUALITY_L1_RADIOMETRIC_SATURATION =
"LC09_L1TP_097018_20211118_20211118_02_T2_QA_RADSAT.TIF"
    FILE_NAME_ANGLE_COEFFICIENT = "LC09_L1TP_097018_20211118_20211118_02_T2_ANG.txt"
    FILE_NAME_ANGLE_SENSOR_AZIMUTH_BAND_4 =
"LC09_L1TP_097018_20211118_20211118_02_T2_VAA.TIF"
    FILE_NAME_ANGLE_SENSOR_ZENITH_BAND_4 =
"LC09_L1TP_097018_20211118_20211118_02_T2_VZA.TIF"
    FILE_NAME_ANGLE_SOLAR_AZIMUTH_BAND_4 =
"LC09_L1TP_097018_20211118_20211118_02_T2_SAA.TIF"
    FILE_NAME_ANGLE_SOLAR_ZENITH_BAND_4 = "LC09_L1TP_097018_20211118_20211118_02_T2_SZA.TIF"
    FILE_NAME_METADATA_ODL = "LC09_L1TP_097018_20211118_20211118_02_T2_MTL.txt"
    FILE_NAME_METADATA_XML = "LC09_L1TP_097018_20211118_20211118_02_T2_MTL.xml"
    DATA_TYPE_BAND_1 = "UINT16"
    DATA_TYPE_BAND_2 = "UINT16"
    DATA_TYPE_BAND_3 = "UINT16"
    DATA_TYPE_BAND_4 = "UINT16"
    DATA_TYPE_BAND_5 = "UINT16"
    DATA_TYPE_BAND_6 = "UINT16"
    DATA_TYPE_BAND_7 = "UINT16"
    DATA_TYPE_BAND_8 = "UINT16"
    DATA_TYPE_BAND_9 = "UINT16"
    DATA_TYPE_BAND_10 = "UINT16"
    DATA_TYPE_BAND_11 = "UINT16"
    DATA_TYPE_QUALITY_L1_PIXEL = "UINT16"
    DATA_TYPE_QUALITY_L1_RADIOMETRIC_SATURATION = "UINT16"
    DATA_TYPE_ANGLE_SENSOR_AZIMUTH_BAND_4 = "INT16"
```

```
  DATA_TYPE_ANGLE_SENSOR_ZENITH_BAND_4 = "INT16"
  DATA_TYPE_ANGLE_SOLAR_AZIMUTH_BAND_4 = "INT16"
  DATA_TYPE_ANGLE_SOLAR_ZENITH_BAND_4 = "INT16"
END_GROUP = PRODUCT_CONTENTS
GROUP = IMAGE_ATTRIBUTES
  SPACECRAFT_ID = "LANDSAT_9"
  SENSOR_ID = "OLI_TIRS"
  WRS_TYPE = 2
  WRS_PATH = 97
  WRS_ROW = 18
  NADIR_OFFNADIR = "NADIR"
  TARGET_WRS_PATH = 97
  TARGET_WRS_ROW = 18
  DATE_ACQUIRED = 2021-11-18
  SCENE_CENTER_TIME = "00:09:42.9336170Z"
  STATION_ID = "LGN"
  CLOUD_COVER = 60.23
  CLOUD_COVER_LAND = 75.79
  IMAGE_QUALITY_OLI = 9
  IMAGE_QUALITY_TIRS = 9
  SATURATION_BAND_1 = "N"
  SATURATION_BAND_2 = "N"
  SATURATION_BAND_3 = "N"
  SATURATION_BAND_4 = "N"
  SATURATION_BAND_5 = "N"
  SATURATION_BAND_6 = "N"
  SATURATION_BAND_7 = "N"
  SATURATION_BAND_8 = "N"
  SATURATION_BAND_9 = "N"
  ROLL_ANGLE = -0.001
  SUN_AZIMUTH = 171.61700481
  SUN_ELEVATION = 10.36432742
  EARTH_SUN_DISTANCE = 0.9885441
END_GROUP = IMAGE_ATTRIBUTES
GROUP = PROJECTION_ATTRIBUTES
  MAP_PROJECTION = "UTM"
  DATUM = "WGS84"
  ELLIPSOID = "WGS84"
  UTM_ZONE = 58
  GRID_CELL_SIZE_PANCHROMATIC = 15.00
  GRID_CELL_SIZE_REFLECTIVE = 30.00
  GRID_CELL_SIZE_THERMAL = 30.00
  PANCHROMATIC_LINES = 16401
  PANCHROMATIC_SAMPLES = 16161
  REFLECTIVE_LINES = 8201
  REFLECTIVE_SAMPLES = 8081
  THERMAL_LINES = 8201
  THERMAL_SAMPLES = 8081
  ORIENTATION = "NORTH_UP"
  CORNER_UL_LAT_PRODUCT = 61.17524
  CORNER_UL_LON_PRODUCT = 162.85426
  CORNER_UR_LAT_PRODUCT = 61.17165
  CORNER_UR_LON_PRODUCT = 167.36123
  CORNER_LL_LAT_PRODUCT = 58.96781
  CORNER_LL_LON_PRODUCT = 162.99306
  CORNER_LR_LAT_PRODUCT = 58.96453
  CORNER_LR_LON_PRODUCT = 167.20851
  CORNER_UL_PROJECTION_X_PRODUCT = 384600.000
  CORNER_UL_PROJECTION_Y_PRODUCT = 6784200.000
  CORNER_UR_PROJECTION_X_PRODUCT = 627000.000
  CORNER_UR_PROJECTION_Y_PRODUCT = 6784200.000
  CORNER_LL_PROJECTION_X_PRODUCT = 384600.000
```

```
    CORNER_LL_PROJECTION_Y_PRODUCT = 6538200.000
    CORNER_LR_PROJECTION_X_PRODUCT = 627000.000
    CORNER_LR_PROJECTION_Y_PRODUCT = 6538200.000
  END_GROUP = PROJECTION_ATTRIBUTES
  GROUP = LEVEL1_PROCESSING_RECORD
    ORIGIN = "Image courtesy of the U.S. Geological Survey"
    DIGITAL_OBJECT_IDENTIFIER = "https://doi.org/10.5066/P975CC9B"
    REQUEST_ID = "P7014iw57qhrf_00002"
    LANDSAT_SCENE_ID = "LC90970182021322LGN00"
    LANDSAT_PRODUCT_ID = "LC09_L1TP_097018_20211118_20211118_02_T2"
    PROCESSING_LEVEL = "L1TP"
    COLLECTION_CATEGORY = "T2"
    OUTPUT_FORMAT = "GEOTIFF"
    DATE_PRODUCT_GENERATED = 2021-11-18T02:17:19Z
    PROCESSING_SOFTWARE_VERSION = "LPGS_15.5.0"
    FILE_NAME_BAND_1 = "LC09_L1TP_097018_20211118_20211118_02_T2_B1.TIF"
    FILE_NAME_BAND_2 = "LC09_L1TP_097018_20211118_20211118_02_T2_B2.TIF"
    FILE_NAME_BAND_3 = "LC09_L1TP_097018_20211118_20211118_02_T2_B3.TIF"
    FILE_NAME_BAND_4 = "LC09_L1TP_097018_20211118_20211118_02_T2_B4.TIF"
    FILE_NAME_BAND_5 = "LC09_L1TP_097018_20211118_20211118_02_T2_B5.TIF"
    FILE_NAME_BAND_6 = "LC09_L1TP_097018_20211118_20211118_02_T2_B6.TIF"
    FILE_NAME_BAND_7 = "LC09_L1TP_097018_20211118_20211118_02_T2_B7.TIF"
    FILE_NAME_BAND_8 = "LC09_L1TP_097018_20211118_20211118_02_T2_B8.TIF"
    FILE_NAME_BAND_9 = "LC09_L1TP_097018_20211118_20211118_02_T2_B9.TIF"
    FILE_NAME_BAND_10 = "LC09_L1TP_097018_20211118_20211118_02_T2_B10.TIF"
    FILE_NAME_BAND_11 = "LC09_L1TP_097018_20211118_20211118_02_T2_B11.TIF"
    FILE_NAME_QUALITY_L1_PIXEL = "LC09_L1TP_097018_20211118_20211118_02_T2_QA_PIXEL.TIF"
    FILE_NAME_QUALITY_L1_RADIOMETRIC_SATURATION =
"LC09_L1TP_097018_20211118_20211118_02_T2_QA_RADSAT.TIF"
    FILE_NAME_ANGLE_COEFFICIENT = "LC09_L1TP_097018_20211118_20211118_02_T2_ANG.txt"
    FILE_NAME_ANGLE_SENSOR_AZIMUTH_BAND_4 =
"LC09_L1TP_097018_20211118_20211118_02_T2_VAA.TIF"
    FILE_NAME_ANGLE_SENSOR_ZENITH_BAND_4 =
"LC09_L1TP_097018_20211118_20211118_02_T2_VZA.TIF"
    FILE_NAME_ANGLE_SOLAR_AZIMUTH_BAND_4 =
"LC09_L1TP_097018_20211118_20211118_02_T2_SAA.TIF"
    FILE_NAME_ANGLE_SOLAR_ZENITH_BAND_4 = "LC09_L1TP_097018_20211118_20211118_02_T2_SZA.TIF"
    FILE_NAME_METADATA_ODL = "LC09_L1TP_097018_20211118_20211118_02_T2_MTL.txt"
    FILE_NAME_METADATA_XML = "LC09_L1TP_097018_20211118_20211118_02_T2_MTL.xml"
    FILE_NAME_CPF = "LC09CPF_20210927_20211231_02.02"
    FILE_NAME_BPF_OLI = "LO9BPF20211117223222_20211118000816.01"
    FILE_NAME_BPF_TIRS = "LT9BPF20211117225516_20211118000344.01"
    FILE_NAME_RLUT = "LC09RLUT_20210927_20531231_02_03.h5"
    DATA_SOURCE_ELEVATION = "GLS2000"
    GROUND_CONTROL_POINTS_VERSION = 5
    GROUND_CONTROL_POINTS_MODEL = 51
    GEOMETRIC_RMSE_MODEL = 21.406
    GEOMETRIC_RMSE_MODEL_Y = 16.370
    GEOMETRIC_RMSE_MODEL_X = 13.792
  END_GROUP = LEVEL1_PROCESSING_RECORD
  GROUP = LEVEL1_MIN_MAX_RADIANCE
    RADIANCE_MAXIMUM_BAND_1 = 804.93738
    RADIANCE_MINIMUM_BAND_1 = -66.47199
    RADIANCE_MAXIMUM_BAND_2 = 837.14374
    RADIANCE_MINIMUM_BAND_2 = -69.13160
    RADIANCE_MAXIMUM_BAND_3 = 771.03668
    RADIANCE_MINIMUM_BAND_3 = -63.67246
    RADIANCE_MAXIMUM_BAND_4 = 639.18402
    RADIANCE_MINIMUM_BAND_4 = -52.78402
    RADIANCE_MAXIMUM_BAND_5 = 379.03827
    RADIANCE_MINIMUM_BAND_5 = -31.30110
    RADIANCE_MAXIMUM_BAND_6 = 94.97116
```

```
    RADIANCE_MINIMUM_BAND_6 = -7.84275
    RADIANCE_MAXIMUM_BAND_7 = 32.11728
    RADIANCE_MINIMUM_BAND_7 = -2.65226
    RADIANCE_MAXIMUM_BAND_8 = 712.98907
    RADIANCE_MINIMUM_BAND_8 = -58.87887
    RADIANCE_MAXIMUM_BAND_9 = 143.33020
    RADIANCE_MINIMUM_BAND_9 = -11.83626
    RADIANCE_MAXIMUM_BAND_10 = 25.00330
    RADIANCE_MINIMUM_BAND_10 = 0.10038
    RADIANCE_MAXIMUM_BAND_11 = 22.97172
    RADIANCE_MINIMUM_BAND_11 = 0.10035
  END_GROUP = LEVEL1_MIN_MAX_RADIANCE
  GROUP = LEVEL1_MIN_MAX_REFLECTANCE
    REFLECTANCE_MAXIMUM_BAND_1 = 1.210700
    REFLECTANCE_MINIMUM_BAND_1 = -0.099980
    REFLECTANCE_MAXIMUM_BAND_2 = 1.210700
    REFLECTANCE_MINIMUM_BAND_2 = -0.099980
    REFLECTANCE_MAXIMUM_BAND_3 = 1.210700
    REFLECTANCE_MINIMUM_BAND_3 = -0.099980
    REFLECTANCE_MAXIMUM_BAND_4 = 1.210700
    REFLECTANCE_MINIMUM_BAND_4 = -0.099980
    REFLECTANCE_MAXIMUM_BAND_5 = 1.210700
    REFLECTANCE_MINIMUM_BAND_5 = -0.099980
    REFLECTANCE_MAXIMUM_BAND_6 = 1.210700
    REFLECTANCE_MINIMUM_BAND_6 = -0.099980
    REFLECTANCE_MAXIMUM_BAND_7 = 1.210700
    REFLECTANCE_MINIMUM_BAND_7 = -0.099980
    REFLECTANCE_MAXIMUM_BAND_8 = 1.210700
    REFLECTANCE_MINIMUM_BAND_8 = -0.099980
    REFLECTANCE_MAXIMUM_BAND_9 = 1.210700
    REFLECTANCE_MINIMUM_BAND_9 = -0.099980
  END_GROUP = LEVEL1_MIN_MAX_REFLECTANCE
  GROUP = LEVEL1_MIN_MAX_PIXEL_VALUE
    QUANTIZE_CAL_MAX_BAND_1 = 65535
    QUANTIZE_CAL_MIN_BAND_1 = 1
    QUANTIZE_CAL_MAX_BAND_2 = 65535
    QUANTIZE_CAL_MIN_BAND_2 = 1
    QUANTIZE_CAL_MAX_BAND_3 = 65535
    QUANTIZE_CAL_MIN_BAND_3 = 1
    QUANTIZE_CAL_MAX_BAND_4 = 65535
    QUANTIZE_CAL_MIN_BAND_4 = 1
    QUANTIZE_CAL_MAX_BAND_5 = 65535
    QUANTIZE_CAL_MIN_BAND_5 = 1
    QUANTIZE_CAL_MAX_BAND_6 = 65535
    QUANTIZE_CAL_MIN_BAND_6 = 1
    QUANTIZE_CAL_MAX_BAND_7 = 65535
    QUANTIZE_CAL_MIN_BAND_7 = 1
    QUANTIZE_CAL_MAX_BAND_8 = 65535
    QUANTIZE_CAL_MIN_BAND_8 = 1
    QUANTIZE_CAL_MAX_BAND_9 = 65535
    QUANTIZE_CAL_MIN_BAND_9 = 1
    QUANTIZE_CAL_MAX_BAND_10 = 65535
    QUANTIZE_CAL_MIN_BAND_10 = 1
    QUANTIZE_CAL_MAX_BAND_11 = 65535
    QUANTIZE_CAL_MIN_BAND_11 = 1
  END_GROUP = LEVEL1_MIN_MAX_PIXEL_VALUE
  GROUP = LEVEL1_RADIOMETRIC_RESCALING
    RADIANCE_MULT_BAND_1 = 1.3297E-02
    RADIANCE_MULT_BAND_2 = 1.3829E-02
    RADIANCE_MULT_BAND_3 = 1.2737E-02
    RADIANCE_MULT_BAND_4 = 1.0559E-02
    RADIANCE_MULT_BAND_5 = 6.2615E-03
```

```
    RADIANCE_MULT_BAND_6 = 1.5689E-03
    RADIANCE_MULT_BAND_7 = 5.3056E-04
    RADIANCE_MULT_BAND_8 = 1.1778E-02
    RADIANCE_MULT_BAND_9 = 2.3677E-03
    RADIANCE_MULT_BAND_10 = 3.8000E-04
    RADIANCE_MULT_BAND_11 = 3.4900E-04
    RADIANCE_ADD_BAND_1 = -66.48529
    RADIANCE_ADD_BAND_2 = -69.14543
    RADIANCE_ADD_BAND_3 = -63.68520
    RADIANCE_ADD_BAND_4 = -52.79458
    RADIANCE_ADD_BAND_5 = -31.30737
    RADIANCE_ADD_BAND_6 = -7.84432
    RADIANCE_ADD_BAND_7 = -2.65279
    RADIANCE_ADD_BAND_8 = -58.89065
    RADIANCE_ADD_BAND_9 = -11.83862
    RADIANCE_ADD_BAND_10 = 0.10000
    RADIANCE_ADD_BAND_11 = 0.10000
    REFLECTANCE_MULT_BAND_1 = 2.0000E-05
    REFLECTANCE_MULT_BAND_2 = 2.0000E-05
    REFLECTANCE_MULT_BAND_3 = 2.0000E-05
    REFLECTANCE_MULT_BAND_4 = 2.0000E-05
    REFLECTANCE_MULT_BAND_5 = 2.0000E-05
    REFLECTANCE_MULT_BAND_6 = 2.0000E-05
    REFLECTANCE_MULT_BAND_7 = 2.0000E-05
    REFLECTANCE_MULT_BAND_8 = 2.0000E-05
    REFLECTANCE_MULT_BAND_9 = 2.0000E-05
    REFLECTANCE_ADD_BAND_1 = -0.100000
    REFLECTANCE_ADD_BAND_2 = -0.100000
    REFLECTANCE_ADD_BAND_3 = -0.100000
    REFLECTANCE_ADD_BAND_4 = -0.100000
    REFLECTANCE_ADD_BAND_5 = -0.100000
    REFLECTANCE_ADD_BAND_6 = -0.100000
    REFLECTANCE_ADD_BAND_7 = -0.100000
    REFLECTANCE_ADD_BAND_8 = -0.100000
    REFLECTANCE_ADD_BAND_9 = -0.100000
  END_GROUP = LEVEL1_RADIOMETRIC_RESCALING
  GROUP = LEVEL1_THERMAL_CONSTANTS
    K1_CONSTANT_BAND_10 = 799.0284
    K2_CONSTANT_BAND_10 = 1329.2405
    K1_CONSTANT_BAND_11 = 475.6581
    K2_CONSTANT_BAND_11 = 1198.3494
  END_GROUP = LEVEL1_THERMAL_CONSTANTS
  GROUP = LEVEL1_PROJECTION_PARAMETERS
    MAP_PROJECTION = "UTM"
    DATUM = "WGS84"
    ELLIPSOID = "WGS84"
    UTM_ZONE = 58
    GRID_CELL_SIZE_PANCHROMATIC = 15.00
    GRID_CELL_SIZE_REFLECTIVE = 30.00
    GRID_CELL_SIZE_THERMAL = 30.00
    ORIENTATION = "NORTH_UP"
    RESAMPLING_OPTION = "CUBIC_CONVOLUTION"
  END_GROUP = LEVEL1_PROJECTION_PARAMETERS
END_GROUP = LANDSAT_METADATA_FILE
END
```

Appendix C L9 Level 1 XML Metadata Example


```xml
<?xml version="1.0" encoding="UTF-8"?>

-<LANDSAT_METADATA_FILE>

-<PRODUCT_CONTENTS>

<ORIGIN>Image courtesy of the U.S. Geological Survey</ORIGIN>

<DIGITAL_OBJECT_IDENTIFIER>https://doi.org/10.5066/P975CC9B</DIGITAL_OBJECT_IDENTIFIER>

<LANDSAT_PRODUCT_ID>LC09_L1TP_097018_20211118_20211118_02_T2</LANDSAT_PRODUCT_ID>

<PROCESSING_LEVEL>L1TP</PROCESSING_LEVEL>

<COLLECTION_NUMBER>02</COLLECTION_NUMBER>

<COLLECTION_CATEGORY>T2</COLLECTION_CATEGORY>

<OUTPUT_FORMAT>GEOTIFF</OUTPUT_FORMAT>

<FILE_NAME_BAND_1>LC09_L1TP_097018_20211118_20211118_02_T2_B1.TIF</FILE_NAME_BAND_1>

<FILE_NAME_BAND_2>LC09_L1TP_097018_20211118_20211118_02_T2_B2.TIF</FILE_NAME_BAND_2>

<FILE_NAME_BAND_3>LC09_L1TP_097018_20211118_20211118_02_T2_B3.TIF</FILE_NAME_BAND_3>

<FILE_NAME_BAND_4>LC09_L1TP_097018_20211118_20211118_02_T2_B4.TIF</FILE_NAME_BAND_4>

<FILE_NAME_BAND_5>LC09_L1TP_097018_20211118_20211118_02_T2_B5.TIF</FILE_NAME_BAND_5>

<FILE_NAME_BAND_6>LC09_L1TP_097018_20211118_20211118_02_T2_B6.TIF</FILE_NAME_BAND_6>

<FILE_NAME_BAND_7>LC09_L1TP_097018_20211118_20211118_02_T2_B7.TIF</FILE_NAME_BAND_7>

<FILE_NAME_BAND_8>LC09_L1TP_097018_20211118_20211118_02_T2_B8.TIF</FILE_NAME_BAND_8>

<FILE_NAME_BAND_9>LC09_L1TP_097018_20211118_20211118_02_T2_B9.TIF</FILE_NAME_BAND_9>

<FILE_NAME_BAND_10>LC09_L1TP_097018_20211118_20211118_02_T2_B10.TIF</FILE_NAME_BAND_10>
```

<FILE_NAME_BAND_11>LC09_L1TP_097018_20211118_20211118_02_T2_B11.TIF</FILE_NAME_BAND_11>

<FILE_NAME_QUALITY_L1_PIXEL>LC09_L1TP_097018_20211118_20211118_02_T2_QA_PIXEL.TIF</FILE_NAME_QUALITY_L1_PIXEL>

<FILE_NAME_QUALITY_L1_RADIOMETRIC_SATURATION>LC09_L1TP_097018_20211118_20211118_02_T2_QA_RADSAT.TIF</FILE_NAME_QUALITY_L1_RADIOMETRIC_SATURATION>

<FILE_NAME_ANGLE_COEFFICIENT>LC09_L1TP_097018_20211118_20211118_02_T2_ANG.txt</FILE_NAME_ANGLE_COEFFICIENT>

<FILE_NAME_ANGLE_SENSOR_AZIMUTH_BAND_4>LC09_L1TP_097018_20211118_20211118_02_T2_VAA.TIF</FILE_NAME_ANGLE_SENSOR_AZIMUTH_BAND_4>

<FILE_NAME_ANGLE_SENSOR_ZENITH_BAND_4>LC09_L1TP_097018_20211118_20211118_02_T2_VZA.TIF</FILE_NAME_ANGLE_SENSOR_ZENITH_BAND_4>

<FILE_NAME_ANGLE_SOLAR_AZIMUTH_BAND_4>LC09_L1TP_097018_20211118_20211118_02_T2_SAA.TIF</FILE_NAME_ANGLE_SOLAR_AZIMUTH_BAND_4>

<FILE_NAME_ANGLE_SOLAR_ZENITH_BAND_4>LC09_L1TP_097018_20211118_20211118_02_T2_SZA.TIF</FILE_NAME_ANGLE_SOLAR_ZENITH_BAND_4>

<FILE_NAME_METADATA_ODL>LC09_L1TP_097018_20211118_20211118_02_T2_MTL.txt</FILE_NAME_METADATA_ODL>

<FILE_NAME_METADATA_XML>LC09_L1TP_097018_20211118_20211118_02_T2_MTL.xml</FILE_NAME_METADATA_XML>

<DATA_TYPE_BAND_1>UINT16</DATA_TYPE_BAND_1>

<DATA_TYPE_BAND_2>UINT16</DATA_TYPE_BAND_2>

<DATA_TYPE_BAND_3>UINT16</DATA_TYPE_BAND_3>

<DATA_TYPE_BAND_4>UINT16</DATA_TYPE_BAND_4>

<DATA_TYPE_BAND_5>UINT16</DATA_TYPE_BAND_5>

<DATA_TYPE_BAND_6>UINT16</DATA_TYPE_BAND_6>

<DATA_TYPE_BAND_7>UINT16</DATA_TYPE_BAND_7>

<DATA_TYPE_BAND_8>UINT16</DATA_TYPE_BAND_8>

<DATA_TYPE_BAND_9>UINT16</DATA_TYPE_BAND_9>

<DATA_TYPE_BAND_10>UINT16</DATA_TYPE_BAND_10>

<DATA_TYPE_BAND_11>UINT16</DATA_TYPE_BAND_11>

<DATA_TYPE_QUALITY_L1_PIXEL>UINT16</DATA_TYPE_QUALITY_L1_PIXEL>

<DATA_TYPE_QUALITY_L1_RADIOMETRIC_SATURATION>UINT16</DATA_TYPE_QUALITY_L1_RADIOMETRIC_SATURATION>

<DATA_TYPE_ANGLE_SENSOR_AZIMUTH_BAND_4>INT16</DATA_TYPE_ANGLE_SENSOR_AZIMUTH_BAND_4>

<DATA_TYPE_ANGLE_SENSOR_ZENITH_BAND_4>INT16</DATA_TYPE_ANGLE_SENSOR_ZENITH_BAND_4>

<DATA_TYPE_ANGLE_SOLAR_AZIMUTH_BAND_4>INT16</DATA_TYPE_ANGLE_SOLAR_AZIMUTH_BAND_4>

<DATA_TYPE_ANGLE_SOLAR_ZENITH_BAND_4>INT16</DATA_TYPE_ANGLE_SOLAR_ZENITH_BAND_4>

</PRODUCT_CONTENTS>

-<IMAGE_ATTRIBUTES>

<SPACECRAFT_ID>LANDSAT_9</SPACECRAFT_ID>

<SENSOR_ID>OLI_TIRS</SENSOR_ID>

<WRS_TYPE>2</WRS_TYPE>

<WRS_PATH>97</WRS_PATH>

<WRS_ROW>18</WRS_ROW>

<NADIR_OFFNADIR>NADIR</NADIR_OFFNADIR>

<TARGET_WRS_PATH>97</TARGET_WRS_PATH>

<TARGET_WRS_ROW>18</TARGET_WRS_ROW>

<DATE_ACQUIRED>2021-11-18</DATE_ACQUIRED>

<SCENE_CENTER_TIME>00:09:42.9336170Z</SCENE_CENTER_TIME>

<STATION_ID>LGN</STATION_ID>

<CLOUD_COVER>60.23</CLOUD_COVER>

<CLOUD_COVER_LAND>75.79</CLOUD_COVER_LAND>

<IMAGE_QUALITY_OLI>9</IMAGE_QUALITY_OLI>

<IMAGE_QUALITY_TIRS>9</IMAGE_QUALITY_TIRS>

<SATURATION_BAND_1>N</SATURATION_BAND_1>

<SATURATION_BAND_2>N</SATURATION_BAND_2>

<SATURATION_BAND_3>N</SATURATION_BAND_3>

<SATURATION_BAND_4>N</SATURATION_BAND_4>

<SATURATION_BAND_5>N</SATURATION_BAND_5>

<SATURATION_BAND_6>N</SATURATION_BAND_6>

<SATURATION_BAND_7>N</SATURATION_BAND_7>

<SATURATION_BAND_8>N</SATURATION_BAND_8>

<SATURATION_BAND_9>N</SATURATION_BAND_9>

<ROLL_ANGLE>-0.001</ROLL_ANGLE>

<SUN_AZIMUTH>171.61700481</SUN_AZIMUTH>

<SUN_ELEVATION>10.36432742</SUN_ELEVATION>

<EARTH_SUN_DISTANCE>0.9885441</EARTH_SUN_DISTANCE>

</IMAGE_ATTRIBUTES>

-<PROJECTION_ATTRIBUTES>

<MAP_PROJECTION>UTM</MAP_PROJECTION>

<DATUM>WGS84</DATUM>

<ELLIPSOID>WGS84</ELLIPSOID>

<UTM_ZONE>58</UTM_ZONE>

<GRID_CELL_SIZE_PANCHROMATIC>15.00</GRID_CELL_SIZE_PANCHROMATIC>

<GRID_CELL_SIZE_REFLECTIVE>30.00</GRID_CELL_SIZE_REFLECTIVE>

<GRID_CELL_SIZE_THERMAL>30.00</GRID_CELL_SIZE_THERMAL>

<PANCHROMATIC_LINES>16401</PANCHROMATIC_LINES>

<PANCHROMATIC_SAMPLES>16161</PANCHROMATIC_SAMPLES>

<REFLECTIVE_LINES>8201</REFLECTIVE_LINES>

<REFLECTIVE_SAMPLES>8081</REFLECTIVE_SAMPLES>

<THERMAL_LINES>8201</THERMAL_LINES>

<THERMAL_SAMPLES>8081</THERMAL_SAMPLES>

<ORIENTATION>NORTH_UP</ORIENTATION>

<CORNER_UL_LAT_PRODUCT>61.17524</CORNER_UL_LAT_PRODUCT>

<CORNER_UL_LON_PRODUCT>162.85426</CORNER_UL_LON_PRODUCT>

<CORNER_UR_LAT_PRODUCT>61.17165</CORNER_UR_LAT_PRODUCT>

<CORNER_UR_LON_PRODUCT>167.36123</CORNER_UR_LON_PRODUCT>

<CORNER_LL_LAT_PRODUCT>58.96781</CORNER_LL_LAT_PRODUCT>

<CORNER_LL_LON_PRODUCT>162.99306</CORNER_LL_LON_PRODUCT>

<CORNER_LR_LAT_PRODUCT>58.96453</CORNER_LR_LAT_PRODUCT>

<CORNER_LR_LON_PRODUCT>167.20851</CORNER_LR_LON_PRODUCT>

<CORNER_UL_PROJECTION_X_PRODUCT>384600.000</CORNER_UL_PROJECTION_X_PRODUCT>

<CORNER_UL_PROJECTION_Y_PRODUCT>6784200.000</CORNER_UL_PROJECTION_Y_PRODUCT>

<CORNER_UR_PROJECTION_X_PRODUCT>627000.000</CORNER_UR_PROJECTION_X_PRODUCT>

<CORNER_UR_PROJECTION_Y_PRODUCT>6784200.000</CORNER_UR_PROJECTION_Y_PRODUCT>

<CORNER_LL_PROJECTION_X_PRODUCT>384600.000</CORNER_LL_PROJECTION_X_PRODUCT>

<CORNER_LL_PROJECTION_Y_PRODUCT>6538200.000</CORNER_LL_PROJECTION_Y_PRODUCT>

<CORNER_LR_PROJECTION_X_PRODUCT>627000.000</CORNER_LR_PROJECTION_X_PRODUCT>

<CORNER_LR_PROJECTION_Y_PRODUCT>6538200.000</CORNER_LR_PROJECTION_Y_PRODUCT>

</PROJECTION_ATTRIBUTES>

-<LEVEL1_PROCESSING_RECORD>

<ORIGIN>Image courtesy of the U.S. Geological Survey</ORIGIN>

<DIGITAL_OBJECT_IDENTIFIER>https://doi.org/10.5066/P975CC9B</DIGITAL_OBJECT_IDENTIFIER>

<REQUEST_ID>P7014iw57qhrf_00002</REQUEST_ID>

<LANDSAT_SCENE_ID>LC90970182021322LGN00</LANDSAT_SCENE_ID>

<LANDSAT_PRODUCT_ID>LC09_L1TP_097018_20211118_20211118_02_T2</LANDSAT_PRODUCT_ID>

<PROCESSING_LEVEL>L1TP</PROCESSING_LEVEL>

<COLLECTION_CATEGORY>T2</COLLECTION_CATEGORY>

<OUTPUT_FORMAT>GEOTIFF</OUTPUT_FORMAT>

<DATE_PRODUCT_GENERATED>2021-11-18T02:17:19Z</DATE_PRODUCT_GENERATED>

<PROCESSING_SOFTWARE_VERSION>LPGS_15.5.0</PROCESSING_SOFTWARE_VERSION>

<FILE_NAME_BAND_1>LC09_L1TP_097018_20211118_20211118_02_T2_B1.TIF</FILE_NAME_BAND_1>

<FILE_NAME_BAND_2>LC09_L1TP_097018_20211118_20211118_02_T2_B2.TIF</FILE_NAME_BAND_2>

<FILE_NAME_BAND_3>LC09_L1TP_097018_20211118_20211118_02_T2_B3.TIF</FILE_NAME_BAND_3>

<FILE_NAME_BAND_4>LC09_L1TP_097018_20211118_20211118_02_T2_B4.TIF</FILE_NAME_BAND_4>

<FILE_NAME_BAND_5>LC09_L1TP_097018_20211118_20211118_02_T2_B5.TIF</FILE_NAME_BAND_5>

<FILE_NAME_BAND_6>LC09_L1TP_097018_20211118_20211118_02_T2_B6.TIF</FILE_NAME_BAND_6>

<FILE_NAME_BAND_7>LC09_L1TP_097018_20211118_20211118_02_T2_B7.TIF</FILE_NAME_BAND_7>

<FILE_NAME_BAND_8>LC09_L1TP_097018_20211118_20211118_02_T2_B8.TIF</FILE_NAME_BAND_8>

<FILE_NAME_BAND_9>LC09_L1TP_097018_20211118_20211118_02_T2_B9.TIF</FILE_NAME_BAND_9>

<FILE_NAME_BAND_10>LC09_L1TP_097018_20211118_20211118_02_T2_B10.TIF</FILE_NAME_BAND_10>

<FILE_NAME_BAND_11>LC09_L1TP_097018_20211118_20211118_02_T2_B11.TIF</FILE_NAME_BAND_11>

<FILE_NAME_QUALITY_L1_PIXEL>LC09_L1TP_097018_20211118_20211118_02_T2_QA_PIXEL.TIF</FILE_NAME_QUALITY_L1_PIXEL>

<FILE_NAME_QUALITY_L1_RADIOMETRIC_SATURATION>LC09_L1TP_097018_20211118_20211118_02_T2_QA_RADSAT.TIF</FILE_NAME_QUALITY_L1_RADIOMETRIC_SATURATION>

<FILE_NAME_ANGLE_COEFFICIENT>LC09_L1TP_097018_20211118_20211118_02_T2_ANG.txt</FILE_NAME_ANGLE_COEFFICIENT>

<FILE_NAME_ANGLE_SENSOR_AZIMUTH_BAND_4>LC09_L1TP_097018_20211118_20211118_02_T2_VAA.TIF</FILE_NAME_ANGLE_SENSOR_AZIMUTH_BAND_4>

<FILE_NAME_ANGLE_SENSOR_ZENITH_BAND_4>LC09_L1TP_097018_20211118_20211118_02_T2_VZA.TIF</FILE_NAME_ANGLE_SENSOR_ZENITH_BAND_4>

<FILE_NAME_ANGLE_SOLAR_AZIMUTH_BAND_4>LC09_L1TP_097018_20211118_20211118_02_T2_SAA.TIF</FILE_NAME_ANGLE_SOLAR_AZIMUTH_BAND_4>

<FILE_NAME_ANGLE_SOLAR_ZENITH_BAND_4>LC09_L1TP_097018_20211118_20211118_02_T2_SZA.TIF</FILE_NAME_ANGLE_SOLAR_ZENITH_BAND_4>

<FILE_NAME_METADATA_ODL>LC09_L1TP_097018_20211118_20211118_02_T2_MTL.txt</FILE_NAME_METADATA_ODL>

<FILE_NAME_METADATA_XML>LC09_L1TP_097018_20211118_20211118_02_T2_MTL.xml</FILE_NAME_METADATA_XML>

<FILE_NAME_CPF>LC09CPF_20210927_20211231_02.02</FILE_NAME_CPF>

<FILE_NAME_BPF_OLI>LO9BPF20211117223222_20211118000816.01</FILE_NAME_BPF_OLI>

<FILE_NAME_BPF_TIRS>LT9BPF20211117225516_20211118000344.01</FILE_NAME_BPF_TIRS>

<FILE_NAME_RLUT>LC09RLUT_20210927_20531231_02_03.h5</FILE_NAME_RLUT>

<DATA_SOURCE_ELEVATION>GLS2000</DATA_SOURCE_ELEVATION>

<GROUND_CONTROL_POINTS_VERSION>5</GROUND_CONTROL_POINTS_VERSION>

<GROUND_CONTROL_POINTS_MODEL>51</GROUND_CONTROL_POINTS_MODEL>

<GEOMETRIC_RMSE_MODEL>21.406</GEOMETRIC_RMSE_MODEL>

<GEOMETRIC_RMSE_MODEL_Y>16.370</GEOMETRIC_RMSE_MODEL_Y>

<GEOMETRIC_RMSE_MODEL_X>13.792</GEOMETRIC_RMSE_MODEL_X>

</LEVEL1_PROCESSING_RECORD>

-<LEVEL1_MIN_MAX_RADIANCE>

<RADIANCE_MAXIMUM_BAND_1>804.93738</RADIANCE_MAXIMUM_BAND_1>

<RADIANCE_MINIMUM_BAND_1>-66.47199</RADIANCE_MINIMUM_BAND_1>

<RADIANCE_MAXIMUM_BAND_2>837.14374</RADIANCE_MAXIMUM_BAND_2>

<RADIANCE_MINIMUM_BAND_2>-69.13160</RADIANCE_MINIMUM_BAND_2>

<RADIANCE_MAXIMUM_BAND_3>771.03668</RADIANCE_MAXIMUM_BAND_3>

<RADIANCE_MINIMUM_BAND_3>-63.67246</RADIANCE_MINIMUM_BAND_3>

<RADIANCE_MAXIMUM_BAND_4>639.18402</RADIANCE_MAXIMUM_BAND_4>

<RADIANCE_MINIMUM_BAND_4>-52.78402</RADIANCE_MINIMUM_BAND_4>

<RADIANCE_MAXIMUM_BAND_5>379.03827</RADIANCE_MAXIMUM_BAND_5>

<RADIANCE_MINIMUM_BAND_5>-31.30110</RADIANCE_MINIMUM_BAND_5>

<RADIANCE_MAXIMUM_BAND_6>94.97116</RADIANCE_MAXIMUM_BAND_6>

<RADIANCE_MINIMUM_BAND_6>-7.84275</RADIANCE_MINIMUM_BAND_6>

<RADIANCE_MAXIMUM_BAND_7>32.11728</RADIANCE_MAXIMUM_BAND_7>

<RADIANCE_MINIMUM_BAND_7>-2.65226</RADIANCE_MINIMUM_BAND_7>

<RADIANCE_MAXIMUM_BAND_8>712.98907</RADIANCE_MAXIMUM_BAND_8>

<RADIANCE_MINIMUM_BAND_8>-58.87887</RADIANCE_MINIMUM_BAND_8>

<RADIANCE_MAXIMUM_BAND_9>143.33020</RADIANCE_MAXIMUM_BAND_9>

<RADIANCE_MINIMUM_BAND_9>-11.83626</RADIANCE_MINIMUM_BAND_9>

<RADIANCE_MAXIMUM_BAND_10>25.00330</RADIANCE_MAXIMUM_BAND_10>

<RADIANCE_MINIMUM_BAND_10>0.10038</RADIANCE_MINIMUM_BAND_10>

<RADIANCE_MAXIMUM_BAND_11>22.97172</RADIANCE_MAXIMUM_BAND_11>

<RADIANCE_MINIMUM_BAND_11>0.10035</RADIANCE_MINIMUM_BAND_11>

</LEVEL1_MIN_MAX_RADIANCE>

-<LEVEL1_MIN_MAX_REFLECTANCE>

<REFLECTANCE_MAXIMUM_BAND_1>1.210700</REFLECTANCE_MAXIMUM_BAND_1>

<REFLECTANCE_MINIMUM_BAND_1>-0.099980</REFLECTANCE_MINIMUM_BAND_1>

<REFLECTANCE_MAXIMUM_BAND_2>1.210700</REFLECTANCE_MAXIMUM_BAND_2>

<REFLECTANCE_MINIMUM_BAND_2>-0.099980</REFLECTANCE_MINIMUM_BAND_2>

<REFLECTANCE_MAXIMUM_BAND_3>1.210700</REFLECTANCE_MAXIMUM_BAND_3>

<REFLECTANCE_MINIMUM_BAND_3>-0.099980</REFLECTANCE_MINIMUM_BAND_3>

<REFLECTANCE_MAXIMUM_BAND_4>1.210700</REFLECTANCE_MAXIMUM_BAND_4>

<REFLECTANCE_MINIMUM_BAND_4>-0.099980</REFLECTANCE_MINIMUM_BAND_4>

<REFLECTANCE_MAXIMUM_BAND_5>1.210700</REFLECTANCE_MAXIMUM_BAND_5>

<REFLECTANCE_MINIMUM_BAND_5>-0.099980</REFLECTANCE_MINIMUM_BAND_5>

<REFLECTANCE_MAXIMUM_BAND_6>1.210700</REFLECTANCE_MAXIMUM_BAND_6>

<REFLECTANCE_MINIMUM_BAND_6>-0.099980</REFLECTANCE_MINIMUM_BAND_6>

<REFLECTANCE_MAXIMUM_BAND_7>1.210700</REFLECTANCE_MAXIMUM_BAND_7>

<REFLECTANCE_MINIMUM_BAND_7>-0.099980</REFLECTANCE_MINIMUM_BAND_7>

<REFLECTANCE_MAXIMUM_BAND_8>1.210700</REFLECTANCE_MAXIMUM_BAND_8>

<REFLECTANCE_MINIMUM_BAND_8>-0.099980</REFLECTANCE_MINIMUM_BAND_8>

<REFLECTANCE_MAXIMUM_BAND_9>1.210700</REFLECTANCE_MAXIMUM_BAND_9>

<REFLECTANCE_MINIMUM_BAND_9>-0.099980</REFLECTANCE_MINIMUM_BAND_9>

</LEVEL1_MIN_MAX_REFLECTANCE>

-<LEVEL1_MIN_MAX_PIXEL_VALUE>

<QUANTIZE_CAL_MAX_BAND_1>65535</QUANTIZE_CAL_MAX_BAND_1>

<QUANTIZE_CAL_MIN_BAND_1>1</QUANTIZE_CAL_MIN_BAND_1>

<QUANTIZE_CAL_MAX_BAND_2>65535</QUANTIZE_CAL_MAX_BAND_2>

<QUANTIZE_CAL_MIN_BAND_2>1</QUANTIZE_CAL_MIN_BAND_2>

<QUANTIZE_CAL_MAX_BAND_3>65535</QUANTIZE_CAL_MAX_BAND_3>

<QUANTIZE_CAL_MIN_BAND_3>1</QUANTIZE_CAL_MIN_BAND_3>

<QUANTIZE_CAL_MAX_BAND_4>65535</QUANTIZE_CAL_MAX_BAND_4>

<QUANTIZE_CAL_MIN_BAND_4>1</QUANTIZE_CAL_MIN_BAND_4>

<QUANTIZE_CAL_MAX_BAND_5>65535</QUANTIZE_CAL_MAX_BAND_5>

<QUANTIZE_CAL_MIN_BAND_5>1</QUANTIZE_CAL_MIN_BAND_5>

<QUANTIZE_CAL_MAX_BAND_6>65535</QUANTIZE_CAL_MAX_BAND_6>

<QUANTIZE_CAL_MIN_BAND_6>1</QUANTIZE_CAL_MIN_BAND_6>

<QUANTIZE_CAL_MAX_BAND_7>65535</QUANTIZE_CAL_MAX_BAND_7>

<QUANTIZE_CAL_MIN_BAND_7>1</QUANTIZE_CAL_MIN_BAND_7>

<QUANTIZE_CAL_MAX_BAND_8>65535</QUANTIZE_CAL_MAX_BAND_8>

<QUANTIZE_CAL_MIN_BAND_8>1</QUANTIZE_CAL_MIN_BAND_8>

<QUANTIZE_CAL_MAX_BAND_9>65535</QUANTIZE_CAL_MAX_BAND_9>

<QUANTIZE_CAL_MIN_BAND_9>1</QUANTIZE_CAL_MIN_BAND_9>

<QUANTIZE_CAL_MAX_BAND_10>65535</QUANTIZE_CAL_MAX_BAND_10>

<QUANTIZE_CAL_MIN_BAND_10>1</QUANTIZE_CAL_MIN_BAND_10>

<QUANTIZE_CAL_MAX_BAND_11>65535</QUANTIZE_CAL_MAX_BAND_11>

<QUANTIZE_CAL_MIN_BAND_11>1</QUANTIZE_CAL_MIN_BAND_11>

</LEVEL1_MIN_MAX_PIXEL_VALUE>

-<LEVEL1_RADIOMETRIC_RESCALING>

<RADIANCE_MULT_BAND_1>1.3297E-02</RADIANCE_MULT_BAND_1>

<RADIANCE_MULT_BAND_2>1.3829E-02</RADIANCE_MULT_BAND_2>

<RADIANCE_MULT_BAND_3>1.2737E-02</RADIANCE_MULT_BAND_3>

<RADIANCE_MULT_BAND_4>1.0559E-02</RADIANCE_MULT_BAND_4>

<RADIANCE_MULT_BAND_5>6.2615E-03</RADIANCE_MULT_BAND_5>

<RADIANCE_MULT_BAND_6>1.5689E-03</RADIANCE_MULT_BAND_6>

<RADIANCE_MULT_BAND_7>5.3056E-04</RADIANCE_MULT_BAND_7>

<RADIANCE_MULT_BAND_8>1.1778E-02</RADIANCE_MULT_BAND_8>

<RADIANCE_MULT_BAND_9>2.3677E-03</RADIANCE_MULT_BAND_9>

<RADIANCE_MULT_BAND_10>3.8000E-04</RADIANCE_MULT_BAND_10>

<RADIANCE_MULT_BAND_11>3.4900E-04</RADIANCE_MULT_BAND_11>

<RADIANCE_ADD_BAND_1>-66.48529</RADIANCE_ADD_BAND_1>

<RADIANCE_ADD_BAND_2>-69.14543</RADIANCE_ADD_BAND_2>

<RADIANCE_ADD_BAND_3>-63.68520</RADIANCE_ADD_BAND_3>

<RADIANCE_ADD_BAND_4>-52.79458</RADIANCE_ADD_BAND_4>

<RADIANCE_ADD_BAND_5>-31.30737</RADIANCE_ADD_BAND_5>

<RADIANCE_ADD_BAND_6>-7.84432</RADIANCE_ADD_BAND_6>

<RADIANCE_ADD_BAND_7>-2.65279</RADIANCE_ADD_BAND_7>

<RADIANCE_ADD_BAND_8>-58.89065</RADIANCE_ADD_BAND_8>

<RADIANCE_ADD_BAND_9>-11.83862</RADIANCE_ADD_BAND_9>

<RADIANCE_ADD_BAND_10>0.10000</RADIANCE_ADD_BAND_10>

<RADIANCE_ADD_BAND_11>0.10000</RADIANCE_ADD_BAND_11>

<REFLECTANCE_MULT_BAND_1>2.0000E-05</REFLECTANCE_MULT_BAND_1>

<REFLECTANCE_MULT_BAND_2>2.0000E-05</REFLECTANCE_MULT_BAND_2>

<REFLECTANCE_MULT_BAND_3>2.0000E-05</REFLECTANCE_MULT_BAND_3>

<REFLECTANCE_MULT_BAND_4>2.0000E-05</REFLECTANCE_MULT_BAND_4>

<REFLECTANCE_MULT_BAND_5>2.0000E-05</REFLECTANCE_MULT_BAND_5>

<REFLECTANCE_MULT_BAND_6>2.0000E-05</REFLECTANCE_MULT_BAND_6>

<REFLECTANCE_MULT_BAND_7>2.0000E-05</REFLECTANCE_MULT_BAND_7>

<REFLECTANCE_MULT_BAND_8>2.0000E-05</REFLECTANCE_MULT_BAND_8>

<REFLECTANCE_MULT_BAND_9>2.0000E-05</REFLECTANCE_MULT_BAND_9>

<REFLECTANCE_ADD_BAND_1>-0.100000</REFLECTANCE_ADD_BAND_1>

<REFLECTANCE_ADD_BAND_2>-0.100000</REFLECTANCE_ADD_BAND_2>

<REFLECTANCE_ADD_BAND_3>-0.100000</REFLECTANCE_ADD_BAND_3>

<REFLECTANCE_ADD_BAND_4>-0.100000</REFLECTANCE_ADD_BAND_4>

<REFLECTANCE_ADD_BAND_5>-0.100000</REFLECTANCE_ADD_BAND_5>

<REFLECTANCE_ADD_BAND_6>-0.100000</REFLECTANCE_ADD_BAND_6>

<REFLECTANCE_ADD_BAND_7>-0.100000</REFLECTANCE_ADD_BAND_7>

<REFLECTANCE_ADD_BAND_8>-0.100000</REFLECTANCE_ADD_BAND_8>

<REFLECTANCE_ADD_BAND_9>-0.100000</REFLECTANCE_ADD_BAND_9>

</LEVEL1_RADIOMETRIC_RESCALING>

-<LEVEL1_THERMAL_CONSTANTS>

<K1_CONSTANT_BAND_10>799.0284</K1_CONSTANT_BAND_10>

<K2_CONSTANT_BAND_10>1329.2405</K2_CONSTANT_BAND_10>

<K1_CONSTANT_BAND_11>475.6581</K1_CONSTANT_BAND_11>

<K2_CONSTANT_BAND_11>1198.3494</K2_CONSTANT_BAND_11>

</LEVEL1_THERMAL_CONSTANTS>

+<LEVEL1_PROJECTION_PARAMETERS>

</LANDSAT_METADATA_FILE>

Appendix D Observatory Component Systems

D.1 Observatory Component Reference Systems

L9 IAS geometry algorithms use ten coordinate systems. These coordinate systems are referred to frequently in this document and are briefly defined here. They are presented in the order in which they would be used to transform a detector and sample time into a ground position.

D.2 OLI-2 Instrument LOS Coordinate System

The OLI-2 LOS coordinate system is used to define the band and detector pointing directions relative to the instrument axes. These pointing directions are used to construct LOS vectors for individual detector samples. This coordinate system is defined so that the Z-axis is parallel to the telescope boresight axis and is positive toward the OLI aperture. The origin is where this axis intersects the OLI-2 focal plane.

The X-axis is parallel to the along-track direction, with the positive direction toward the leading, odd numbered SCAs (see Figure D-1). The Y-axis is in the across-track direction with the positive direction toward SCA01. This definition makes the OLI-2 coordinate system nominally parallel to the spacecraft coordinate system, with the difference being due to residual misalignment between the OLI-2 and the spacecraft body.

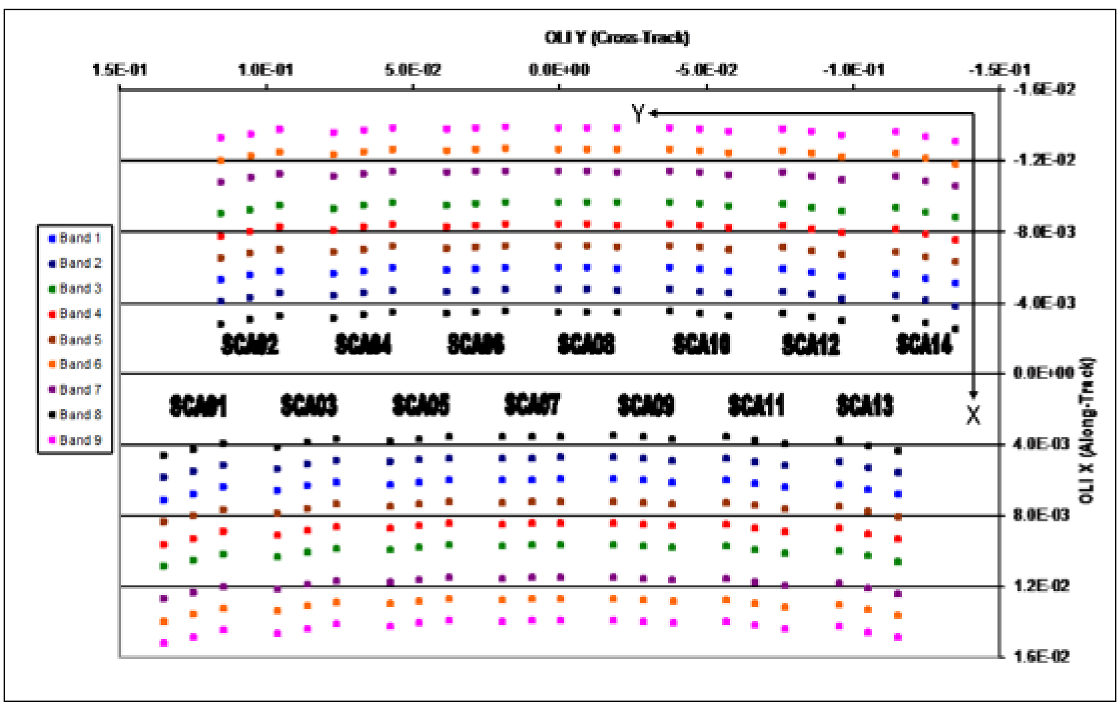

Figure D-1. OLI Line-of-Sight Coordinate System

D.3 TIRS-2 Instrument Coordinate System

The orientations of the TIRS-2 detector LOS directions and of the TIRS-2 SSM are both defined within the TIRS-2 instrument coordinate system. TIRS-2 LOS coordinates define the band and detector-pointing directions relative to the instrument axes. These pointing directions are used to construct LOS vectors for individual detector samples. The vectors are then reflected off the SSM to direct them out of the TIRS aperture for Earth viewing. The TIRS-2 LOS model is formulated so that the effect of a nominally pointed SSM is included in the definition of the detector lines-of-sight, with departures from nominal SSM pointing causing perturbations to these lines-of-sight. This formulation allows TIRS-2 LOS construction to be very similar to OLI-2. This is described in detail below, in the TIRS-2 LOS Model Creation algorithm.

The TIRS-2 coordinate system is defined so that the Z-axis is parallel to the TIRS-2 boresight axis and is positive toward the TIRS aperture. The origin is where this axis intersects the TIRS-2 focal plane. The X-axis is parallel to the along-track direction, with the positive direction toward the leading SCA (SCA02 in Figure D-2). The Y-axis is in the across-track direction with the positive direction toward SCA03. This definition makes the TIRS-2 coordinate system nominally parallel to the spacecraft coordinate system, with the difference being due to residual misalignment between the TIRS-2 and the spacecraft body.

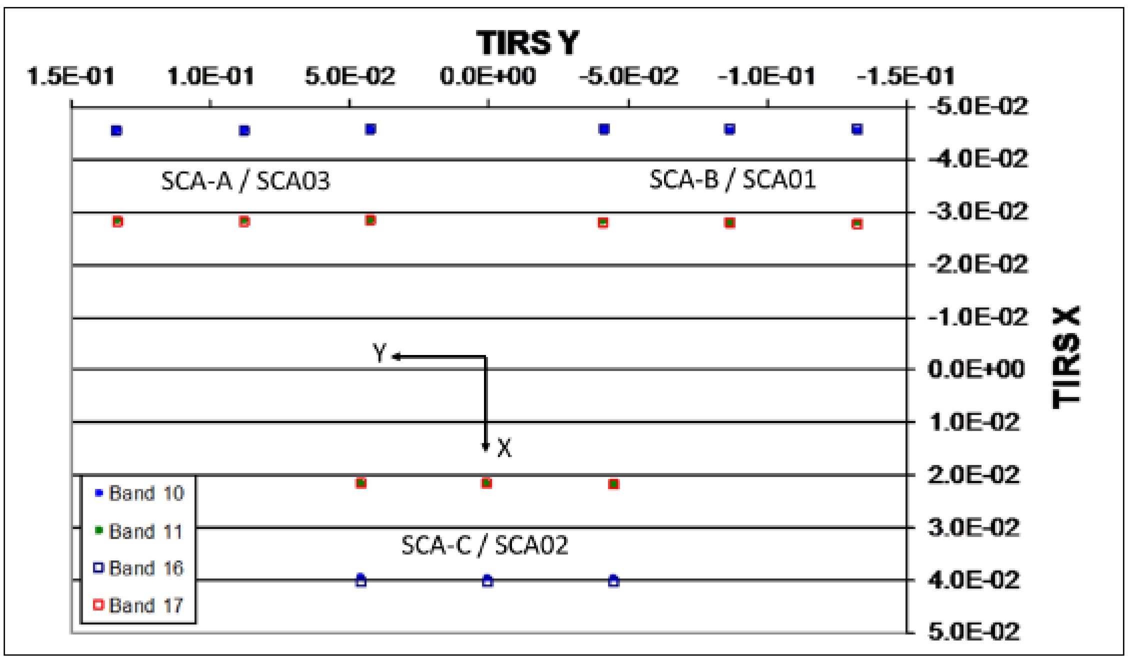

Figure D-2. TIRS Line-of-Sight Coordinates

D.4 Spacecraft Coordinate System

The spacecraft coordinate system is the spacecraft-body-fixed coordinate system used to relate the locations and orientations of the various spacecraft components to one another and to the OLI-2 and TIRS-2 instruments. It is defined with the +Z axis in the

Earth-facing direction, the +X axis in the nominal direction of flight, and the +Y axis toward the cold side of the spacecraft (opposite the solar array). This coordinate system is used during Observatory integration and prelaunch testing to determine prelaunch positions, alignments of the attitude control sensors (star trackers and SIRU), and the OLI-2 and TIRS-2 instrument payloads. The spacecraft coordinate system is nominally the same as the navigation reference system (see below) used for spacecraft attitude determination and control. However, for reasons explained below, these two coordinate systems are treated separately.

D.5 Navigation Reference Coordinate System

The navigation reference frame (a.k.a., the attitude control system reference) is the spacecraft-body-fixed coordinate system used for spacecraft attitude determination and control. The coordinate axes are defined by the spacecraft ACS, which attempts to keep the navigation reference frame aligned with the (yaw-steered) orbital coordinate system (for nominal nadir pointing) so that the OLI-2 and TIRS-2 boresight axes are always pointing toward the center of the Earth. The orientation of this coordinate system relative to the inertial coordinate system is captured in spacecraft attitude data.

Ideally, the navigation reference frame is the same as the spacecraft coordinate system. In practice, the navigation frame is based on the orientation of the absolute attitude sensor (i.e., star tracker) being used for attitude determination. Any errors in the orientation knowledge for this tracker with respect to the spacecraft body frame will lead to differences between the spacecraft and navigation coordinate systems. This becomes important if the absolute attitude sensor is changed, for example, by switching from the primary to the redundant star tracker during on-orbit operations. Such an event would effectively redefine the navigation frame to be based on the redundant tracker, with the difference between the spacecraft and navigation frames now resulting from redundant tracker alignment knowledge errors, rather than from primary tracker alignment knowledge errors. This redefinition would require updates to the on-orbit instrument-to-ACS alignment calibrations. Therefore, the spacecraft and navigation reference coordinate systems are different because the spacecraft coordinate system is fixed but the navigation reference can change.

D.6 SIRU Coordinate System

The spacecraft orientation rate data provided by the spacecraft attitude control system's inertial measurement unit are referenced to the SIRU coordinate system. The SIRU consists of four rotation-sensitive axes. This configuration provides redundancy to protect against the failure of any one axis. The four SIRU axis directions are determined relative to the SIRU coordinate system, the orientation of which is itself measured relative to the spacecraft coordinate system both prelaunch and on-orbit, as part of the ACS calibration procedure. The IAS uses this alignment transformation to convert the SIRU data contained in the L9 spacecraft ancillary data to the navigation reference coordinate system for blending with the ACS quaternions.

D.7 Orbital Coordinate System

The orbital coordinate system is centered at the spacecraft, and its orientation is based on the spacecraft position in inertial space (see Figure D-3). The origin is the spacecraft's center of mass, with the Z-axis pointing from the spacecraft's center of mass to the Earth's center of mass. The Y-axis is the normalized cross product of the Z-axis and the instantaneous (inertial) velocity vector and corresponds to the negative of the instantaneous angular momentum vector direction. The X-axis is the cross product of the Y- and Z-axes. The orbital coordinate system is used to convert spacecraft attitude, expressed as Earth-Centered Inertial (ECI) quaternions, to roll-pitch-yaw Euler angles.

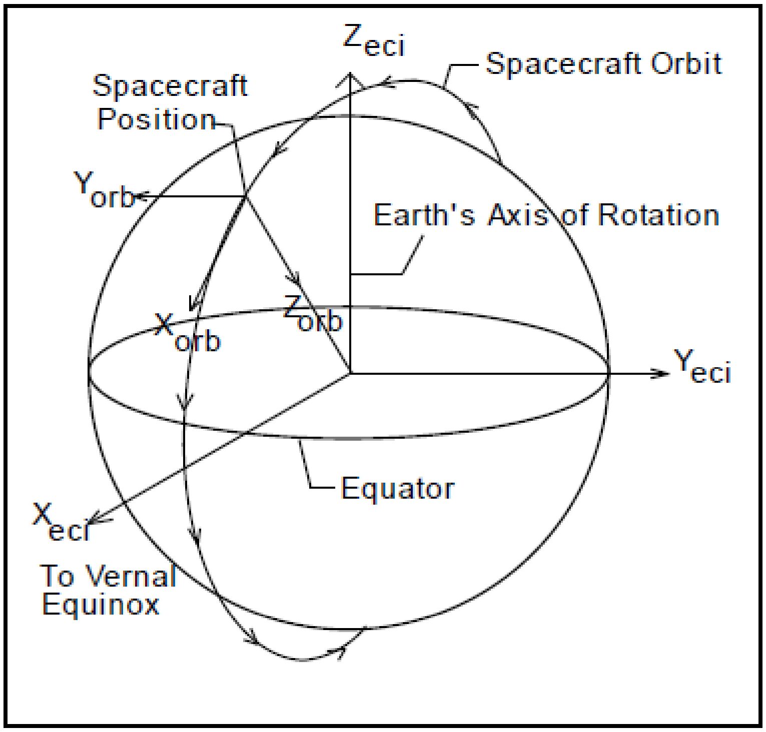

Figure D-3. Orbital Coordinate System

D.8 ECI J2000 Coordinate System

The ECI coordinate system of epoch J2000 is space-fixed with its origin at the Earth's center of mass (see Figure D-4). The Z-axis corresponds to the mean north celestial pole of epoch J2000.0. The X-axis is based on the mean vernal equinox of epoch J2000.0. The Y-axis is the cross product of the Z and X axes. This coordinate system is described in detail in the Explanatory Supplement to the Astronomical Almanac published by the U.S. Naval Observatory. Data in the ECI coordinate system are present in the L9 spacecraft ancillary data form of attitude quaternions that relate the navigation frame to the ECI J2000 coordinate system.

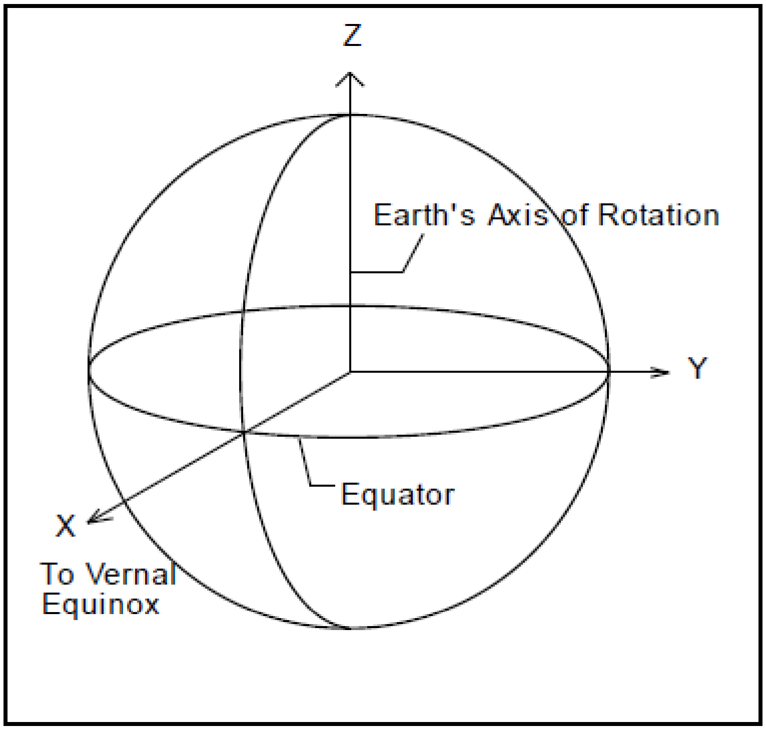

Figure D-4. Earth-Centered Inertial (ECI) Coordinate System

D.9 ECEF Coordinate System

The Earth-Centered, Earth-Fixed (ECEF) coordinate system is Earth-fixed with its origin at the Earth’s center of mass (see Figure D-5). It corresponds to the Conventional Terrestrial System defined by the Bureau International de l’Heure (BIH), which is the same as the WGS84 geocentric reference system. This coordinate system is described in the Supplement to Department of Defense World Geodetic System 1984 Technical Report, Part 1: Methods, Techniques, and Data Used in WGS84 Development, TR 8350.2-A, published by the NGA.

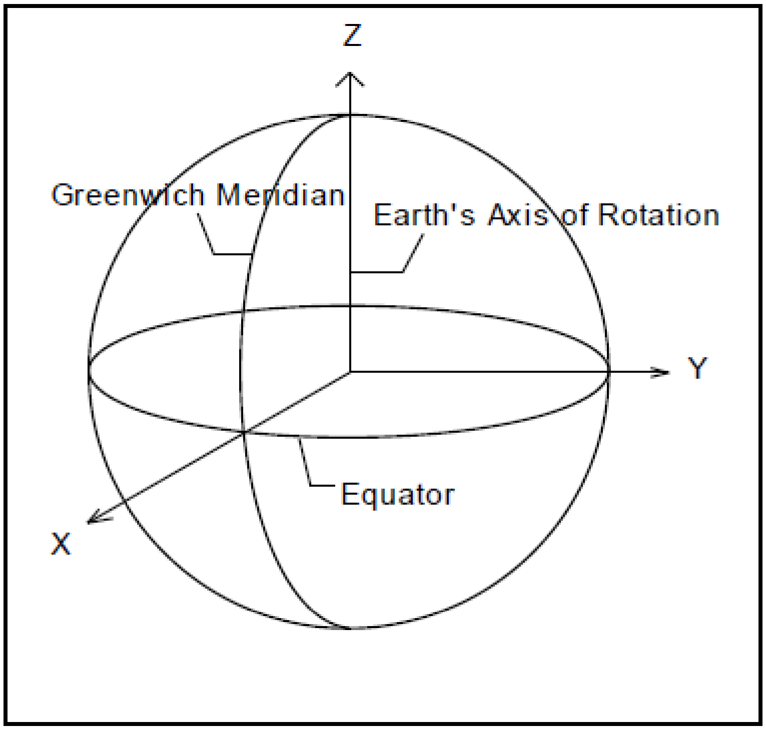

Figure D-5. Earth-Centered Earth-Fixed (ECEF) Coordinate System

D.10 Geodetic Coordinate System

The geodetic coordinate system is based on the WGS84 reference frame, with coordinates expressed in latitude, longitude, and height above the reference Earth ellipsoid (see Figure D-6). No ellipsoid is required by the definition of the ECEF coordinate system, but the geodetic coordinate system depends on the selection of an Earth ellipsoid. Latitude and longitude are defined as the angle between the ellipsoid normal and its projection onto the Equator, and the angle between the local meridian and the Greenwich meridian, respectively. The scene center and scene corner coordinates in the Level 0R product metadata are expressed in the geodetic coordinate system.

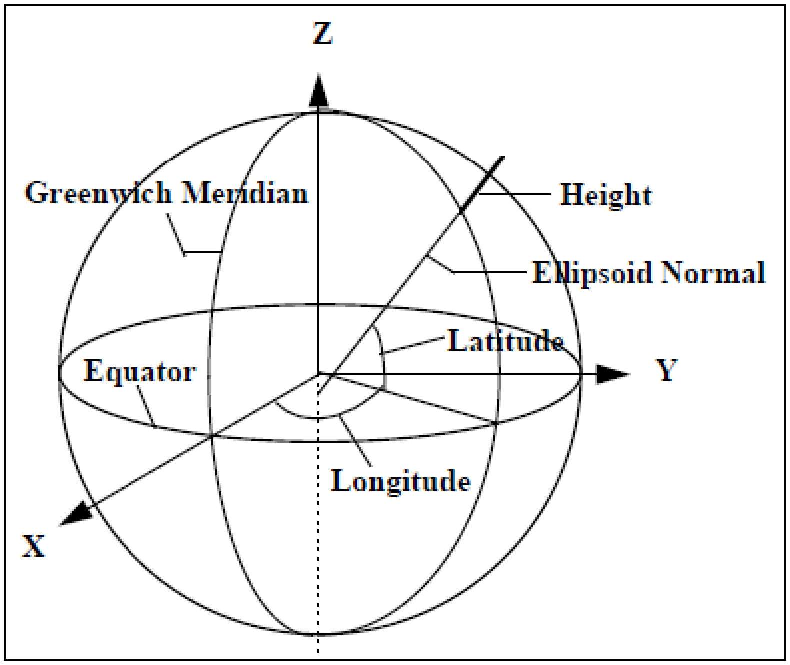

Figure D-6. Geodetic Coordinate System

D.11 Map Projection Coordinate System

L1 products are generated with respect to a map projection coordinate system, such as the UTM, which provides mapping from latitude and longitude to a plane coordinate system that approximates a Cartesian coordinate system for a portion of the Earth's surface. It is used for convenience as a method of providing digital image data in an Earth-referenced grid that is compatible with other ground-referenced datasets. Although the map projection coordinate system is only an approximation of a true local Cartesian coordinate system at the Earth's surface, the mathematical relationship between the map projection and geodetic coordinate systems is defined precisely and unambiguously.

Appendix E Acronyms

0R	Zero Reformatted Data
AAS	Anomaly Analysis Subsystem
ACS	Attitude Control System
ADD	Algorithm Description Document
ALI	Advanced Land Imager
ANG	Angle Band
ASTER	Advanced Spaceborne Thermal Emission and Reflection Radiometer
ATRAN	Atmospheric Transmittance
BIH	Bureau International de l'Heure
bLMOC	Backup Multi-Satellite Operations Center
BPF	Bias Parameter File
BRDF	Bi-directional Reflectance Distribution Function
C1	Collection 1
C2	Collection 2
CalCR	Calibration Collection Request
Cal/Val	Calibration/Validation
CCA	Cloud Cover Assessment
CCB	Configuration Control Board
CDED	Canadian Digital Elevation Dataset
CDIST	Distance to Cloud
CE	Circular Error
CFMask	C Function of Mask
CMGDEM	Climate Modeling Grid Digital Elevation Model
COG	Cloud Optimized GeoTIFF
CPF	Calibration Parameter File
CR	Change Request
CVT	Calibration/Validation Team
DCRS	Data Collection and Routing System
DEM	Digital Elevation Model
DFCB	Data Format Control Book
DMS	Data Management Subsystem
DN	Digital Numbers
DOI	Department of the Interior
DOQ	Digital Orthophoto Quadrangle
DPAS	Data Processing and Archive System
DRAD	Downwelled Radiance
DTED	Digital Terrain Elevation Data
ECEF	Earth-Centered, Earth-Fixed
ECI	Earth-Centered Inertial
EE	EarthExplorer

EMIS	Emissivity
EMSD	Emissivity Standard Deviation
EROS	Earth Resources Observation and Science
ERS	EROS Registration Service
ERTS-1	Earth Resources Technology Satellite
ETOPO5	Earth Topography Five Minute Grid
ETM+	Enhanced Thematic Mapper Plus
FASCAL	Facility for Spectroradiometric Calibrations
FMask	Function of Mask
FOT	Flight Operations Team
FOV	Field of View
FPA	Focal Plane Array
FP-IT	Forward Processing for Instrument Teams
FPM	Focal Plane Module
FRB	Full Resolution Browse
GCP	Ground Control Point
GED	Global Emissivity Database
GEOS	Goddard Earth Observing System
GeoTIFF	Geographic Tagged Image File Format
GLAMR	Goddard Laser for Absolute Measurement of Radiance
GLS	Global Land Survey
GLS2000	Global Land Survey 2000
GNE	Ground Network Element
GPS	Geometric Processing Subsystem
GRI	Global Reference Image
GS	Ground System
GSD	Ground Sampling Distance
GSE	Ground Support Equipment
GSFC	Goddard Space Flight Center
GUI	Graphical User Interface
HCA	Horizontal Collimator Assembly
HDF	Hierarchical Data Format
HgCdTe	Mercury–Cadmium–Telluride
IAS	Image Assessment System
IC	International Cooperator
IFOV	Instrument Field of View
IGS	International Ground Stations
ISO	International Standards Organization
JPEG	Joint Photographic Experts Group
K	Kelvin
km	kilometer
L0R	Level 0 Reformatted
L1	Level 1 Data Product

L1GT	Level 1 Systematic Terrain (Corrected)
L1T	Level 1 Terrain (Corrected)
L1TP	Level 1 Terrain Precision (Corrected)
L2	Level 2 Data Product
L2PS	Level 2 Processing Subsystem
L2SP	Level 2 Science Product
L2SR	Level 2 Surface Reflectance
L7	Landsat 7
L8	Landsat 8
L9	Landsat 9
LaSRC	Land Surface Reflectance Code
LCR	LTAP Collection Request
LDCMLUT	Landsat Data Continuity Mission Look-Up Table
LE90	Linear Error 90 Percent
LGN	Landsat Ground Network
LMOC	Landsat Multi-Satellite Operations Center
LOS	Line of Sight
LPGS	Landsat Product Generation System
LSDS	Landsat Satellites Data System
LTAP	Long-Term Acquisition Plan
LTAP-9	Landsat 9 Long-Term Acquisition Plan
LUT	Look-Up Table
LV	Launch Vehicle
m	meter
Mbps	Megabit per Second
MD5	Message-Digest Algorithm 5
MERRA-2	Modern-Era Retrospective Analysis for Research and Applications, Version 2
MLT	Mean Local Time
MMS	Multi-Mission Modular Spacecraft
MODIS	Moderate Resolution Imaging Spectroradiometer
MSS	Multispectral Scanner
MTF	Modulation Transfer Function
MTL	Metadata Text File Extension
NASA	National Aeronautics and Space Administration
NDVI	Normalized Difference Vegetation Index
NED	National Elevation Dataset
NEdL	Noise Equivalent Delta Radiance
NEN	Near Earth Network
NEOG	National Earth Observation Group
NEΔT	Noise Equivalent Change in Temperature
NGA	National Geospatial Intelligence Agency
Ni-H2	Nickel–Hydrogen

NIST	National Institute for Standards and Technology
NMAS	National Map Accuracy Standards
NSLRSDA	National Satellite Land Remote Sensing Data Archive
OBC	On-Board Calibrator
ODL	Object Description Language
OIV	On-orbit Initialization and Verification
OLI-2	Operational Land Imager-2
PCS	Process Control Subsystem
PICS	Pseudo-Invariant Calibration Site
PIE	Payload Interface Electronics
QA	Quality Assessment
QA_PIXEL	QA Pixel-level Band
QA_RADSAT	QA Radiometric Saturation and Terrain Occlusion Band
QAS	Quality Assessment Subsystem
QB	Quality Band
QWIP	Quantum Well Infrared Photodetector
RBV	Return Beam Vidicon
RF	Radio Frequency
RLUT	Response Linearity Look-Up Table
RMSE	Root Mean Square Error
ROIC	Read-Out Integrated Circuit
RPS	Radiometric Processing Subsystem
RSR	Relative Spectral Response
SAA	Solar Azimuth Angle
SCA	Sensor Chip Assemblies
SCR	Special Collection Request
SiPIN	Silicon PIN
SIRU	Scalable Inertial Reference Unit
SLC	Scan Line Corrector
SN	Space Network
SNR	Signal-to-Noise Ratio
SPOT	Satellite Pour l'Observation de la Terre
SR	Surface Reflectance
SRTM	Shuttle Radar Topography Mission
SSM	Scene Select Mirror
SSR	Solid State Recorder
ST	Surface Temperature
STAC	Spatio-Temporal Asset Catalog
SWIR	Short Wavelength Infrared
SZA	Solar Zenith Angle
TIRS-2	Thermal Infrared Sensor-2
TM	Thematic Mapper
TOA	Top of Atmosphere

TRAD	Thermal Radiance Layer
UI	User Interface
URAD	Upwell Radiance Layer
USGS	U.S. Geological Survey
UT1	UTC Corrected
UTC	Universal Time Code
VAA	Sensor Azimuth Angle
VC	Virtual Channel
VNIR	Visible and Near Infrared
VSFB	Vandenberg Space Force Base
VZA	Sensor Zenith Angle
WAN	Wide Area Network
WGS84	World Geodetic System 1984
WRS-2	Worldwide Reference System-2
XML	Extensible Markup Language

References

Please see https://www.usgs.gov/landsat-missions/landsat-acronyms for a complete list of acronyms.

LSDS-1328 Landsat 8-9 OLI/TIRS Collection 2 Level 2 Data Format Control Book (DFCB)

LSDS-1329 Landsat Atmospheric Auxiliary Data Data Format Control Book (DFCB)

LSDS-1388 Landsat Cloud Optimized GeoTIFF (COG) Data Format Control Book (DFCB).

LSDS-1724 Landsat 9 Long-Term Acquisition Plan (LTAP-9)

LSDS-1747 Landsat 8-9 Calibration and Validation (Cal/Val) Algorithm Description Document (ADD)

LSDS-1822 Landsat 8-9 OLI/TIRS Collection 2 Level 1 Data Format Control Book (DFCB)

LSDS-1823 Landsat 1-9 Full Resolution Browse (FRB) Data Format Control Book (DFCB)

LSDS-1834 Landsat 8-9 OLI/TIRS Calibration Parameter File (CPF) Data Format Control Book (DFCB)

LSDS-1835 Landsat 8-9 OLI/TIRS BIAS Parameter File (BPF) Data Format Control Book (DFCB)

LSDS-2032 Landsat Commercial Cloud Direct Access User Guide

Storey JC, Rengarajan R, Choate MJ. Bundle Adjustment Using Space-Based Triangulation Method for Improving the Landsat Global Ground Reference. *Remote Sensing*. 2019; 11(14):1640. https://doi.org/10.3390/rs11141640

Steve Foga, Pat L. Scaramuzza, Song Guo, Zhe Zhu, Ronald D. Dilley, Tim Beckmann, Gail L. Schmidt, John L. Dwyer, M. Joseph Hughes, Brady Laue. Cloud detection algorithm comparison and validation for operational Landsat data products, *Remote Sensing of Environment*. 2017; https://doi.org/10.1016/j.rse.2017.03.026

Landsat Missions Website
https://www.usgs.gov/landsat-missions

Landsat 9 (Collection 2) Data Products Information
https://www.usgs.gov/landsat-missions/landsat-collection-2